

COLLEGE OF AGRICULTURE, ENGINEERING AND SCIENCE



**INVESTIGATION OF THE THERMOPHYSICAL PROPERTIES OF
COCONUT FIBRE BASED GREEN NANOFLUID FOR HEAT
TRANSFER APPLICATIONS**

By

ADEWUMI, GLORIA ADEDAYO

Dissertation submitted in fulfilment of the academic requirements for the degree of Doctor of
Philosophy in Mechanical Engineering

Supervisor: PROFESSOR FREDDIE L. INAMBAO
School of Engineering, Discipline of Mechanical Engineering,
Howard College, Durban.

May, 2018

“As the candidate’s supervisor I agree to the submission of this thesis”.

Professor Freddie Inambao

NAME OF SUPERVISOR



SIGNATURE

DECLARATION 1: PLAGIARISM

I, Adewumi, Gloria Adedayo declare that:

1. The research reported in this thesis, except where otherwise indicated, is my original research.
2. This thesis has not been submitted for any degree or examination at any other university.
3. This thesis does not contain other persons' data, pictures, graphs or other information, unless specifically acknowledged as being sourced from other persons.
4. This thesis does not contain other persons' writing, unless specifically acknowledged as being sourced from other researchers. Where other written sources have been quoted, then:
 - a. Their words have been re-written but the general information attributed to them has been referenced;
 - b. Where their exact words have been used, then their writing has been placed in italics and inside quotation marks, and referenced.
5. This thesis does not contain text, graphics or tables copied and pasted from the Internet, unless specifically acknowledged, and the source being detailed in the thesis and in the references sections.



Signature

DECLARATION 2: PUBLICATIONS

This section includes publications that have been submitted, accepted, published or in press.

ISI/SCOPUS/DoHET Accredited Journals

Publication 1: Adewumi, G.A., Eloka-Eboka, A.C. and Inambao, F.L., 2017. Thermal Conductivity and Viscosity of Bio-based Carbon Nanotubes: Review, *International Journal of Renewable Energy Research (IJRER)*, 7(4), pp. 1752-1766. (Published)

Publication 2: Adewumi, G.A., Inambao, F.L., Eloka-Eboka, A.C. and Revaprasadu, N, 2018. Synthesis of Carbon Nanotubes and Nanospheres from Coconut Fibre and the Role of Synthesis Temperature on their Growth. *Journal of Electronic Materials*. <https://doi.org/10.1007/s11664-018-6248-z>. (Published)

Publication 3: Adewumi, G.A., Inambao, F.L., Sharifpur, M and Meyer J. Investigation of the Viscosity and Stability of Green Nanofluids from Coconut Fibre Carbon Nanoparticles: Effect of Temperature and Mass Fraction. *International Journal of Applied Engineering Research ISSN 0973-4562 Volume 13, Number 10 (2018) pp. 8336-8342*. (Published)

Conference Proceedings

Publication 4: Adewumi, G.A., Eloka-Eboka, A.C. and Inambao, F.L., 2016. A Review on Thermal Conductivity of Bio-Based Carbon Nanotubes. *In proceedings of World Academy of Science, Engineering and Technology: International Conference on Nanotechnology and Biotechnology*, Miami USA Mar 24-25, 2016, pp. 1633-1642.

Publication 5: Adewumi, G.A., Revaprasadu, N., Eloka-Eboka, A.C., Inambao, F. and Gervas, C, 2017. A Facile Low-cost Synthesis of Carbon Nanosphere from Coconut Fibre. *In proceedings of the World Congress on Engineering and Computer Science 2017 Vol II WCECS* San Francisco, USA, October 25-27, 2017, pp. 577-582.

Publication 6: Adewumi, G.A., Inambao, F.L., Sharifpur, M and Meyer J. Thermal Conductivity of Nanofluids Prepared from Bio-based Nanomaterials Dispersed

in 60:40 Ethylene Glycol/Water Base Fluid. *Submitted to NANOSMAT Africa Conference, 2018 Capetown South Africa.*

Book Chapters

Publication 7: Adewumi, G.A., Inambao, F.L., Sharifpur, M and Meyer J. Investigation into the Electrical Conductivity of Carbon Nanosphere-Based Green Nanofluids. *Transactions on Engineering Technologies: World Congress on Engineering and Computer Science 2017*. https://doi.org/10.1007/978-981-13-2191-7_6. (Accepted)

In all the above publications, I, Gloria Adedayo Adewumi was the main and corresponding author, whilst Professor Freddie Inambao was the co-author and research supervisor. All other authors were collaborators who served at a supervisory capacity.

ACKNOWLEDGEMENTS

I will like to convey my deepest gratitude to my supervisor Professor Freddie Inambao who has been of immense help by offering guidance, support and assistance throughout the duration of this research.

I would also like to thank Professor Neerish Revaprasadu and Professor Mohsen Sharifpur at the University of Zululand and University of Pretoria respectively who gave me the opportunity to use their labs for my experiments.

My profound gratitude goes to my family, Professor and Mrs S. E. Adewumi who taught me virtues that guide me daily; my siblings, who taught me teamwork; and my in-laws Pastor and Mrs Akinrinde for your relentless prayers and love.

My gratitude goes to my friends and colleagues at the Green Energy Solutions Group (GES) for the information shared with me.

Finally, I would love to say a huge thank you to my dearest husband and friend 'Jibola whom I love deeply, and my little princess Morire for having been my support and motivation during the course of my studies.

ABSTRACT

Significant resources are being channelled toward research on carbon nanomaterials obtained from biomass precursors because of their overall environmental acceptability, stability, low toxicity and simplistic use. Due to their unique nature, they have excellent thermo-physical properties which include improved thermal conductivity, electrical conductivity and viscosity. In this study, carbon nanotubes and nanospheres were successfully synthesized from coconut fibre activated carbon. The biomass was first carbonized, then physically activated followed by treatment using ethanol vapor at 700 °C to 1100 °C at 100 °C intervals. The effect of synthesis temperature on the formation of the nanomaterials was studied using scanning electron microscope (SEM), transmission electron microscope (TEM), energy dispersive X-ray powder diffraction (XRD), Fourier transform infrared microscopy (FTIR) and thermo-gravimetric analysis (TGA). SEM analysis revealed nanospheres were formed at higher temperatures of 1000 °C and 1100 °C, while lower temperatures of 800 °C and 900 °C favoured the growth of carbon nanotubes. At 700 °C however, no tubes or spheres were formed. TEM and FTIR were used to observe spectral features, such as the peak positions, intensity and bandwidth which are linked to some structural properties of the samples investigated. All these provided facts on the nanosphere and nanotube dimensions, vibrational modes and the degree of purity of the obtained samples. In general, the TEM results showed spheres of diameter in the range 30 nm to 250 nm while the tubes had diameters between 50 nm to 100 nm. XRD analysis revealed that the materials synthesized were amorphous in nature with a hexagonal graphite structure. Experimental measurements of the thermal conductivity, electrical conductivity and viscosity of the synthesized nanomaterials dispersed in 60%:40% ethylene glycol (EG) and water (W) nanofluids containing gum arabic (GA) were performed, considering the effects of temperature and mass fraction. Stability testing of the nanofluids were determined by zeta potential, viscosity and UV spectroscopy measurements of nanofluids for 720 minutes. The green nanofluids prepared were observed to very stable for more than 720 minutes. Also the results of experiments showed that the addition of nanomaterials to the base fluid increased the viscosity and that with the increase in temperature, the viscosity decreased while the electrical conductivity improved when compared to the base fluid. On the other hand, the thermal conductivity results were observed to decrease with the addition of nanoparticles. This decrease observed has been attributed to high thermal boundary resistance, ratio of surfactant and inconsistent size of the nanoparticles.

TABLE OF CONTENTS

DECLARATION 1: PLAGIARISM.....	ii
DECLARATION 2: PUBLICATIONS	iii
ACKNOWLEDGEMENTS	v
ABSTRACT.....	vi
TABLE OF CONTENTS.....	vii
LIST OF FIGURES.....	x
LIST OF APPENDICES	xi
NOMENCLATURE.....	xii
ACRONYMS	xv
CHAPTER 1: INTRODUCTION	1
1.1 General Introduction	1
1.2 Preparation of nanofluids	2
1.2.1 One-Step Method of Nanofluid Preparation	2
1.2.2 Two-Step Method of Nanofluid Preparation.....	2
1.3 Negative Impact of Nanoparticles.....	2
1.4 Research Questions	3
1.4 Research Rationale.....	4
1.5 Research Motivation	4
1.6 Statement of Purpose.....	5
1.7 Aims and Objectives	5
1.8 Hypotheses.....	5
1.9 Thesis Outline	6
References	6
CHAPTER 2: THERMAL CONDUCTIVITY AND VISCOSITY OF BIO-BASED CARBON NANOTUBES.....	8
CHAPTER 3: SYNTHESIS OF CARBON NANOSPHERES FROM COCONUT FIBRE	24
Part 1: A FACILE LOW-COST SYNTHESIS OF CARBON NANOSPHERES FROM COCONUT FIBRE	25

Part 2: SYNTHESIS OF CARBON NANOTUBES AND NANOSPHERES FROM COCONUT FIBRE AND THE ROLE OF SYNTHESIS TEMPERATURE ON THEIR GROWTH	31
CHAPTER 4: VISCOSITY AND STABILITY OF GREEN NANOFLUIDS FROM COCONUT FIBRE CARBON NANOPARTICLES.....	38
CHAPTER 5: THE ELECTRICAL CONDUCTIVITY OF CARBON NANOSPHERE-BASED GREEN NANOFLUIDS	46
INVESTIGATION INTO THE ELECTRICAL CONDUCTIVITY OF CARBON NANOSPHERE-BASED GREEN NANOFLUIDS	47
Abstract	47
5.1 Introduction	47
5.2 Experimental Method.....	51
5.2.1 Materials and Stable Nanofluid Preparation	51
5.3 Measurement of Electrical Conductivity	52
5.4 Results and Discussion.....	52
5.4.1 XRD and Stability of Nanofluid.....	52
5.4.2 Electrical Conductivity Evaluation	54
5.5 Conclusion.....	56
Acknowledgement.....	57
References	57
CHAPTER 6: THERMAL CONDUCTIVITY OF NANOFLUIDS PREPARED FROM BIOBASED NANOMATERIALS	60
THERMAL CONDUCTIVITY OF NANOFLUIDS PREPARED FROM BIOBASED NANOMATERIALS DISPERSED IN 60:40 ETHYLENE GLYCOL/WATER BASE FLUID	61
Abstract	61
6.1 Introduction	61
6.2 Theory	63
6.3 Experimental	64
6.3.1 Preparation of Stable Nanofluids	64
6.3.2 Thermal Conductivity Measurements	64
6.4 Results and Discussion.....	65

6.4.1 Morphology and Stability of Nanofluids	65
6.5 Measurement of Thermal Conductivity	68
6.6 Conclusion.....	70
References	70
CHAPTER 7: CONCLUSION AND FUTURE WORK	73
7.1 Conclusion.....	73
7.2 Future Work	74

LIST OF FIGURES

Fig. 5.1. Nanosphere particle size distribution.....	52
Fig. 5.2. XRD pattern of carbon nanospheres synthesized at 1100 °C	53
Fig. 5.3. EDX of CNS	53
Fig. 5.4. Stability test using viscosity at a constant temperature for 720 min.....	54
Fig. 5.5. Electrical conductivity at different temperatures for different volume concentrations	54
Fig. 5.6. Electric conductivity at various mass fractions	55
Fig. 5.7. Electrical conductivity enhancements at various temperatures for different volume concentrations.....	56
Fig. 5.8. Electrical conductivity enhancement at different volume fractions	56
Fig. 6.1. Particle size distribution and TEM image of green nanoparticles synthesized from bio-based precursor and used in the present study	66
Fig. 6.2. X-ray diffractogram of nanoparticles.....	67
Fig. 6.3. UV-Vis spectroscopy for stability analysis of nanofluids	67
Fig. 6.4. Comparison of measured data and ASHRAE.....	68
Fig. 6.5. Thermal conductivity at different mass fractions	69
Fig. 6.6. Temperature effect on thermal conductivity of prepared nanofluids.....	70

APPENDIX

Appendix 1: A review on the Thermal Conductivity of Bio-based Carbon Nanotubes 75

NOMENCLATURE

a_1 and a_2	Graphene sheets 1 and 2
B_c	Boltzmann constant
C	Length of the chiral vector
C_p	Specific heat (J/kg K)
\hat{C}_{jj}^q	Quantum canonical correlation function
d	Tube diameter (nm)
E	Electric field
F_s	Hydrodynamic force (N)
F_d	Hydrodynamic drag force (N)
G	Reciprocal lattice vector
\hbar	Planck's constant
J	Resulting heat flux density
m	Mass
n_{+ve}	Number of positive ions
n_{-ve}	Number of negative ions
q, q' and q''	Phonon wave vectors
q_{+ve}	Charge on positive ion
q_{-ve}	Charge on negative ion
r_{c-c}	The c-c distance of the grapheme layer (1.42 Å)
r_i	Radius of i ion
r	Radius

T	Temperature (°C)
V	Volume (cm ³)
∇T	Temperature gradient

Greek Symbols

α	Thermal diffusivity of CNT (m ² /s)
k	Thermal conductivity (W/mK)
μ	Viscosity (Pa s)
v	Velocity (m/s)
v_i	Velocity of i ion
v_e	Counter-current velocity
v_{+ve}	Positive ion drift velocity
v_{-ve}	Negative ion drift velocity
ρ	Density (Kg/m ³)
σ	Electrical conductivity ($\mu S/cm$)
τ_f	Mean free time
τ_U	Three-phonon Umklapp scattering process
τ_B	Relaxation time for boundary scattering
\emptyset	Volume fraction ($\emptyset/100$)
\emptyset_{ecs}	Effective volume fraction of cluster spheres
\emptyset_m	Maximum particle volume fraction usually taken as 0.605
$\theta_{D.eff}$	Efficient temperature (°C)
θ	Helical angle (degrees)

Subscript

<i>eff</i>	Effective
<i>bf</i>	Base fluid
<i>nf</i>	Nanofluids
<i>np</i>	Nanoparticle
<i>-ve</i>	Negative
<i>+ve</i>	Positive

ACRONYMS

CNS	Carbon nanosphere
CNT	Carbon nanotube
CVD	Chemical vapour deposition
EDX	Energy dispersive X-ray spectrometer
EG	Ethylene glycol
FESEM	Field emission scanning electron microscopy
FTIR	Fourier transform infrared spectroscopy
MD	Molecular dynamics
MEMS	Microelectromechanical
MWCNT	Multi-walled carbon nanotube
NEMS	Nanoelectromechanical
PCM	Phase change materials
SAED	Selected area electron diffraction
SEM	Scanning electron microscopy
SWCNT	Single-walled carbon nanotube
TGA	Thermo-gravimetric analysis
UV	Ultraviolet
TEM	Transmission electron microscopy
XRD	X-ray diffraction

CHAPTER 1: INTRODUCTION

1.1 General Introduction

In many industrial and automotive applications, fluids such as ethylene glycol, water, refrigerants, oil etc., are used to either add or remove heat. Addition or withdrawal of heat is done to enhance the energy efficiency of the system as well as to save cost through reducing processing time and increasing the equipment's working life. The principle of heat transfer generally centres on reducing thermal resistance by increasing the effective heat transfer surface area or by generating turbulence in the fluid flow [1].

More research was therefore required on the enhancement of the heat flow process as complex systems emerged. About two decades ago, two researchers at Argonne National Laboratory discovered that adding nanometer scale materials to existing heat transfer fluids had the ability to enhance their thermo-physical properties and subsequently improve heat transfer [2]. These materials possess a very high aspect ratio and special surface area which are essential criteria for heat transfer enhancement. The discovery of these classes of fluids opened the possibility of designing miniature and lighter heat exchanger systems.

Nanofluids are a novel class of fluids with particles in the nanometer scale dispersed and suspended in suitable base fluids in order to improve their properties for a desired application. They can also be described as colloidal suspensions containing nanoparticles. Nanofluids possess thermophysical properties such as thermal conductivity, viscosity, density, and electrical conductivity. These have been revealed to change under varying temperature, particle loading and particle geometry, with these variations originating from the changes in the nanofluids' internal structure and flow hydrodynamic properties. For nanofluids to be used in heat transfer applications, an understanding of the thermo-physical properties is essential in order to be able to control and manipulate the nanofluids for their target applications. Poor thermo-physical properties are a primary limitation in developing energy-efficient heat transfer fluids that are required for ultrahigh performance cooling. Nanofluids have been found to exhibit improved thermo-physical properties and lead to an astonishing reduction in heat exchanger pumping power. Choi [2] and his team established that copper nanoparticles dispersed in water improved thermal conductivity and pumping power was reduced which is an important advantage in heat exchangers. They are also believed to reduce erosion and clogging which occurs when using micro particles, leading to significant energy savings.

1.2 Preparation of nanofluids

Preparation of stable nanofluids is a key necessity in their applications in heat transfer. Due to the small size of nanoparticles, they contain very high surface charge and strong Van der Waals forces which leads to agglomeration in base fluids. The following are the drawbacks of an unstable nanofluid [3]:

- i. Rapid settlement of the nanoparticles in the base fluid, thereby resulting in poor thermal conductivity and subsequently poor heat transfer capacity.
- ii. Increase in erosion and clogging of pipes and flow channels.
- iii. Drop in pressure.

These agglomerates must therefore be broken up for the nanofluids to be termed as stable. Nanofluids can be prepared by using either a one-step (single step) method or a two-step method.

1.2.1 One-Step Method of Nanofluid Preparation

The one-step method of nanofluid preparation involves a process of combining the synthesis of the nanoparticles and their dispersion in the base-fluid [4]. Some researchers have reported this method to be fast and efficient for the preparation of nanofluids containing metallic nanoparticles as it eliminates the Van der Waals forces present in powder nanoparticles [5]. However a downside of this method is its high cost and inability to be produced on a large scale [6]. In addition, complexes may be formed during the process of nanofluids preparation from residual reactants which may affect the purity of the nanofluids [4].

1.2.2 Two-Step Method of Nanofluid Preparation

The two-step method of nanofluid preparation is the most widely used method for preparing stable nanofluids and it works well for nanoparticles containing oxides and carbon based nanomaterials. This method involves the use of high shear and ultrasonic vibration to break up agglomerates giving rise to a stable suspension. The first step is to prepare nanoparticles by physical or chemical means and disperse these in a base-fluid with or without the addition of a surfactant. Next, the mixture is subjected to stirring using a magnetic stirrer to break down agglomerates. Finally, the mixture is further homogenized using a high power ultrasonic homogenizer to further break down agglomerates to produce a stable suspension.

1.3 Negative Impact of Nanoparticles

During research scale synthesis or commercial synthesis of nanomaterials, engineers, scientists and technicians come in contact with these materials. Recent studies have discovered the negative impact nanoparticles have on humans who have some degree of exposure to them. For example, metallic

nanoparticles such as silver (Ag), cerium dioxide (CeO₂) and titanium dioxide (TiO₂) were found to have the ability to penetrate the plasma membrane and ultimately lead to cell death [7]. Occupational exposure is the most common exposure method whereby nanoparticles interact with human skin and cells. The mechanisms through which nanomaterials are taken up in human cells are still not very well known and are presently under investigation. While it is important that certain measures need to be adopted in order to have a greener route for synthesis of nanomaterials, it is imperative that issues of toxicity and environmental unfriendliness be addressed appropriately as failure to do so may lead to adverse health effects.

Bio-based carbon nanoparticles are a promising substitute for metal-based nanoparticles. Past studies of bio-based carbon nanoparticles have shown an increase in thermal conductivity, latent heat, thermal resistance and overall thermal efficiency [8]. The precursor used is very important in controlling the morphology and yield of carbon nanoparticles. Precursors such as graphite powder, petroleum pitch, carbon rich polymers, and other types of hydrocarbons have been used previously and research is ongoing in this area. However, due to toxicity and environmental hazards it is important to produce nanomaterials from green sources that would pose no harm to humans and the environment.

Greener routes through which carbon nanomaterials can be synthesized have been investigated and the results indicate that there is a future in green nanotechnology from bio-based precursors. These natural products, some of which have been used as either reductants, capping agents or for surface functionalization [9] during synthesis, have proven to mitigate issues relating to environmental contamination and toxicity. Plant parts such as the leaves, roots, fruits, seeds and stems are being used for metal nanoparticle synthesis [10]. The use of plant parts during synthesis is possible due to the presence of polyphenols, their verified stability in acidic solutions, and their oxidative defence systems in cells [11]. Plant extracts contain molecules which have the capacity to reduce metal ions or act as capping agents to nanoparticles [12]. Plant extracts have the benefit of being readily synthesized at room temperature and easily scaled up. The polyphenols present in tea extracts can also act as both chelating and reducing agents which prevents agglomeration in nanoparticle formation and consequently leads to an increase in stability and longevity [10].

1.4 Research Questions

The following are the research questions to be considered:

- a. How can carbon nanomaterials be synthesized from coconut fibre?
- b. What morphology and structural properties of carbon nanomaterials will be obtained?
- c. Are the prepared nanofluids stable?

- d. Are the thermo-physical properties of bio-based green nanofluids improved compared to the base fluid (60:40 EG/W)?

1.4 Research Rationale

Fifty-five billion coconuts are harvested annually while the maximum total production of coconut fibre is estimated to be 5-6 million tonnes per annum. Natural fibres, of which coconut fibre is one, are easily sourced worldwide and are considered to be cheap and environmentally friendly due to their renewability, non-microbial degradability and light weight. They have been used as components in composites in which tensile strength, flexural strength and hardness of the composites are paramount [13-15]. Coconut fibre makes up about 54 % of the coconut fruit [16] and of this, only about 15 % of the fibres find use in various applications [15]. They are generally used as domestic fuel and for making ropes and mats. Channelling these cheap and abundant materials into applications relating to nanotechnology will not only reduce heavy dependence on other toxic chemical precursors, but will also help in achieving a bio-economy strategy. Activated carbon derived from coconut fibre contains metals which eliminate the use of additional catalysts during preparation of the carbon nanomaterials; this is an advantage during synthesis as this helps to reduce costs incurred from catalysts which contributes to the overall low-cost preparation procedure.

1.5 Research Motivation

Bio-based carbon nanotubes are a promising substitute for synthetic carbon nanotubes because they form lesser agglomerates and they are thermally stable. The precursor material used is important in controlling the morphology and yield of carbon nanotubes. Precursors such as graphite powder, petroleum pitch, carbon rich polymers, and other types of hydrocarbons have been used previously and research is ongoing in this area. However, due to toxicity and environmental hazards that can be caused, it is important to produce nanomaterials from green sources that pose no harm to humans and the environment.

The motivations behind this research are:

- i. Absence of literature on the synthesis of carbon nanomaterials from coconut fibre.
- ii. No previous literature on the preparation of green nanofluids from coconut fibre nanomaterials dispersed in 60:40 EG/W nanofluids.
- iii. No previous studies have been found in the literature on the thermo-physical properties of bio-based green nanofluids.

1.6 Statement of Purpose

As the applications of nanoparticles expand, the issue of safety and toxicity becomes more prominent because they have been reported to have the ability to harm humans and wildlife as they can penetrate the skin through inhalation, ingestion and dermal contact [17, 18]. Recently, the use of bio-based precursors in the synthesis of carbon nanomaterials has been investigated regarding environmental friendliness and renewability. The results reveal that nanomaterials from biomass have a huge potential to be used in nanotechnology as they can put agricultural waste to good use. Bio-based materials, apart from improving environmental protection, also enhance national energy security and rural economic growth [19]. According to the South African bio-economy strategy launched in 2014, bio-based products should be derived from non-fossil products such as biomass.

The purpose of this study is therefore to synthesize carbon nanomaterials from a coconut fibre bio-based precursor to be dispersed in 60:40 EG/W nanofluids.

1.7 Aims and Objectives

The aim of this study was to investigate the thermophysical properties (electrical conductivity and viscosity) of green nanofluids prepared from dispersing coconut fibre nanomaterials in 60:40 EG/W. The objectives were:

- i. To synthesize and characterise carbon nanomaterials from a coconut fibre bio-based precursor.
- ii. To prepare nanofluids by dispersing the synthesized carbon nanomaterials in 60:40 EG/W base fluid.
- iii. To determine the stability of the nanofluid using zeta potential, UV spectroscopy and viscosity measurements over a period of 720 mins.
- iv. To determine the viscosity of bio-based green nanofluids under different temperatures and concentrations.
- v. To determine the electrical conductivity of the prepared green nanofluids at varying temperatures and concentration.
- vi. To determine the thermal conductivity of the nanofluids and to compare the results with the thermal conductivity of the base fluid (60:40 EG/W)

1.8 Hypotheses

The following were the hypotheses of this research:

- i. Carbon based nanomaterials can be synthesized from coconut fibre by ethanol vapour treatment.

- ii. The morphology and size of the synthesized carbon nanomaterials is dependent on the synthesis temperature.
- iii. Stable nanofluids can be prepared from the dispersion of bio-based carbon nanomaterials in 60:40 EG/W base fluids with gum arabic (GA) as surfactant.
- iv. The viscosity, thermal conductivity and electrical conductivity of the prepared nanofluids are improved compared to the base fluid.

1.9 Thesis Outline

In the present chapter, the background information on nanofluids has been discussed. In addition, the research question, rationale, motivation, statement of purpose, hypothesis, aims and objectives have also been outlined. The remaining chapters are organized as follows:

Chapter 2 is a review paper that presents past research in the area of thermal conductivity and viscosity of carbon nanotubes. The chapter explores thermal conductivity of individual carbon nanotubes and carbon nanotube-based nanofluids.

Chapter 3 is divided into two parts comprising a conference proceeding and a journal publication which reports a general time and cost effective approach which was implemented for preparing carbon nanospheres from coconut fibre bio-based feedstock and the effects of synthesis temperature. Carbon nanospheres and nanotubes were successfully synthesized by passing ethanol vapour through activated carbon obtained from coconut fibre at 700 °C to 1100 °C at 100 °C increments.

Chapter 4 presents the effect of temperature and mass fraction on the viscosity and stability of green nanofluids prepared from bio-based carbon nanomaterials.

Chapter 5 presents results from the electrical conductivity measurements of green nanofluids taking into consideration the effect of temperature and mass fraction.

Chapter 6 is an investigation into the thermal conductivity of the prepared green nanofluids and its comparison with the thermal conductivity of the base fluid (60:40 EG/W).

Chapter 7 summarizes the conclusions and future work related to this study.

References

- [1] C. Maradiya, "The heat transfer enhancement techniques and their thermal performance factor," *Beni-Suef University Journal of Basic and Applied Sciences*, 2017.
- [2] S. U. Choi and J. A. Eastman, "Enhancing thermal conductivity of fluids with nanoparticles," Argonne National Lab., IL (United States)1995.

- [3] S. K. Das, S. U. Choi, W. Yu, and T. Pradeep, *Nanofluids: science and technology*. John Wiley & Sons, 2007.
- [4] M. Uddin, K. S. Al Kalbani, M. Rahman, M. Alam, N. Al-Salti, and I. Eltayeb, "Fundamentals of nanofluids: evolution, applications and new theory," *International Journal of Biomathematics and Systems Biology*, vol. 2, no. 1, pp. 1-32, 2016.
- [5] H.-t. Zhu, Y.-s. Lin, and Y.-s. Yin, "A novel one-step chemical method for preparation of copper nanofluids," *Journal of Colloid and Interface Science*, vol. 277, no. 1, pp. 100-103, 2004.
- [6] W. Yu and H. Xie, "A review on nanofluids: preparation, stability mechanisms, and applications," *Journal of Nanomaterials*, vol. 2012, p. 1, 2012.
- [7] L. P. Franchi *et al.*, "Cyto- and genotoxic effects of metallic nanoparticles in untransformed human fibroblast," *Toxicology in Vitro*, vol. 29, no. 7, pp. 1319-1331, 2015.
- [8] S.-G. Jeong, O. Chung, S. Yu, S. Kim, and S. Kim, "Improvement of the thermal properties of Bio-based PCM using exfoliated graphite nanoplatelets," *Solar Energy Materials and Solar Cells*, vol. 117, pp. 87-92, 2013.
- [9] R. Sadri *et al.*, "A facile, bio-based, novel approach for synthesis of covalently functionalized graphene nanoplatelet nano-coolants toward improved thermo-physical and heat transfer properties," *Journal of Colloid and Interface Science*, 2017.
- [10] O. V. Kharissova, H. V. Dias, B. I. Kharisov, B. O. Perez, and V. M. Perez, "The greener synthesis of nanoparticles," *Trends Biotechnol*, vol. 31, no. 4, pp. 240-8, Apr 2013.
- [11] R. Tsao, "Chemistry and biochemistry of dietary polyphenols," *Nutrients*, vol. 2, no. 12, pp. 1231-46, Dec 2010.
- [12] A. K. Mittal, Y. Chisti, and U. C. Banerjee, "Synthesis of metallic nanoparticles using plant extracts," *Biotechnology Advances*, vol. 31, no. 2, pp. 346-56, Mar-Apr 2013.
- [13] L. Kuburi *et al.*, "Effects of coir fiber loading on the physio-mechanical and morphological properties of coconut shell powder filled low density polyethylene composites," *Procedia Manufacturing*, vol. 7, pp. 138-144, 2017.
- [14] I. Bujang, M. Awang, and A. Ismail, "Study on the dynamic characteristic of coconut fibre reinforced composites," in *Proceedings of the Regional Conference on Engineering Mathematics, Mechanics, Manufacturing & Architecture*, 2007.
- [15] P. Muensri, T. Kunanopparat, P. Menut, and S. Siri wattanayotin, "Effect of lignin removal on the properties of coconut coir fiber/wheat gluten biocomposite," *Composites Part A: Applied Science and Manufacturing*, vol. 42, no. 2, pp. 173-179, 2011.
- [16] S. Bello, J. Agunsoye, J. Adebisi, F. Kolawole, and B. Suleiman, "Physical properties of coconut shell nanoparticles," *Kathmandu University Journal of Science, Engineering and Technology*, vol. 12, no. 1, pp. 63-79, 2016.
- [17] M. Sajid *et al.*, "Impact of nanoparticles on human and environment: review of toxicity factors, exposures, control strategies, and future prospects," *Environmental Science and Pollution Research*, vol. 22, no. 6, pp. 4122-4143, March 01 2015.
- [18] B. Nowack and T. D. Bucheli, "Occurrence, behavior and effects of nanoparticles in the environment," *Environmental Pollution*, vol. 150, no. 1, pp. 5-22, 2007.
- [19] S. P. Singh, E. Ekanem, T. Wakefield Jr, and S. Comer, "Emerging importance of bio-based products and bio-energy in the US economy: information dissemination and training of students," *International Food and Agribusiness Management Review*, vol. 5, no. 3, p. 14, 2003.

CHAPTER 2: THERMAL CONDUCTIVITY AND VISCOSITY OF BIO-BASED CARBON NANOTUBES

Adewumi, G.A., Eloka-Eboka, A.C. and Inambao, F.L., 2017. Thermal Conductivity and Viscosity of Bio-based Carbon Nanotubes. *International Journal of Renewable Energy Research (IJRER)*, 7(4), pp.1752-1766. (Published)

Thermal Conductivity and Viscosity of Bio-based Carbon Nanotubes: Review

Gloria A. Adewumi*‡, Andrew Eloka-Eboka**, Freddie Inambao***

*Discipline of Mechanical Engineering, School of Engineering, PhD candidate, Room 138B, Discipline of Mechanical Engineering, University of KwaZulu-Natal, Howard College

** Discipline of Mechanical Engineering, School of Engineering, Post-doctoral Fellow, Green Energy Solutions, Discipline of Mechanical Engineering, University of KwaZulu-Natal, Howard College

*** Discipline of Mechanical Engineering, School of Engineering, Professor, Discipline of Mechanical Engineering University of KwaZulu-Natal, Howard College

(adewumigloria@gmail.com, fatherfounder@yahoo.com, inambaof@ukzn.ac.za)

‡

Corresponding Author; Gloria Adewumi, Room 138B Discipline of Mechanical Engineering, University of KwaZulu Natal, Durban, South Africa, Tel: +27749423154, adewumigloria@gmail.com

Received: 10.04.2017 Accepted: 16.07.2017

Abstract- Significant research focus is being channeled to carbon nanotubes (CNTs) obtained from biomass precursors because of their overall environmental acceptability, stability, low toxicity and simplistic use. They contain unique properties such as high viscosity, high aspect ratio, special surface area and high thermal conductivity which have been identified to be responsible for their improved heat transfer applications. High thermal conductivity of this class of nanomaterials is linked to the presence of phonons. Thus, knowledge of the principle of heat conductivity in carbon nanotubes encompasses investigations relating to the dissimilarity in the different phonon modes. Also, an in-depth understanding in which phonon modes play the governing role is necessary. Herein the authors have carried out a critical review of past and current literature, the function of phonon relaxation rate primarily governed by three-phonon Umklapp scattering process and boundary scattering have been explored. Also the roles of temperature and shearing time on viscosity of CNT fluids are discussed. Results indicate that the sensitivity of the phonon modes is due to several nanotube parameters like: temperature, diameter, axial strain, defects and length. The various viscosity experiments from literature shows that the kinematics viscosity of nanofluids improved with a decrease in the temperature and increase of the CNT concentration.

Keywords- Bio-based carbon nanotubes, Phonons, Thermal conductivity, Umklapp process, Viscosity.

1. Introduction

A “biomaterial” or a “bio-based material” is produced from existing living organisms including residues and agricultural crops, algae and trees. “Sustainable bio-based materials” are materials obtained from mature and reaped cropland or plantations which are sustainable; synthesized without harmful contributions and influences; are harmless and healthy for the environment during usage [1-5], and are intended to be reused at the end of their proposed use via composting and recycling.

Due to their unique mechanical, electrical and thermal properties, a growing effort is being made to deviate from the heavy dependence on petroleum sources for energy. Bio-materials obtained from green sources pose no health hazards and is friendlier on ozone depletion. Past study has suggested a focus towards the formation of value added materials obtained from bio-mass instead of using biomass as a direct source of fuel [6-10].

In 1991 after their discovery, research on Carbon Nanotube (CNTs) has emerged, branching open new discoveries and opportunities. CNTs have wonderful heat and electrical transfer properties which makes them a sort of wonder material. The diversity in property which is an advantage stems from their abilities to be rolled up in different tube axis based on different helicities [11] and this is decided by a chiral vector which categorizes CNTs into “zigzag”, “armchair”, and “chiral” forms. Carbon nanotubes are one-dimensional cylinders and can be multiple or single layers of carbon. Nanotubes with a one layer are called Single Wall Carbon Nanotubes (SWCNTs) while carbon nanotubes with multiple walls are called Multi-wall Carbon Nanotubes (MWCNTs) [12]. The diameters of the tubes are in the range of a few nanometers (0.4nm-1.4nm) and a length in micrometers, which confers high aspect ratios [11]. MWCNTs are easier to synthesize when compared to SWCNT because they can be grown from most hydrocarbons at a low temperature (600-900°C). SWCNTs are usually synthesized by infusing

metals in the transition metals group in catalytic amounts in the arc-discharge process while being able to grow from selected hydrocarbons [11]. Earlier studies determined that CNT immersed in suitable base fluids had the ability to reduce erosion and clogging which is seen in micro particles and this has led to significant energy savings and high efficiency in micro-channels [11],[13],[14]. The knowledge of the thermal conductivity of CNTs is very useful in the design of nanoelectromechanical systems (NEMS) and microelectromechanical systems (MEMS) used for efficient thermal transport system in electrical, mechanical and chemical applications, solar energy systems and central air conditioning systems. It is also necessary in the development of molecular theories in nanofluids and nanofluid mixtures [15]. Low thermal conductivity are presently a major disadvantage in the synthesis of heat transfer fluids with high energy-efficiency needed for very high performance cooling [11]. Nanofluids however, are seen to have high thermal conductivities which depends not only on forces acting on nanoparticles but also on particle motion and interaction with turbulent eddies which leads to an astonishing reduction in heat exchanger pumping power [13]. After reviewing previous works, we find that the reported thermal conductivities of CNT is as high as 3000W/mK [16]. For bio-based CNT on the other hand, there is less literature available. Recently, the thermal conductivity of bio-based phase change (PCM) was enhanced by adding carbon nanotubes and the thermal conductivity reported is 0.557W/mK [17]. In comparison to tested carbon black, studies by [18] revealed a 36% in the thermal conductivity of carbonized ball milled lignin after synthesis by ball-milling. This review presents the various methods of synthesis of carbon nanoparticles and equally important, an investigation of the thermal conductivity measurements of MWCNT and SWCNT. The effects of temperature, length, substrate and diameter of the nanotubes have been analyzed. The current trend towards miniaturization and the global need for a renewable and sustainable heat transfer source has motivated this study.

2. Synthesis of Carbon Nanoparticles

The tube diameter (d) and the helical angle θ are the two factors that describe the structure of a nanotube, not to forget the helical vector $C = na_1 + ma_2$ (where a_1 and a_2 are the graphene sheets). Tubes are characterized by (x,y) notation depending on how they are rolled. The diameter and helical angle of nanotubes can be found from x and y [11] and given in equation (1) and equation (2).

$$d = \frac{c}{\pi} = \frac{\sqrt{3r_{c-c}(y^2+xy+x^2)}^{1/2}}{\pi} \quad (1)$$

$$\theta = \tan^{-1} \frac{\sqrt{3}m}{(y+2x)} \quad (2)$$

r_{c-c} The c-c distance of the graphene layer (1.421Å)

C Length of the chiral vector

From a broad view, there exist three methods of synthesizing carbon nanotubes [11],[19],[20]:

- Formation of single-walled nanotubes (SWNT) by the incorporation of transition metals in catalytic amounts in the arc-discharge process;
- Laser evaporation which forms nanotubes with rope-like structures; and
- Chemical vapor deposition.

Bio-based carbon nanoparticles are a promising substitute for the metal based nanoparticles. Past studies on CNTs have shown increase in thermal conductivity, latent heat, thermal resistance, environmental friendliness, renewability and overall thermal efficiency [17],[18],[21-23]. Synthesis methods for CNT production depends largely on its application. The precursor used during synthesis is important in governing the yield and morphology of carbon nanoparticles. Precursors like petroleum pitch, graphite powders, carbon rich polymers, petroleum pitch, and other types of hydrocarbons have been successfully used in synthesizing CNT and research is still ongoing in this area, [11, 24-28]. However due to toxicity and environmental hazards that can be caused, it is important to produce nanomaterials which are free from amorphous carbon. They should be obtained from green sources that would pose no harm to humans and the environment.

The authors in [29] reviewed greener routes used for nanoparticle production. Greener routes sourced from plant extracts and natural products used in past research were studied. These natural products, some of which were used as capping agents and reductants during synthesis have proven to assist with problems relating to environmental contamination, while using non-toxic solvents like water. Parts of plants like the roots, leaf, fruits, stem and seeds are being adopted for synthesis of nanoparticles from metallic nanoparticle synthesis. [15, 29-33]. This is identified to be due to the presence of polyphenols because they are stable in acidic solutions and they also modulate the oxidative defense system in cells [34]. The bio-molecules present in plant are reported to reduce metal ions or act as capping agents to particles in nano-size in a one-step green synthesis methods developed by [33]. The authors emphasized their advantages of being readily conducted at room temperature, easily scaled up and rapid. Micro-organisms have been used to synthesize nanoparticles; however the rate at which production occurred was found to be slow and only limited number of sizes and shapes are amenable compared to that of biomass-based. The polyphenols contained in tea extracts can act as both reducing and chelating agents which prevents agglomeration in nanoparticle formation and consequently leads to an increase in stability and longevity [29].

Authors [21] and [35], synthesized carbon nanoparticles from glucose and alkali or acid additives. However the former carried out their experiments under ultra-sonication condition, while the latter utilized hydrothermal synthesis. From their results, the method

based on ultrasonic synthesis was more efficient in terms of particle size agglomeration as the particle size obtained (5nm) as opposed to the particle sizes from [35] which was 70-100nm. Ultrasound has been known to produce alternating high pressure and low-pressure waves in solution, resulting in the collapse and formation of small vacuum bubbles [21]. Zhang et al. [22] have also applied a simple hydrothermal method using L-ascorbic acid as a carbon source. There were no acidic additives and there was no need for any surface modification. However, the addition of ethanol enhanced the surface state of the carbon nanoparticle. Gonugunta et al. [36] studied the production of bio-based carbon nanoparticle using lignin as the carbon source. The freeze drying process was used in order to avoid lumps or aggregates formed from carbonization. It was observed that there was an increase in thermal stability with a corresponding increase in KOH. This was as a result of the influence of KOH on the particle size as lignin samples modified with KOH yielded ultrafine particles even though it forms agglomeration at higher concentrations of 15% [36]. To avoid the problem of lump formation (agglomeration) which usually arises from carbonization, thermal pyrolysis method was recently used by Roshni and Ottoor [37] to synthesize bio-based nanoparticles from coconut milk. The authors used the pyrolysis method because it does not involve any surface passivating agent or any acid treatment. The result however shows a large size range (20nm-50-nm) which could be due to non-homogeneity in the pyrolysis method adopted. Apart from the chemical methods used for synthesis, physical approaches are also being used for synthesis of nanoparticles [18, 27, 38, 39]. Physical methods include: ball milling and mechanical grinding. A bottom-up mechano-chemical approach using milling of inorganic precursors was also reported by Rak et al. [27]. Conventionally, ball milling is a top down approach because the particles are broken down into nanometer sized particles.

A. *Effects of synthesis parameters on the growth of CNT*

The parameters involved in the synthesis of CNT plays a significant role on the final characteristics of the CNT structures. The influence of synthesis time on CNT yield from literature increases with increasing time [40-44]. This is evident from studies by Niu et al. [40], where at 2 minutes, isolated and short SWCNT with high defects and poor quality were obtained while CNTs with lesser defects were achieved for synthesis carried out in 30 minutes. Conversely, it has been observed that CNTs obtained after much longer synthesis time were likely to possess weaker crystallinity [42]. This report stated that increasing the reaction time of synthesis led to a constant inner diameter while the outer diameter increased. The effect of temperature on synthesis of CNT using nickel substrates generated results which points toward a major synthesis of MWCNT at lower temperature and nickel thickness [45]. The temperature was varied between 900°C, 800°C and 700°C and the varied temperatures formed radical results in the CNT structure produced. The

study showed that higher temperatures supports core-shell configuration and for declining temperatures, the formation of CNT is enhanced. Toussi et al. [44] showed that when the temperature of synthesis is lower than 750°C, CNT formation was lesser; however CNT formation was higher for higher temperatures (>900°C). The best temperature for CNT growth by Toussi et al. [44] occurred between 800°C and 900°C and the optimum growth temperature was at 850°C, while Shamsudin et al. [46] obtained an optimum growth of about 99.99% at 900°C. Apart from synthesizing from high temperatures, carbon nanotubes can also be synthesized from carbonaceous solids at low temperature (450°C) [47].

In the chemical vapor deposition (CVD) method, a hydrocarbon gas which is the carbon source is used together with a metal catalyst that acts as seed for the development of CNTs. CVD takes place at a lower temperature (500-1000°C) [11]. Synthesis of CNTs is usually followed by purification, deposition and suspension in an organic solvent [12]. Using CVD method of synthesis allows more precision control of CNT orientation, lower cost and more defined product(s). The electrical properties of CNT's have been improved by synthesizing SWCNT using CVD on supported catalyst. They have proven to be semiconducting in nature and also quasi-metallic with small band gaps [20]. Selecting a proper precursor, catalyst and suitable vapor pressure optimizes the yield of growth rate and quality of produced CNTs [48].

The choice of catalyst and substrate is important for the successive growth and desired orientation of CNTs [49]. The use of transition metals as catalyst for CNT synthesis have been reported by [50-52]. The most common transition metal catalysts used are Ni, Co and Fe due to their extraordinary solubility and carbon diffusion rate. They are desirable due to high melting points and strong adhesion qualities. Higher quality nanotubes growth is obtained when Fe is used as catalyst during synthesis compared to Co and Ni. This has been attributed to its greater carbon solubility. Increasing the Fe quantity decreases the quality of the nanotubes synthesized due to general aggregation of the Fe particles. It was concluded that lower metal loading percentage is preferable for the production of better quality CNTs with identical diameters [53]. MgO and Mo have also been recognized to be an appropriate catalyst support for Fe as it produces nanotubes with enhanced graphitization, smaller and more uniform nanoparticles [50, 51]. A uniform diameter CNT was synthesized using Mn₁₂ as a catalyst precursor [54]. The diameter grown is 1.5±0.31nm and the result indicates that an adhesion strength exists which can determine the diameter of as-grown SWCNT needed for controlled synthesis [54]. Cheng et al. [55], revealed that the dimension of the catalytic particles and amount dispersed on the support was useful in controlling nanotube shape. A novel method of synthesis was reported by the authors using an improved floating catalyst approach produced by catalytically pyrolyzing benzene at 1100°C-1200°C [55].

Solid organo-metallocenes are have been used due to their metal liberating qualities which catalyzes hydrocarbon deposits efficiently [48, 56]. Alloy of metals also play a substantial role in catalyzing the growth CNTs and through them a better yield of CNTs are derived [57-60]. As more research continues on enhancing the growth of CNTs, noble metals have been discovered to effectively synthesize CNTs. However, they are most effective when their particle sizes are very small (<5nm) [48]. A robust and cost effective method of CNT synthesis was reported by Jeong et al. [17], in which catalytic particles solution and carbon sources were atomized without the use of a special heating system. This method of synthesis proved more effective than thermal pyrolysis based catalytic vapor deposition (CVD) in which there is difficulty in controlling the quantity of particles entrained in carrier gas due to steep temperature gradient between furnaces. The method also proved more effective than aerosol pyrolysis [17]. Catalytic pyrolysis involving annealing of carbonaceous solid containing cobalt has been used to synthesize MWCNT [47]. The cobalt is used as a catalyst to decompose carbonaceous solid, form carbon gas species and eventually growth of CNTs. The use of cobalt can also lead to the deposition of carbon at high temperatures and are hazardous [51]. This mentioned downside of cobalt and other transition metals motivated Abdullahi et al. [51] to use a systematic approach based on catalyst loading, pre-treatment and selection of the right operating conditions for the improvement of a monometallic catalytic system for the growth of SWCNT. High quality SWCNTs with high yield was achieved by using a 2 wt.% Fe-MgO catalyst with diameters ranging from 0.8-2.0nm.

Understanding the growth and controlling the diameter of CNT facilitates the research of new applications and basic properties of CNTs [20, 61]. The major function of a catalyst in describing the nanotube diameter synthesized by chemical vapor deposition can be seen from the investigation of the diameter distribution which shows a close connection between diameters of nanocluster nanotubes and catalysts [61]. This discovery was made when the authors Cheung et al. [61] prepared iron nanoclusters having three distinctive diameters which were utilized in the development of CNTs with comparable diameters. Diameter-controlled synthesis of SWCNT using Mn₁₂ cluster as a catalyst precursor by means of mist flow CVD has also been reported by Sun et al. [54]. The mist flow CVD was reported to be effective for the diameter controlled growth of SWCNTs. Site selective synthesis based on CVD is able to grow CNTs at controllable locations and with desired orientations on surfaces [20]. CVD are described to be effective in the production of materials which are hybrid in nature and based on CNT from various supports where superficial located growth is desired [49]. The study was on the comparison and utilization of synthetic hematite and natural nontronites as interface adaptation nanoparticles for local growth of carbon nanotubes at required support.

3. Thermal Conductivity of Carbon Nanotubes

A. Thermal conductivity in a base fluid

Thermal conductivity and heat transfer of nanofluids depends not only on the forces acting on nanoparticles, but also on particle motion and interaction with turbulent eddies [14]. Convective heat transfer can be passively improved by altering the boundary conditions, flow geometry or by increasing the thermal conductivity of the base fluid [62]. Decrease in diameter of nanoparticles brings about a more uniform temperature distribution. However, this leads to a corresponding increase in cost and complexity of nanoparticle production [63]. Previous study reveals that the thermal conductivity of fluids with sphere-shaped particles improved with an increase in the ratio of the surface area to volume ratio of the particle and volume fraction of the particles [13]. It has also been pointed that since transfer of heat takes place at the surface, nanoparticles with a wide surface area should be used. Compared to micrometer and millimeter-sized particle fluids, nanofluids have enhanced rheological properties and extended stability which makes them possess increased thermal compatibility [64]. Carbon nanoparticles are being utilized in the enhancement of the thermal conductivity of their applications [17, 64-67]. The high aspect ratio of CNTs, their special surface area and high conductivity is responsible in making them suitable for heat transfer purposes in nanofluids [64, 66]. The improved thermal conductivity is due to a well formed arrangement at the solid/liquid interface and the mode of heat conduction in nanotube suspensions [64]. Brownian motion has also been suggested to be a major phenomenon in controlling a nanofluids thermal conductivity [64].

The study by [17] considered the preparation of thermally enhanced bio-based phase change materials (PCM) by utilizing a method known as vacuum impregnation with exfoliated graphite nano-platelets. The results show a 375% improvement in thermal conductivity. There was also an improvement in the latent heat and thermal resistance. Nanomaterials added to a working fluid in a vapour compression cycle was theoretically and experimentally tested for performance and an increase of 10.5% was observed with 13.5% less energy consumption [68]. The thermal conductivity of synthetic engine oil and ethylene glycol were improved by dispersing multi-walled carbon nanotubes and measurement was carried out using the transient hot wire method [64]. The authors stated an enhancement in thermal conductivity with an increase in volume fraction. Thermal conductivity enhancements up to 12.4% was achieved for CNT/ethylene glycol suspensions at a volume fraction of 1 vol% when compared to CuO based nanoparticles. In addition, up to 30% thermal conductivity enhancement was achieved for CNT-engine oil suspension with 2 vol%. These outcomes evidently point to the fact that there exists an enhanced thermal conductivity ratios improvement with a corresponding rise in the volume fraction of CNTs and it is almost non-linear [64].

B. Thermal conductivity of MWCNT

The need to measure the intrinsic thermal properties and thermal conductivity of individual carbon nanotubes in order to get an accurate estimation prompted the study by Kim et al. [16] and Choi et al. [69]. The studies of the thermal properties of MWCNTs by taking bulk measurements had a disadvantage of yielding a joint average in a sample made of different tubes. This is as a result of the existence of various tube-tube junctions which can be an obstacle to thermal transport in bundle nanotubes [16]. These tube-tube interactions are primarily created from van der Waals forces with an exception for unique instances when local charge introduce additional electrostatic fields [70]. It was proposed that the nanotubes should touch each other over less than 2-3% of their total length in order to achieve high thermal conductivity in long MWCNT [70]. A hybridized device with MWCNT to investigate thermal transportation was developed by Kim et al [16]. A mechanical approach was used to place MWCNT on the device and this approach produced a device of nanotube structure which has the ability to quantify the thermal conductivity of individual MWCNT. The thermal conductivity reported is over 3000W/mK at room temperature. On the other hand, Choi et al. [69] placed a single CNT across the electrodes for thermal conductivity measurements using 3- ω using a combination of electric fields with an alternating current and direct current. This approach is based on selective deposition technique which has a benefit of permitting the control of single nanotube placement. The thermal conductivity was reported as 650 and 830 W/mK respectively. The technique is reported to operate on a narrow-band detection technique and is said to give better signal-to-noise ratio [71]. In order to produce reliable data on the thermal conductivity of different nanotube sizes, an outstanding measurement technique was developed based on the four-point-probe third-harmonic (3- ω) method with assistance of a focused ion beam (FIB) for electric field supply [72]. When likened to the two point probe 3- ω technique used by Choi et al. [69], the precision of the measurement is considerably improved by disregarding the contact contribution in the measurement which was previously done by annealing the nanotube samples at 600°C. The measured value for the CNTs investigated by the authors in [72] is 300 ± 20 W/mK. The variation in thermal conductivity is likely to depend on the size and type of carbon nanotube employed which results in diverse mean free paths of the energy carriers. The 3- ω technique of measuring thermal conductivity recently used by Vollebregt et al. [73], was employed to determine the thermal conductivity for a low temperature grown vertical MWCNT bundles. This is important because CNT bundles which are required to obtain a low electrical and heat resistance applications need to possess low thermal conductivity. The thermal conductivity reported was 1.7-3.5 W/mK. The disadvantage of this method is a low quality sample arising from a low growth temperature.

The notable technical difficulty in fabricating devices used by the authors from literature [16, 69, 71, 72], motivated the research by Xie et al. [74]. The authors made an estimate of the thermal conductivity of individual CNTs from the obtained thermal diffusivity measurement of MWCNT array based on a laser flash technique. The following correlation was used to determine the thermal conductivity [74]:

$$\lambda = \alpha \rho C_p \tag{3}$$

Where:

C_p Specific heat;

ρ Density; and

α Thermal diffusivity of CNT.

The thermal conductivity at room temperature was reported to be about 750W/mK and it increased smoothly with an increased temperature. Measuring the thermal conductivity of a film of MWNTs using pulsed photo-thermal reflectance technique was used by Yang et al. [75] and Samani et al. [76]. This non-contact method is said to have an advantage of having no boundary scattering due to reservoir junction which was detected in electrical junction [76]. The thermal conductivity for CNT bundle length of 10 – 50 μm and diameter 40-100 nm was measured and was found to be about 15W/mK [75] while Samani et al. [76] reported a thermal conductivity of 2586 W/mK for an individual CNT of length 2 μm and diameter 150nm. The high thermal conductivity of the individual MWCNT by Samani et al. [76] has been proposed to arise from the existence of ballistic flux of long-wave acoustic phonon, which originates from all the walls having equal contribution to thermal transport. These phonons enable heat transport in MWCNT, and are therefore an essential factor of the thermal conductivity. For novel materials for which quantitative measurements cannot be carried out, simulations involving molecular dynamics are applied. The need to comprehend the lattice thermal transport properties of carbon nanotubes for nano-electromechanical systems (NEMS) and microelectromechanical systems (MEMS) devices prompted the study by Che et al. [77] and Berber et al. [78]. The molecular dynamics (MD) approach is critical to note the influence of various defects speculative calculations and the thermal conductivity of CNT. One major concern of using MD however, is the effect of size of the simulation box as a result of the periodic boundary simulations [77]. The thermal conductivity is extracted from the Green-Kubo relationship in (4).

$$\Lambda(\omega) = \frac{1}{2\kappa_B T^2 V} \hat{C}_{jj}^q(\omega) \tag{4}$$

Where:

κ_B Boltzmann constant;

V Volume;

T Temperature of the sample; and

\hat{C}_{jj}^q Quantum canonical correlation function.

The thermal conductivity obtained was 950 W/mK along the tube axis and 5.6 W/mK in a perpendicular direction to the tube.

C. Thermal conductivity in SWCNT

The thermal conductivity of SWCNTs from most studies in literature have been seen to depend on several CNT parameters ranging from nanotube length, simulation method for free boundary and periodic boundary conditions [79, 80]; temperature [81, 82]; axial strain [83]; radius and chirality of the tube [84], defect influence [77] and interaction between the nanotube with the substrate [85]. Several other studies also emphasized the fact that dependence of thermal conductivity below 30K is reliant on phonons rather than electrons [81]. Table 1 lists the thermal conductivity and measurements of SWCNT from literature.

Table 1. Thermal conductivity of carbon nanotube from literature

Author	Thermal conductivity technique	Result
Hone et al. [81]	Measured using a comparative method. Temperature drops are measured using constatan rod.	Room temperature thermal conductivity of 1750-5800W/mK
Che et al. [77]	Empirical bond under dependent force field, based on equilibrium molecular dynamics simulation.	950W/mK (Nanotube bundle along tube axis) 5.6W/mK (nanotube bundle perpendicular to the tube)
Silotia et al. [86]	A suitable form of relaxation time that represents phonon-phonon scattering and interaction with an appropriate anisotropic dynamical model.	At increased temperatures thermal conductivity in SWNT ropes tends towards that of a two-dimensional material while at lower temperatures, it behaves as a quasi-two-dimensional material because of the curvature of graphene sheets
Duzynska et al. [87]	Optothermal technique.	26W/mK at 300K 9W/mK at 450K

Li-Jun et al. [88]	Physical property measurement system (PPMS, from Quantum design Corporation).	650W/mK at 100K decreases to 480W/mK and keeps almost constant from 100-300K
Osman and Strivastava [89]	Molecular dynamics simulations.	The thermal conductivities beginning from 100K first show a peaking behaviour after which it drops off at higher temperatures.
Gu and Chen [90]	Analysis of all possible combining and splitting Umklapp scattering process based on total phonon dispersion relations.	474W/mK at 300K
Berber et al. [78]	Molecular dynamics simulations using the Tersoff potential, augmented by Van der Waals interaction in graphite.	6000W/mK at room temperature for an isolated (10,10)
Pan et al. [91]	Non-equilibrium molecular dynamics method with Brenner II potential.	The thermal conductivity at 300K of (10,0) is 237W/mK
Lukes and Zhong [79]	Molecular dynamics simulation	Thermal conductivity improvement with nanotube length, from about 10 W/m to 375 W/m K
Pop et al. [92]	Joule self-heating.	3,500W/mK at room temperature
Saavin et al. [85]	Molecular dynamics simulations centered on the green Kubo formalism.	360W/mK and 88W/mK

Hence, an in-depth knowledge of the principle of conduction of heat in SWCNTs comprises studying the variance between the different phonon modes and to determine which types of phonon modes play the governing role.

D. Temperature dependent thermal conductivity of single-walled carbon nanotubes

The thermal conductivity of SWCNT measured by [81] was focused on the low temperature range (<100K), which had a linear behavior. At this low temperature, a small diameter most probably affects the phonon properties of single-walled carbon nanotubes [81, 82]. A significant decrease in thermal conductivity was observed as the temperature decreased (Fig. 1). The results from the studies revealed an intrinsic thermal conductivity of nanotube bundles rather than sample dependent effects like joints between bundles. Cao et al. [82] reported a peak behavior at about 85K accompanied by a rapid decrease in the temperature dependent thermal conductivity which is caused by the Umklapp scattering freezing out. The peak behavior will shift to higher temperatures as diameter increases while neglecting dependence on tube chirality [89]. This is because as the temperature improved, the Umklapp scattering which is strong becomes more effective due to the thermal population of higher-energy phonons (Fig. 2) [82].

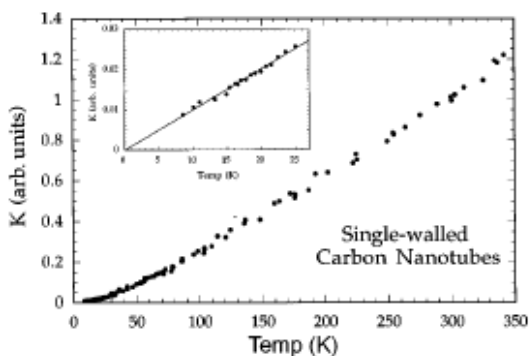


Fig. 1. Thermal conductivity of SWNT as a function of temperature [81].

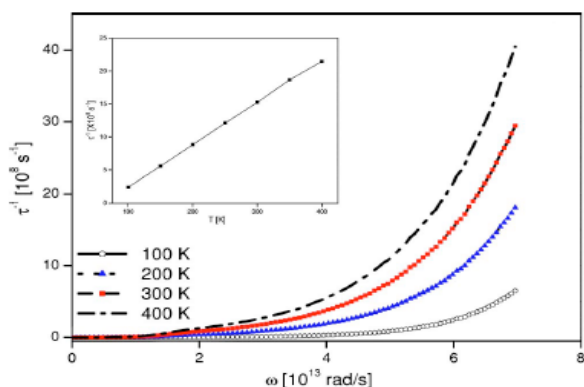


Fig. 2. Relaxation rates of Umklapp process of (6,0) SWNT [82].

Silotia et al. [86] attempted to make an explanation of the experimental variation in temperature in the thermal conductivity stated by Hone et al. [81] using a theoretical anisotropic model. The thermal conductivity centered on the studied model is given as:

$$\kappa = \frac{B_c^2 \theta_{D,eff}^2}{\hbar^2 (6\pi^2 n)^{2/3}} \frac{\pi \hbar}{B_c} \theta_{D,eff}^{d-1} \frac{1}{3} \times I \quad (5)$$

Where: \hbar is the Planck's constant, B_c is Boltzmann constant and $\theta_{D,eff}$ is the efficient temperature. The anisotropic model is used because other models like Debye and the extended Debye model do not take into account the presence of the anisotropic nature of SWCNT especially at low temperatures below 30K. In addition, the anisotropic model illuminates in detail the variation in temperature of specific heat for the entire temperature range of 2-300K [86]. The thermal conductivity involves phonon-phonon interaction and phonon-phonon scattering that produces phonon relaxation time τ or phonon mean free path l . Figure 3 shows the thermal conductivity measurements by [86]. From the Figure, it is observed that the highest thermal conductivity was observed at the highest temperature (350°K) and the lowest conductivity at the lowest temperature (8°K).

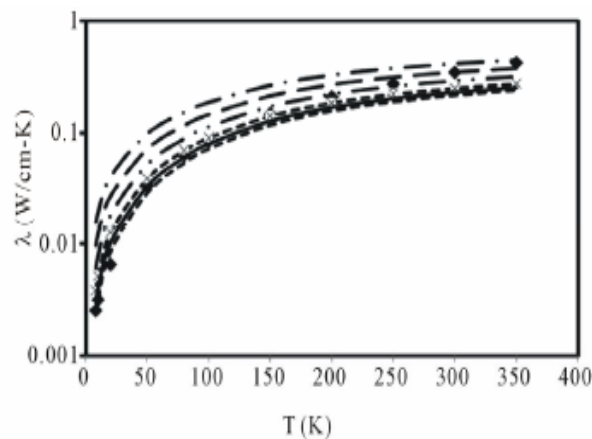


Fig. 3. Thermal conductivity of SWCNT in the temperature range 8-350 at different diameters (0.7, 0.75, 0.8, 0.9, 1, and 1.1,) [86].

At 100K, a clear peak was observed in the study carried out by Li-Jun et al. [88], which gradually decreases with an increasing temperature till it gets to 200K and from 200K-300K, the temperature becomes constant. This behavior is said to be due to the temperature dependent property of phonon. At low temperature, the phonon relaxation time is inversely proportional to the temperature which translates into a decrease in thermal conductivity with increasing temperature. However at high temperatures, phonon-phonon scattering contributes to the phonon-decay and shows no temperature dependence (the thermal conductivity is constant) [88]. This peaking behavior is also seen in the studies by Osman and Srivastava [89]. It was observed by the authors that the peak changes to greater temperatures with increasing diameter of nanotube which is due to the beginning of Umklapp scattering, which is said to lower the thermal conductivity at greater temperatures, and also depends on nanotube radius. The peak in this study occurred at 400K and then a drop followed at 500K. Recently a technique known as opto-thermal method was used to determine the intrinsic thermal conductivity and interfacial thermal

conductance on thin nanotube films deposited on silicon substrates as a function of temperature in the range 300-450K [87]. The tube diameter was in the range of 1.2-1.7nm with a mean length of 1 μ m. The value of K was found to decrease non-linearly by nearly 60%. This was due to the increase of multi phonon scattering at higher temperatures. The thermal conductivity decreased from 26.4 to 9.2W/mK in the temperature range of 300-450K.

The thermal conductivity in higher temperature range of 300-800K has been determined by [92] using reverse fitting based on an existing electro-thermal transport model. The results indicated a restrained decrease in the thermal conductivity of SWCNT close to the extreme end of the temperature range inversely proportional to T^2 . The presence of Umklapp phonon-phonon scattering that leads to a temperature dependence of $1/T$ is seen from the graph. In addition, at the upper end of the graph can be seen a drop in thermal conductivity at a rate sharper than $1/T$. The reason given to this is the effect of second order scattering process with scattering rates proportional to T^2 . At the low end of the temperature range, a levelling of thermal conductivity was observed signifying a shift towards thermal transportation restricted by phonon boundary scattering as a result of the limited sample size as seen in Fig. 4.

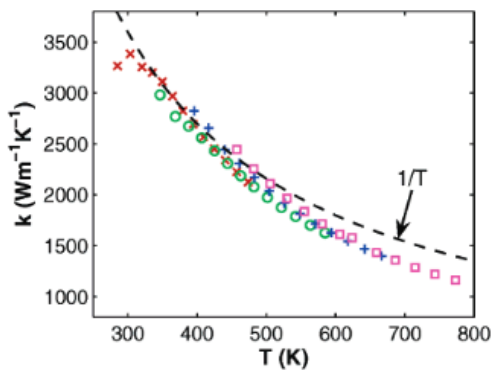


Fig. 4. Thermal conductivity of SWCNT in the temperature range 300-800K [92].

4. The Effect of Substrates on the Thermal Conductivity of SWCNT

The question arose on whether the thermal conductivity of SWCNTs was related to the effects of substrates [85]. This question was answered by carrying out a straight modelling of the heat transfer by using molecular dynamics models and also by studying the equilibrium multi-particle dynamics which is centered on the Green-Kubo formula. The study discovered a finite conductivity for nanotubes that were placed on substrates unlike remote carbon nanotubes that displayed an unusual thermal conductivity. The mean free path that is conducted by heat is larger or of the same order for the Knudsen number ($Kn > 1$) and of the nanotube length. This show the relations of CNT with a substrate can radically alter the character of thermal conductivity which is as a result of the

presence of a constricted gap at the extremity of the frequency spectrum of acoustic phonons.

5. The Role of Phonon-phonon Scattering in Carbon Nanotubes

Heat conduction by phonons is an general process that encompasses an extensive scope of physics and plays a critical role in applications ranging from LED lighting to space power generation [93]. Acoustic phonons play a dominant role in phonon state [81, 82, 92]. Additional phonon mode, scattering process and rolling-up of graphene sheets have major outcome on the temperature dependence of the thermal conductivity at both high and low temperature [81, 86]. In a perfect isolated SWCNT, an analysis of the physical mechanics can be carried out using phonon relaxation rate which is majorly controlled by three-phonon Umklapp scattering process and boundary scattering [82, 90]. The Umklapp process is made up of the combining process and the splitting process which both contribute to thermal resistance. The total relaxation time can be derived from Matthiessen's rule and given as [82]:

$$\frac{1}{\tau} = \frac{1}{\tau_B} + \frac{1}{\tau_U} \quad (6)$$

$$\text{With } \frac{1}{\tau_U} = \frac{1}{c_p} + \frac{1}{s_p},$$

Therefore the total relaxation rate can be rewritten as:

$$\frac{1}{\tau} = \frac{1}{\tau_B} + \frac{1}{c_p} + \frac{1}{s_p} \quad (7)$$

Where τ_U is the three-phonon Umklapp scattering process and τ_B is the relaxation time for boundary scattering. It was observed that there exists additional low lying doubled over phonon subdivisions as the tubes diameter increases which invariably contributes to thermal conductivity. The use of complete dispersion relations for SWCNT by Gu and Chen [90], concentrated on the three-phonon interactions to derive thermal conductivity. Han [94] has shown that the relaxation rate of Umklapp process is obtained from the given lattice characteristics and dispersion data. Because the role of low frequency phonon is more intense compared to that of high frequency, the combining process has been assumed to be of greater importance than the splitting process in the assessment of thermal resistance.

The combining process and the splitting process respectively satisfy the selection rule:

$$q + q' = q'' + G \quad (8)$$

$$q = q' + q'' + G \quad (9)$$

Where q, q', q'' are phonon wave vectors and G is the reciprocal-lattice vector [90]. From equation (9), the rate of relaxation for the three-phonon Umklapp process can be given as [90]:

$$\frac{1}{\tau} = \frac{4h\gamma^2}{3\rho l v^2} \sum_{j'=1-N/2}^{N/2} \sum_{p'=1}^6 \frac{\omega \omega' \omega''}{v_g} \delta(\delta_\omega) N(\omega', \omega'') \quad (10)$$

The thermal conductivity calculated for the tube was found to be 474 W/m K at 300 K. The outcome of orderly functionalization on the thermal conductivity of SWCNT at 300K was carried out by [91] using a non-equilibrium molecular dynamics (NEMD) simulations. The simulation was carried out to find the character of the thermal conductivity by means of decorated hydrogen atoms. This was done by calculating the phonon power spectra of the SWCNTs from Fourier transform of the velocity autocorrelation function. From Fourier’s equation, the thermal conductivity is defined thus:

$$J = -\lambda \nabla T \tag{11}$$

Where: T and J is the resulting heat flux density and ∇T is the gradient of the temperature. The results show that the functionalized CNTs show considerably lesser thermal conductivity than pristine CNT (CNT with attached hydrogen). It was also ascertained that there exists more repressed axial phonon modes of the unsystematically functionalized SWCNTs than the systematic functionalized tube. The atoms of hydrogen which attach to the CNTs act as defects which consequently decrease the thermal conductivity. The study of the phonon spectra shows that the density of phonon modes is considerably altered for functionalized tubes, which leads to the suppression of some vibrational modes and a decrease in the length of phonon scattering. This results in the degeneration of thermal conductivity. At room temperature, the phonon-phonon Umklapp scattering is negligible and therefore the phonon transport is nearly ballistic with the phonons having only a small number of scattering events between the thermal reservoirs. This feature is not present in bulk measurements of MWCNT which is conceivably because of the added extrinsic phonon scattering mechanisms like tube-tube interactions [16].

6. Viscosity of Carbon Nanotubes Based Nanofluids

Since the advent of carbon nanotubes, it has been shown that the thermo-physical properties of base fluids like water and ethylene glycol can be enhanced by adding carbon nanoparticles in precise quantity. Nanofluid viscosity is a crucial property for uses involving flow of fluid and it determines the pumping power [95]. Changing the viscosity of a base fluid by adding nanoparticles can lead to a direct impact of the systems overall efficiency. The viscosity of CNT nanofluid is dependent on the temperature, shear rate for different nanotube concentration and agglomeration effects on rheological characteristics [96].

Table 2. Viscosity measurements of CNT nanofluid from literature

Sadri et al. [97]	Rotational rheometer	15,30 and 45°C	Nanofluid viscosity improved with increasing sonication time up to a maximum value and then decreased with further increase in sonication time.
Halefadl et al. [95]	Stress controlled rheometer in a cone and plate configuration.	40°C	Results show that the shear viscosity increases with nanotube concentration for a specific shear rate
Jo and Banerjee [96]	A rotational rheometer and a cone and plate test.	Fixed temperature of 550°C	Nanofluid viscosity is significantly enhanced up to 93% in the concentration of 2wt%
Aladag et al. [98]	Stress controlled rheometer	2-10°C	Viscosity of the CNT suspension decreases when the shear rate increases
Vakili-Nezhaad and Dorany [99]	Bohlin CVO rheometer (Malvern Instrument).	Between 24°C and 100°C.	Enhancement of the viscosity index is 14.11%

A. Shear rate and temperature effects on the viscosity of CNT nanofluids

The study by Aladag et al [98] investigated the influence of temperature on viscosity for CNT/Water and Al₂O₃/Water nanofluids at small concentration and for a temperature range of 2-10°C. The effect of pressure drop and viscosity is important and should to be taken into consideration when used in low temperature application like air conditioning systems. The rheological study was carried out by observing the hysteresis phenomenon. The results showed that viscosity increased when the temperature decreased as shown in Fig. 5, and also the

Author	Viscosity measurement technique	Temperature	Results
--------	---------------------------------	-------------	---------

behavior of the CNT suspension was described as non-Newtonian shear thinning fluid when observed in the experimental condition of the study. Similarly results by Sadri et al [97] indicates a decline in viscosity when temperature was increased (Fig. 6). The study [97] also reported that MWCNT/water based nanofluids behaved as a non-Newtonian fluid. This is because the dynamic viscosity differs as a result of an increase in shear rate. The result of shear thinning effects from the two studies discussed can be credited to realignment of the clusters in the direction of the shearing flow due to the formation of primary particles and the de-aggregation of the nanotube clusters leading to a less viscous force [98],[95].

A recent study has shown that using molten salt as base fluid was advantageous for high temperature applications like concentrated solar power (CSP) [100]. This gave way to the studies by Jo et al [96], who investigated the rheological behavior of CNT dispersed in molten salts under high temperature. A highly non-linear rheological behavior was observed, typical of shear thinning liquid which was more distinct for increased mass concentrations of the nanoparticle. A non-Newtonian behavior was observed in low shear rate region, consistent with literature. The viscosity of the base fluid was significantly enhanced by doping MWCNT which is likely attributed to the agglomeration of the nanotubes [96].

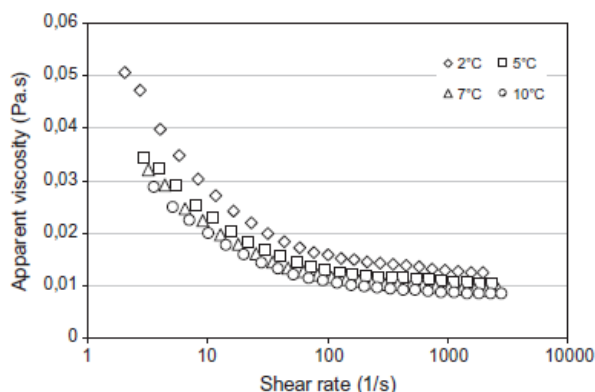


Fig. 5. Influence of temperature apparent viscosity versus shear rate of CNT nanofluid [98].

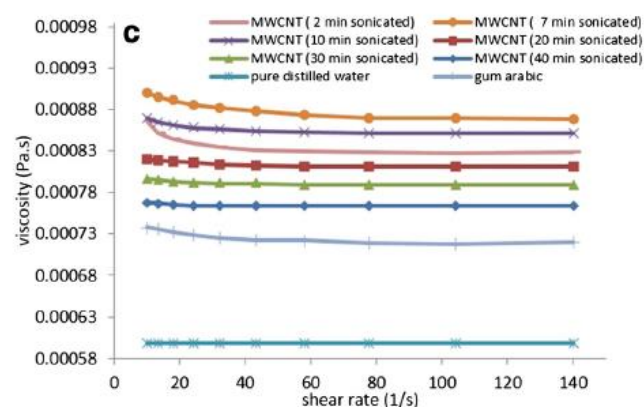
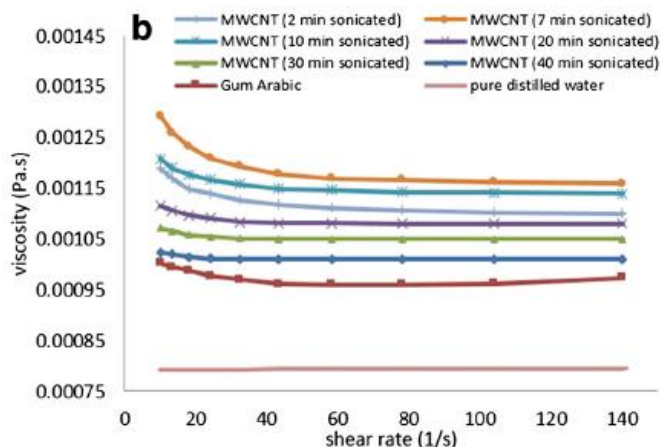
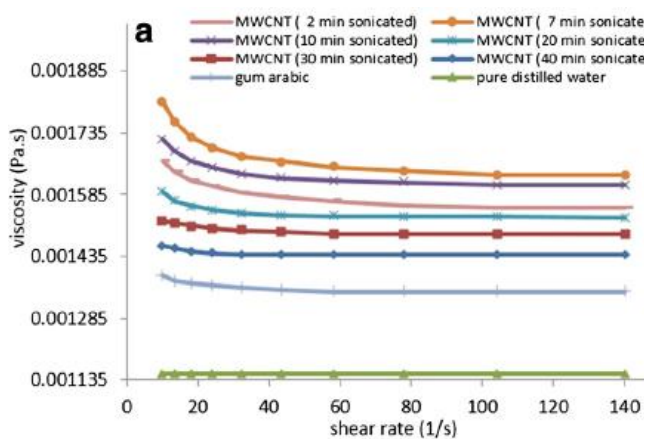


Fig. 6(a,b,c). Dynamic viscosity vs shear rate at various times of sonication [97]

B. The role of surfactant on the viscosity of CNT

Halefadl et al [95] reported results on the experimental investigation on the rheological properties of CNT water based nanofluids stabilized by sodium dodecyl benzene sulfonate (SDBS) as surfactant. The shear viscosity of the base fluids slowly decreases with the decrease of SDBS volume fraction.

C. The effect of particle volume fraction on the viscosity of CNT nanofluid

Nanofluids sample prepared from volume fraction 0.278%, 0.111%, 0.055% and 0.0055% respectively tested at 20,30 and 40°C respectively shows that nanofluids with particle concentration of 0.278% and 0.111% behaved as shear thinning fluids [101]. The shear thinning region was up to 200S^{-1} ; for higher shear rate, the viscosity tends to a Newtonian plateau. For lower particle content (0.055% and 0.0055%) however, the nanotube behaved in a Newtonian manner [101]. Experimental results by Vakili Nezhaad [99] shows that the kinematic viscosity of nanofluids was improved with decline in the temperature and increase in the concentration of MWCNT concentration. It was also pointed out from the studies that a non-linear relationship existed between MWCNT concentration, viscosity and temperature.

7. Discussion and Conclusion

Carbon nanotubes undoubtedly are an intriguing next generation materials, which are being continuously improved upon for application in diverse areas including chemical, mechanical and electrical systems. Their synthesis, growth and application is an area of active research.

From literature, significant milestones have been achieved in the field of CNT synthesis with a focus on CVD. Synthesis parameters have been shown to have a direct output on the shape and morphology of as-grown CNTs. The parameters include precursor, synthesis time, temperature, diameter, among others. The inconsistent heat transfer properties such as thermal conductivity of CNTs are attributed to the various conditions such as temperature, diameter, length, and the morphology of growth of the CNT. The present review validates the similarities in the thermal behavior of MWCNTs and graphite. The thermal conductivity of multiwalled carbon nanotubes can be modelled by making assumptions on the parameters and properties of graphite, even though it is probable that the interlayer coupling in multiwalled carbon nanotubes could be different than it is in graphite. It was also presented that the phonon confinement effects in MWCNTs are significant only at very low temperatures. At these temperatures, the thermal conductivity in SWCNT is dominated by phonon boundary scattering. A linear temperature profile exists at low temperatures less than 80K but shows peak behavior at 85K and falls off at higher temperatures.

Past studies on viscosity shows that viscosity can be enhanced by increasing the CNT concentration and decreasing temperature. In addition CNT/water nanofluids act as non-Newtonian fluid since the dynamic viscosity varies accordingly with a corresponding increase in shear rate.

Acknowledgement

The authors wish to acknowledge the supports from NRF of South Africa and the College of Agriculture, Engineering and Science of the University of KwaZulu-Natal, South Africa.

References

- [1] M. R. Kamesh and D. Madhu, "Effect of Nanoparticles on the Emissions of a CI Engine," *International Journal of Renewable Energy Research*, Journal vol. 7, no. 2, 2017.
- [2] I. Carlucci, G. Mutani, and M. Martino, "Assessment of potential energy producible from agricultural biomass in the municipalities of the Novara plain," in *Renewable Energy Research and Applications (ICRERA), 2015 International Conference on*, 2015, pp. 1394-1398: IEEE.
- [3] Y. İ. Tosun, "5MW hybrid power generation with agriculture and forestry biomass waste co-incineration in stoker and subsequent solar panel (CSP) ORC station," in *Renewable Energy Research and Applications (ICRERA), 2015 International Conference on*, 2015, pp. 583-589: IEEE.
- [4] Y. İ. Tosun, "The proposed design of co-combustion stoker for Şırnak agricultural biomass waste and Şırnak asphaltite in 35MW electricity production," in *Renewable Energy Research and Applications (ICRERA), 2015 International Conference on*, 2015, pp. 358-363: IEEE.
- [5] O. Nakagoe, Y. Furukawa, S. Tanabe, Y. Sugai, and R. Narikiyo, "Hydrogen production from steam reforming of woody biomass with cobalt catalyst," in *Renewable Energy Research and Applications (ICRERA), 2012 International Conference on*, 2012, pp. 1-4: IEEE.
- [6] S. Mohapatra and K. Gadgil, "Biomass: The Ultimate Source of Bio Energy," *International Journal of Renewable Energy Research*, vol. 3, no. 1, p. 4, 2013 2013.
- [7] M. Ahiduzzaman and A. S. Islam, "Assessment of Rice Husk Briquette Fuel Use as an Alternative Source of Wood Fuel," *international Journal of Renewable Energy Research*, vol. 6, no. 4, 2016.
- [8] D. D. Guta, "Assessment of biomass fuel resource potential and utilization in Ethiopia: sourcing strategies for renewable energies," *International Journal of Renewable Energy Research (IJRER)*, vol. 2, no. 1, pp. 131-139, 2012.
- [9] G. Di Giacomo and L. Taglieri, "Development and evaluation of a new advanced solid bio-fuel and related production process," *International Journal of Renewable Energy Research (IJRER)*, vol. 3, no. 2, pp. 255-260, 2013.
- [10] K. A. Fayemiwo, S. H. Awojide, and C. A. Beckley, "Potential Use of Jatropha Curcas Stem for Ethanol Production," *International Journal of Renewable Energy Research (IJRER)*, vol. 3, no. 1, pp. 68-72, 2013.
- [11] S. K. Das, S. U. Choi, W. Yu, and T. Pradeep, *Nanofluids: science and technology*. John Wiley & Sons, 2007.
- [12] X. Qi, C. Qin, W. Zhong, C. Au, X. Ye, and Y. Du, "Large-Scale Synthesis of Carbon Nanomaterials by Catalytic Chemical Vapor Deposition: A Review of the Effects of Synthesis Parameters and Magnetic Properties," *Materials*, vol. 3, no. 8, pp. 4142-4174, 2010.
- [13] S. U. S. Choi and J. A. Eastman, *Enhancing thermal conductivity of fluids with nanoparticles*. 1995, p. Medium: ED; Size: 8 p.
- [14] S.-S. Choi, "Nanofluid technology: current status and future research," Argonne National Lab., IL (US)1998.
- [15] S. Sharma, P. Ranjan, S. Das, S. Gupta, R. Bhati, and A. Majumdar, "Synthesis of Carbon Nanotube Using Olive Oil and its Application in Dye Sensitized Solar Cell," *Intenational Journal*

- of *Renewable Energy Research*, vol. 2, no. 2, 2012.
- [16] P. Kim, L. Shi, A. Majumdar, and P. L. McEuen, "Thermal Transport Measurements of Individual Multiwalled Nanotubes," *Physical Review Letters*, vol. 87, no. 21, 2001.
- [17] S.-G. Jeong, O. Chung, S. Yu, S. Kim, and S. Kim, "Improvement of the thermal properties of Bio-based PCM using exfoliated graphite nanoplatelets," *Solar Energy Materials and Solar Cells*, vol. 117, pp. 87-92, 2013.
- [18] M. R. Snowdon, A. K. Mohanty, and M. Misra, "A Study of Carbonized Lignin as an Alternative to Carbon Black," *ACS Sustainable Chemistry & Engineering*, vol. 2, no. 5, pp. 1257-1263, 2014.
- [19] J. Prasek et al., "Methods for carbon nanotubes synthesis—review," *Journal of Materials Chemistry*, vol. 21, no. 40, pp. 15872-15884, 2011.
- [20] H. Dai, "Carbon nanotubes: synthesis, integration, and properties," *Accounts of chemical research*, vol. 35, no. 12, pp. 1035-1044, 2002.
- [21] H. Li, X. He, Y. Liu, H. Yu, Z. Kang, and S.-T. Lee, "Synthesis of fluorescent carbon nanoparticles directly from active carbon via a one-step ultrasonic treatment," *Materials Research Bulletin*, vol. 46, no. 1, pp. 147-151, 2011.
- [22] B. Zhang, C. y. Liu, and Y. Liu, "A Novel One-Step Approach to Synthesize Fluorescent Carbon Nanoparticles," *European Journal of Inorganic Chemistry*, vol. 2010, no. 28, pp. 4411-4414, 2010.
- [23] B. De and N. Karak, "A green and facile approach for the synthesis of water soluble fluorescent carbon dots from banana juice," *Rsc Advances*, vol. 3, no. 22, pp. 8286-8290, 2013.
- [24] S. Manafi, M. Amin, M. Rahimpour, E. Salahi, and A. Kazemzadeh, "High-yield synthesis of multiwalled carbon nanotube by mechanochemical method," *Nanoscale research letters*, vol. 4, no. 4, pp. 296-302, 2009.
- [25] A. Szabó, C. Perri, A. Csató, G. Giordano, D. Vuono, and J. B. Nagy, "Synthesis methods of carbon nanotubes and related materials," *Materials*, vol. 3, no. 5, pp. 3092-3140, 2010.
- [26] Ö. Güler and E. Evin, "Carbon nanotubes formation by short-time ball milling and annealing of graphite," *Optoelectronics And Advanced Materials*, vol. 6, no. 1-2, pp. 183-187, 2012.
- [27] M. J. Rak, T. Friscic, and A. Moores, "Mechanochemical synthesis of Au, Pd, Ru and Re nanoparticles with lignin as a bio-based reducing agent and stabilizing matrix," *Faraday Discuss*, vol. 170, pp. 155-67, 2014.
- [28] K. Xu et al., "Controllable synthesis of single-and double-walled carbon nanotubes from petroleum coke and their application to solar cells," *Carbon*, vol. 68, pp. 511-519, 2014.
- [29] O. V. Kharissova, H. V. Dias, B. I. Kharisov, B. O. Perez, and V. M. Perez, "The greener synthesis of nanoparticles," *Trends Biotechnol*, vol. 31, no. 4, pp. 240-8, Apr 2013.
- [30] J. Qu, C. Luo, Q. Cong, and X. Yuan, "Carbon nanotubes and Cu-Zn nanoparticles synthesis using hyperaccumulator plants," *Environmental chemistry letters*, vol. 10, no. 2, pp. 153-158, 2012.
- [31] J. Qu, C. Luo, and X. Yuan, "Synthesis of hybrid carbon nanotubes using Brassica juncea L. application to photodegradation of bisphenol A," *Environmental Science and Pollution Research*, vol. 20, no. 6, pp. 3688-3695, 2013.
- [32] J. Zhu, J. Jia, F. L. Kwong, D. H. L. Ng, and S. C. Tjong, "Synthesis of multiwalled carbon nanotubes from bamboo charcoal and the roles of minerals on their growth," *biomass and bioenergy*, vol. 36, pp. 12-19, 2012.
- [33] A. K. Mittal, Y. Chisti, and U. C. Banerjee, "Synthesis of metallic nanoparticles using plant extracts," *Biotechnol Adv*, vol. 31, no. 2, pp. 346-56, Mar-Apr 2013.
- [34] R. Tsao, "Chemistry and biochemistry of dietary polyphenols," *Nutrients*, vol. 2, no. 12, pp. 1231-46, Dec 2010.
- [35] X. He, H. Li, Y. Liu, H. Huang, Z. Kang, and S.-T. Lee, "Water soluble carbon nanoparticles: hydrothermal synthesis and excellent photoluminescence properties," *Colloids and Surfaces B: Biointerfaces*, vol. 87, no. 2, pp. 326-332, 2011.
- [36] P. Gonugunta, S. Vivekanandhan, A. K. Mohanty, and M. Misra, "A study on synthesis and characterization of biobased carbon nanoparticles from lignin," *World Journal of Nano Science and Engineering*, vol. 2, no. 03, p. 148, 2012.
- [37] V. Roshni and D. Ottoor, "Synthesis of carbon nanoparticles using one step green approach and their application as mercuric ion sensor," *Journal of Luminescence*, vol. 161, pp. 117-122, 2015.
- [38] T. A. Hassan, V. K. Rangari, V. Fallon, Y. Farooq, and S. Jeelani, "Mechanochemical and sonochemical synthesis of bio-based nanoparticles," in *Proceedings of the Nanotechnology Conference*, 2010, pp. 278-281.
- [39] T. S. Syamsudin, E. M. Alamsyah, and B. S. Purwasmita, "Synthesis of Bio-based Nanomaterial from Surian (*Toona sinensis* Roem) Wood Bark Using Conventional Balls Milling Method and its Characterization," *Journal of Biological Sciences*, vol. 14, no. 3, p. 204, 2014.
- [40] Z. Niu and Y. Fang, "Effects of synthesis time for synthesizing single-walled carbon nanotubes over Mo-Fe-MgO catalyst and suggested growth mechanism," *Journal of crystal growth*, vol. 297, no. 1, pp. 228-233, 2006.
- [41] S. D. Mhlanga, K. C. Mondal, R. Carter, M. J. Witcomb, and N. J. Coville, "The effect of

- synthesis parameters on the catalytic synthesis of multiwalled carbon nanotubes using Fe-Co/CaCO₃ catalysts," *South African Journal of Chemistry*, vol. 62, pp. 67-76, 2009.
- [42] W. Zhao, H. S. Kim, H. T. Kim, J. Gong, and I. J. Kim, "Synthesis and Growth of Multi-Walled Carbon Nanotubes (MWNTs) by CCDV Using Fe-Supported Zeolite Templates," *Journal of Ceramic Processing Research*, vol. 12, no. 4, pp. 392-397, 2011.
- [43] E. Dündar-Tekkaya and N. Karatepe, "Effect of reaction time, weight ratio, and type of catalyst on the yield of single-wall carbon nanotubes synthesized by chemical vapor deposition of acetylene," *Fullerenes, Nanotubes and Carbon Nanostructures*, vol. 23, no. 6, pp. 535-541, 2015.
- [44] S. M. Toussi, A. Fakhru'l-Razi, and A. Suraya, "Optimization of Synthesis Condition for Carbon Nanotubes by Catalytic Chemical Vapor Deposition (CCVD)," in *IOP Conference Series: Materials Science and Engineering*, 2011, vol. 17, no. 1, p. 012003: IOP Publishing.
- [45] D. Lopez, I. Abe, and I. Pereyra, "Temperature effect on the synthesis of carbon nanotubes and core-shell Ni nanoparticle by thermal CVD," *Diamond and Related Materials*, vol. 52, pp. 59-65, 2015.
- [46] M. Shamsudin, N. Asli, S. Abdullah, S. Yahya, and M. Rusop, "Effect of synthesis temperature on the growth iron-filled carbon nanotubes as evidenced by structural, micro-Raman, and thermogravimetric analyses," *Advances in Condensed Matter Physics*, vol. 2012, 2012.
- [47] Y. Jiang and C. Lan, "Low temperature synthesis of multiwall carbon nanotubes from carbonaceous solid prepared by sol-gel autocombustion," *Materials Letters*, 2015.
- [48] M. Kumar, "Carbon Nanotube Synthesis and Growth Mechanism " in *Carbon Nanotubes - Synthesis, Characterization, Applications*, D. S. Y. (Ed.), Ed.: InTech, 2011, p. 514.
- [49] Š. Kavecký, J. Valúchová, M. Čaplovičová, S. Heissler, P. Šajgalík, and M. Janek, "Nontronites as catalyst for synthesis of carbon nanotubes by catalytic chemical vapor deposition," *Applied Clay Science*, vol. 114, pp. 170-178, 2015.
- [50] Y. Li, J. Liu, Y. Wang, and Z. L. Wang, "Preparation of monodispersed Fe-Mo nanoparticles as the catalyst for CVD synthesis of carbon nanotubes," *Chemistry of Materials*, vol. 13, no. 3, pp. 1008-1014, 2001.
- [51] I. Abdullahi, N. Sakulchaicharoen, and J. E. Herrera, "Selective synthesis of single-walled carbon nanotubes on Fe-MgO catalyst by chemical vapor deposition of methane," *Diamond and Related Materials*, vol. 41, pp. 84-93, 2014.
- [52] G. Allaedini, S. M. Tasirin, and P. Aminayi, "Synthesis of CNTs via chemical vapor deposition of carbon dioxide as a carbon source in the presence of NiMgO," *Journal of Alloys and Compounds*, vol. 647, pp. 809-814, 2015.
- [53] W.-W. Liu, A. Aziz, S.-P. Chai, A. R. Mohamed, and U. Hashim, "Synthesis of single-walled carbon nanotubes: Effects of active metals, catalyst supports, and metal loading percentage," *Journal of Nanomaterials*, vol. 2013, p. 63, 2013.
- [54] Y. Sun, T. Nakayama, and H. Yoshikawa, "Synthesis of uniform single-wall carbon nanotubes using Mn₁₂ clusters as the catalyst precursor," *Diamond and Related Materials*, vol. 56, pp. 42-46, 2015.
- [55] H. Cheng et al., "Large-scale and low-cost synthesis of single-walled carbon nanotubes by the catalytic pyrolysis of hydrocarbons," *Applied Physics Letters*, vol. 72, no. 25, pp. 3282-3284, 1998.
- [56] M. Kumar and Y. Ando, "Chemical vapor deposition of carbon nanotubes: a review on growth mechanism and mass production," *Journal of nanoscience and nanotechnology*, vol. 10, no. 6, pp. 3739-3758, 2010.
- [57] A. L. M. Reddy, M. Shaijumon, and S. Ramaprabhu, "Alloy hydride catalyst route for the synthesis of single-walled carbon nanotubes, multi-walled carbon nanotubes and magnetic metal-filled multi-walled carbon nanotubes," *Nanotechnology*, vol. 17, no. 21, p. 5299, 2006.
- [58] P. M. Parthangal, R. E. Cavicchi, and M. R. Zachariah, "A generic process of growing aligned carbon nanotube arrays on metals and metal alloys," *Nanotechnology*, vol. 18, no. 18, p. 185605, 2007.
- [59] M. Shaijumon, A. L. M. Reddy, and S. Ramaprabhu, "Single step process for the synthesis of carbon nanotubes and metal/alloy-filled multiwalled carbon nanotubes," *Nanoscale Research Letters*, vol. 2, no. 2, pp. 75-80, 2007.
- [60] F. Xu, H. Zhao, and D. T. Stephen, "Carbon nanotube synthesis on catalytic metal alloys in methane/air counterflow diffusion flames," *Proceedings of the Combustion Institute*, vol. 31, no. 2, pp. 1839-1847, 2007.
- [61] C. L. Cheung, A. Kurtz, H. Park, and C. M. Lieber, "Diameter-controlled synthesis of carbon nanotubes," *The Journal of Physical Chemistry B*, vol. 106, no. 10, pp. 2429-2433, 2002.
- [62] X.-Q. Wang and A. S. Mujumdar, "Heat transfer characteristics of nanofluids: a review," *International Journal of Thermal Sciences*, vol. 46, no. 1, pp. 1-19, 2007.
- [63] V. Khullar and H. Tyagi, "A study on environmental impact of nanofluid-based concentrating solar water heating system," *International Journal of Environmental Studies*, vol. 69, no. 2, pp. 220-232, 2012.
- [64] M.-S. Liu, M. Ching-Cheng Lin, I. T. Huang, and C.-C. Wang, "Enhancement of thermal conductivity with carbon nanotube for nanofluids," *International Communications in*

- Heat and Mass Transfer*, vol. 32, no. 9, pp. 1202-1210, 2005.
- [65] Y. Ding, H. Alias, D. Wen, and R. A. Williams, "Heat transfer of aqueous suspensions of carbon nanotubes (CNT nanofluids)," *International Journal of Heat and Mass Transfer*, vol. 49, no. 1-2, pp. 240-250, 2006.
- [66] M. Xing, J. Yu, and R. Wang, "Experimental study on the thermal conductivity enhancement of water based nanofluids using different types of carbon nanotubes," *International Journal of Heat and Mass Transfer*, vol. 88, pp. 609-616, 2015.
- [67] T. Maré, S. Halelfadl, S. Van Vaerenbergh, and P. Estellé, "Unexpected sharp peak in thermal conductivity of carbon nanotubes water-based nanofluids," *International Communications in Heat and Mass Transfer*, vol. 66, pp. 80-83, 2015.
- [68] A. M. A. Soliman, A. K. Abdel-Rahman, S. H. Taher, and S. Ookawara, "Performance Enhancement of Vapor Compression Cycle Using Nanomaterial," presented at the 4th International Conference on Renewable Energy research and Applications, Paterno, Italy, 22-25 November 2015, 2015.
- [69] T. Y. Choi, D. Poulikakos, J. Tharian, and U. Sennhauser, "Measurement of thermal conductivity of individual multiwalled carbon nanotubes by the 3ω method," *Applied Physics Letters*, vol. 87, no. 1, p. 013108, 2005.
- [70] A. E. Aliev, M. H. Lima, E. M. Silverman, and R. H. Baughman, "Thermal conductivity of multi-walled carbon nanotube sheets: radiation losses and quenching of phonon modes," *Nanotechnology*, vol. 21, no. 3, p. 035709, 2010.
- [71] L. Lu, W. Yi, and D. L. Zhang, " 3ω method for specific heat and thermal conductivity measurements," *Review of Scientific Instruments*, vol. 72, no. 7, p. 2996, 2001.
- [72] S. K. Das, S. U. Choi, and H. E. Patel, "Heat transfer in nanofluids—a review," *Heat transfer engineering*, vol. 27, no. 10, pp. 3-19, 2006.
- [73] S. Vollebregt, S. Banerjee, K. Beenakker, and R. Ishihara, "Thermal conductivity of low temperature grown vertical carbon nanotube bundles measured using the three- ω method," *Applied Physics Letters*, vol. 102, no. 19, p. 191909, 2013.
- [74] H. Xie, A. Cai, and X. Wang, "Thermal diffusivity and conductivity of multiwalled carbon nanotube arrays," *Physics Letters A*, vol. 369, no. 1-2, pp. 120-123, 2007.
- [75] D. J. Yang et al., "Thermal conductivity of multiwalled carbon nanotubes," *Physical Review B*, vol. 66, no. 16, 2002.
- [76] M. K. Samani, N. Khosravian, G. C. K. Chen, M. Shakerzadeh, D. Baillargeat, and B. K. Tay, "Thermal conductivity of individual multiwalled carbon nanotubes," *International Journal of Thermal Sciences*, vol. 62, pp. 40-43, 2012.
- [77] J. Che, T. Cagin, and W. A. Goddard III, "Thermal conductivity of carbon nanotubes," *Nanotechnology*, vol. 11, no. 2, p. 65, 2000.
- [78] S. Berber, Y.-K. Kwon, and D. Tománek, "Unusually high thermal conductivity of carbon nanotubes," *Physical review letters*, vol. 84, no. 20, p. 4613, 2000.
- [79] J. R. Lukes and H. Zhong, "Thermal Conductivity of Individual Single-Wall Carbon Nanotubes," *Journal of Heat Transfer*, vol. 129, no. 6, p. 705, 2007.
- [80] Z. Wang, D. Tang, X. Zheng, W. Zhang, and Y. Zhu, "Length-dependent thermal conductivity of single-wall carbon nanotubes: prediction and measurements," *Nanotechnology*, vol. 18, no. 47, p. 475714, 2007.
- [81] J. Hone, M. Whitney, C. Piskoti, and A. Zettl, "Thermal conductivity of single-walled carbon nanotubes," *Physical Review B*, vol. 59, no. 4, p. R2514, 1999.
- [82] J. X. Cao, X. H. Yan, Y. Xiao, and J. W. Ding, "Thermal conductivity of zigzag single-walled carbon nanotubes: Role of the umklapp process," *Physical Review B*, vol. 69, no. 7, 2004.
- [83] C. Ren, W. Zhang, Z. Xu, Z. Zhu, and P. Huai, "Thermal conductivity of single-walled carbon nanotubes under axial stress," *The Journal of Physical Chemistry C*, vol. 114, no. 13, pp. 5786-5791, 2010.
- [84] A. Nasir Imtani, "Thermal conductivity for single-walled carbon nanotubes from Einstein relation in molecular dynamics," *Journal of Physics and Chemistry of Solids*, vol. 74, no. 11, pp. 1599-1603, 2013.
- [85] A. V. Savin, Y. S. Kivshar, and B. Hu, "Effect of substrate on thermal conductivity of single-walled carbon nanotubes," *EPL (Europhysics Letters)*, vol. 88, no. 2, p. 26004, 2009.
- [86] P. Silotia, S. Dabas, A. Saxena, and S.-P. Tewari, "On the Thermal Conductivity of Single-Walled Carbon Nanotube Ropes," *Soft Nanoscience Letters*, vol. 03, no. 01, pp. 7-10, 2013.
- [87] A. Duzynska, A. Taube, K. Korona, J. Judek, and M. Zdrojek, "Temperature-dependent thermal properties of single-walled carbon nanotube thin films," *Applied Physics Letters*, vol. 106, no. 18, p. 183108, 2015.
- [88] H. Li-Jun, L. Ji, L. Zheng, Q. Cai-Yu, Z. Hai-Qing, and S. Lian-Feng, "Thermal properties of single-walled carbon nanotube crystal," *Chinese Physics B*, vol. 20, no. 9, p. 096101, 2011.
- [89] M. A. Osman and D. Srivastava, "Temperature dependence of the thermal conductivity of single-wall carbon nanotubes," *Nanotechnology*, vol. 12, no. 1, p. 21, 2001.
- [90] Y. Gu and Y. Chen, "Thermal conductivities of single-walled carbon nanotubes calculated from the complete phonon dispersion relations," *Physical Review B*, vol. 76, no. 13, 2007.

- [91] R. Pan, Z. Xu, Z. Zhu, and Z. Wang, "Thermal conductivity of functionalized single-wall carbon nanotubes," *Nanotechnology*, vol. 18, no. 28, p. 285704, 2007.
- [92] E. Pop, D. Mann, Q. Wang, K. Goodson, and H. Dai, "Thermal conductance of an individual single-wall carbon nanotube above room temperature," *Nano Lett*, vol. 6, no. 1, pp. 96-100, Jan 2006.
- [93] A. Minnich, "Advances in the measurement and computation of thermal phonon transport properties," *Journal of Physics: Condensed Matter*, vol. 27, no. 5, p. 053202, 2015.
- [94] Y.-J. Han, "Intrinsic thermal-resistive process of crystals: Umklapp processes at low and high temperatures," *Physical Review B*, vol. 54, no. 13, p. 8977, 1996.
- [95] S. Halelfadl, P. Estellé, B. Aladag, N. Doner, and T. Maré, "Viscosity of carbon nanotubes water-based nanofluids: Influence of concentration and temperature," *International Journal of Thermal Sciences*, vol. 71, pp. 111-117, 2013.
- [96] B. Jo and D. Banerjee, "Viscosity measurements of multi-walled carbon nanotubes-based high temperature nanofluids," *Materials Letters*, vol. 122, pp. 212-215, 2014.
- [97] R. Sadri et al., "An experimental study on thermal conductivity and viscosity of nanofluids containing carbon nanotubes," *Nanoscale Res Lett*, vol. 9, no. 1, p. 151, 2014.
- [98] B. Aladag, S. Halelfadl, N. Doner, T. Maré, S. Duret, and P. Estellé, "Experimental investigations of the viscosity of nanofluids at low temperatures," *Applied Energy*, vol. 97, pp. 876-880, 2012.
- [99] G. R. Vakili-Nezhaad and A. Dorany, "Investigation of the Effect of Multiwalled Carbon Nanotubes on the Viscosity Index of Lube Oil Cuts," *Chemical Engineering Communications*, vol. 196, no. 9, pp. 997-1007, 2009.
- [100] M. Schuller et al., "Molten Salt-Carbon Nanotube Thermal Energy Storage for Concentrating Solar Power Systems Final Report," DOE/GO18154; TRN: US201209%258 United States10.2172/1036948TRN: US201209%258Wed Dec 05 11:24:59 EST 2012GFOEnglish, 2012, Available: <http://www.osti.gov/scitech//servlets/purl/1036948/>.
- [101] S. Halelfadl, T. Maré, and P. Estellé, "Efficiency of carbon nanotubes water based nanofluids as coolants," *Experimental Thermal and Fluid Science*, vol. 53, pp. 104-110, 2014.

CHAPTER 3: SYNTHESIS OF CARBON NANOSPHERES FROM COCONUT FIBRE

- Part 1:** Adewumi, G.A., Revaprasadu, N., Eloka-Eboka, A.C., Inambao, F. and Gervas, C, 2017. A Facile Low-cost Synthesis of Carbon Nanosphere from Coconut Fibre. *In proceedings of the World Congress on Engineering and Computer Science 2017 Vol II WCECS* San Francisco, USA, October 25-27, 2017, pp. 577-582.
- Part 2:** Adewumi, G.A., Inambao, F., Eloka-Eboka, A.C. and Revaprasadu, N, 2018. Synthesis of Carbon Nanotubes and Nanospheres from Coconut Fibre and the Role of Synthesis Temperature on their Growth. *Journal of Electronic Materials*. <https://doi.org/10.1007/s11664-018-6248-z>. (Published)

A Facile Low-cost Synthesis of Carbon Nanosphere from Coconut Fibre

Gloria A. Adewumi, *Member, IAENG*, Neerish Revaprasadu, Andrew C. Eloka-Eboka, *Member, IAENG*, Freddie L. Inambao and Charles Gervas

Abstract— Carbon nanospheres have been synthesized using coconut fibre as a renewable feedstock in a three step process which involves pyrolyzation, physical activation and ethanol vapour treatment. The synthesis method produced nanomaterials consisting of nanospheres which have been analysed using field emission scanning electron microscope (FESEM), transmission electron microscopy (TEM), energy dispersive X-ray spectroscopy (EDX), powder x-ray diffraction (p-XRD), fourier transform infra-red spectroscopy (FTIR) and thermogravimetric analysis (TGA). Scanning Electron Microscope (SEM) investigations confirm the production of carbon nanospheres with diameter between 30nm-150nm. The synthesized carbon nanospheres can be used as base particles in nanofluids, in lithium-ion batteries and in the medical field for drug delivery.

Index Terms—, Bio-based feedstock, carbon nanospheres, coconut fibre, low-cost synthesis.

I. INTRODUCTION

ANNUALLY, 12,280 hectares of land are cultivated for coconut trees, from which 64.3 billion nuts are harvested [1]. Fibres from coconut have the highest ductility compared to other fibres obtained from vegetation sources as they have the capability of taking 4-6 times of their strain which is more than that of other fibres comprising of cellulose, hemi cellulose and lignin as major composition [2]. Coconut fibre (CF) is obtained from the pericarp of coconut fruit and a coconut is made up of 33 to 35% of husk. Presently, CF are being used as fuel in the processing of coconut-based products, as a fibre source for manufacturing ropes and mats and as a fuel for domestic application [3]. To benefit from this plentiful and low-cost agricultural waste, coconut fibre has been transformed into a carbon nanomaterial. The conversion of CF into carbon nanomaterials will function as an important raw material

Manuscript received June 22, 2017; revised June, 2017. This work was supported in part by the National Research Foundation South under Grant 109819.

G.A. Adewumi is a Doctoral candidate at the University of KwaZulu-Natal, South Africa. She is with the Mechanical Engineering Department (phone:+27749423154; e-mail: adewumigloria@gmail.com).

N. Revaprasadu is with the University of Zululand X1001, Kwadlangezwa 3886, South Africa (e-mail: revaprasadun@unizulu.ac.za).

A.C Eloka-Eboka is a Postdoctoral Fellow at the University of KwaZulu-Natal, South Africa. Dr. Eloka-Eboka is with the Mechanical Engineering Department of the (e-mail: fatherfounder@yahoo.com).

F.L. Inambao is a Professor in Mechanical Engineering at the University of KwaZulu-Natal South Africa (e-mail inambaof@ukzn.ac.za).

C. Gervas is a Doctoral fellow in Chemistry Department at the University of Zululand X1001, Kwadlangezwa 3886, South Africa (e-mail rufcharles@gmail.com).

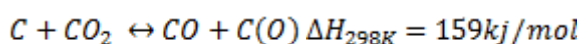
obtained from agricultural waste. Carbon is a group 14 element that is distributed very widely in nature. It also has a remarkable ability to bond with several other elements as a result of its polyvalent properties. The three allotropes of carbon are amorphous, diamond and graphite which occur naturally. Recent research has tuned carbon into nanoscale, resulting into carbon nanotubes, carbon nanofibers and carbon nanospheres.

Carbon has the remarkable capability to bond in several exceptional ways thereby creating structures with distinct properties. This can be seen in the filament-like arrangement of graphene sheets corresponding to carbon nanotubes (CNTs) and carbon nanofibres (CNFs). Heptagonal and in pentagonal pairing of carbon atoms can result in the creation of carbon nanospheres. The graphite sheets in nanospheres occur as waving flakes instead of closed shells which takes the form of the sphere, hence having several open ends at the surface and establishing carbon nanospheres (CNS) as suitable materials for catalytic and adsorption application [4].

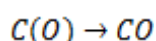
Laboratory fabrication of carbon nanospheres involve methods such as chemical vapour deposition (CVD) [5-8], hydrothermal treatment [9], pyrolysis of polymers [10], ultrasonic treatments and chlorination of cobaltocene [11]. Generally, chemical vapour deposition (CVD) occurs when rare earth metal oxides or metal oxides are used as catalysts which results in a need for purification of the synthesized carbon spheres in order to get rid of the catalyst. This makes the process limited to a small scale [12]. Various sources of biomass are being used for the production of nanomaterials derived from carbon [13, 14] because of their low toxicity and availability. These biomasses are often first carbonized, and then activated before being converted to carbon nanomaterials using different methods [15-20]. The method of activation used can either be physical (thermal), chemical or a combination of both physical and chemical processes [3]. The physical process involves the use of CO₂, steam or air and takes place at higher temperatures while the chemical process which is one-step, takes place at lower temperatures and involves the co-carbonization of a parent feedstock with a suitable chemical compound. Three chemicals, which have been frequently used, include zinc chloride, phosphoric acid and potassium hydroxide or potassium carbonate. Even though any carbon rich material can be used to produce activated carbon, the bio-mass precursor to be used has to possess factors like reliability and consistency in order to be considered sustainable [21].

A study was carried out on natural sources by Kumar *et al.* [22] as a means of synthesizing carbon nanomaterials. The study revealed the use of fossil hydrocarbons, waste natural products natural and botanical hydrocarbon

precursors as sources of hydrocarbon for CNT and graphene synthesis. Those based on fossil hydrocarbon are mostly costly and not readily accessible. In addition, a lot of the liquid and gaseous fossil hydrocarbons are explosive or toxic in nature and are not acceptable for both atmospheric and human health. On the other hand, carbon nanomaterials derived from carbon based natural precursors have the advantage of producing scalable amounts, they are safe to use in the environment, cheap and allows for fast production techniques. Activated carbon has been prepared from oil palm fibre and oil palm shell [23] using physical activation process. The process was optimized by adjusting retention time and CO₂ conditions (activation temperature, flow rate). Tan *et al.* [3] prepared activated carbon from coconut fibre using a combination of physical and chemical methods of activation made up of carbon dioxide (CO₂) gasification and potassium hydroxide (KOH) treatment. The rate of reaction between carbon [24] and carbon dioxide was inhibited by the reaction products of hydrogen and carbon monoxide. The mechanism is as follows [21, 25]:



Initially, a surface oxygen complex (C(O)) is formed, which afterwards acquires some stability under the conditions of reaction:



In this study, the authors present the results from the green synthesis and characterization of carbon nanospheres from coconut fibre biomass using a scalable, time efficient (210 mins) and cost effective process. The materials were synthesized from agricultural waste in the absence of catalysts and acids. The production of the nanospheres involved a three step technique which consists of pyrolyzation, physical activation and ethanol vapour treatment at high temperature followed by characterization using SEM, TEM, EDX, FTIR, TGA and XRD. The produced nanomaterial can be applied in thermal applications for the enhancement of heat transfer working fluids, lithium-ion battery and medical drug delivery.

II. EXPERIMENTAL METHOD

Coconut fibre used in the study was purchased from farmers in a local market in Nigeria and taken to South Africa for research studies. It was received in fibre form and was first washed then dried to reduce moisture content after which it was cut with scissors to size ranges of about 1 mm. Both carbonization in an inert atmosphere and physical activation were carried out in a heat resistant quartz tube (maximum temperature: 1200°C) which was placed into a horizontal tube furnace (Carbolite furnace type MTF 12/25/250, Parsons Lane, with maximum temperature of 1200°C at 700 watts, 50-60 Hertz and 220 volts). Some 14.0 g of the dried specimens were put in a quartz tube, and then placed in the centre of the horizontal tube furnace (Fig. 1). While pyrolysis was ongoing, pure

nitrogen gas at a flow rate of 80 scfm⁻¹ was used as purge gas and introduced into the system at one end. The other end of the tube was exhausted into a beaker of water. The temperature of the furnace was elevated from 25 to 600°C and held for 2 h. The resulting char was physically activated at 800°C for 30 mins under CO₂ gas. A heating rate of 60°C/min was used.

The activated carbon obtained above was inserted into a tube placed in a tube furnace, flushed with argon gas and heated at a temperature of 1100°C at 60°C min⁻¹ for 1hr. At a desired target temperature, 75.0 mL of argon gas passing through a flask of ethanol vapour placed on an ultrasonic humidifier (99.9 %) was introduced into the system. After 60 min treatment, the system was allowed to cool down at a rate of 5 °C min⁻¹ under the flow of argon gas.



Fig. 1. Experimental setup

A. Material characterization

The coconut fibre charcoal, activated charcoal as well as synthesized carbon nanospheres were analysed using FESEM, TEM, EDX, XRD, FTIR and TGA. The synthesis of CNS was carried out in a Carbolite wire-wound tube furnace - single zone (model MTF 12/38/400). The morphology of the samples was examined in a field emission scanning electron microscope (Zeiss, Germany (Ultra Plus, FEGSEM)). The FESEM was equipped with an energy dispersive X-ray spectrometer (EDX) for elemental composition analysis. The microstructure and the phase identification of the samples were studied further by transmission electron microscopy (TEM) using a JEOL 1400 TEM. The sample preparation was carried out by placing a drop of dilute solution of nanoparticles on Formvar-coated Cu grids (150 meshes) for TEM. The samples were left to completely dry at room temperature and viewed at an accelerating voltage of 100 kV (TEM), and images captured digitally using a Megaview III camera; stored and measured using Soft Imaging Systems iTEM software (TEM) and Gatan camera. The sample (a very fine powder) for XRD analysis was prepared by utilising the back loading preparation method. The sample was then analyzed with a PANalytical Empyrean Diffractometer (made in the Netherlands) with an X'Celerator detector and Co-K α radiation. The generator setting was 40 kV (voltage) and 40 mA (current). The coconut fibre carbon nanospheres were

directly dispersed in 95% ethanol directly. After being sonicated for 15 minutes, the samples were placed onto carbon coated copper grids and dried for TEM investigation. The FTIR was analysed using a Perkin Elmer Product FT-IR Spectrum 100 Series while for thermal gravimetric analysis (TGA), [simultaneous thermal analyzer \(STA\) 6000 | PerkinElmer](#) was used.

III. RESULTS AND DISCUSSION

A. Particle Size Distribution and Morphology

Fig. 2 shows a histogram which analyses the size distribution of the nanospheres synthesized. The nanospheres are in the size range of 10 -150 nm and the size with the highest occurrence is 60-89 nm. From the fig., nanospheres of diameter in the range 60-89 nm constituted almost 50% (48.5%) while nanospheres of diameter 30-59 nm constituted 41%. This shows uniformity in the size range of the nanospheres. In the process of carbonization, porosity begins to develop at 600 °C; however the porosity is irregular and not defined. Fig. 3 depicts some typical SEM images of the carbonized coconut fibre at 600 °C for 2hrs. In order to increase porosity, the pyrolyzed coconut fibre was activated under CO₂ for 30 mins. Fig. 3c shows the SEM image of coconut fibre charcoal after being physically activated which indicates some porosity.

The morphology obtained from SEM analysis of the as-synthesized nanospheres is shown in Fig. 3d. The morphology indicates agglomeration between the particles which is as a result of the high surface energy present. The TEM image obtained shows solid nanospheres of high purity graphite as shown in Fig. 4. The particle size obtained agrees with that obtained from the SEM analysis (30-100 nm).

TEM and SEM images show mono-dispersed carbon nanospheres without impurities. These carbon nanospheres have diameters of 30-150 nm. More than 80% of the carbon nanospheres have sizes in the range of 30-100 nm. Fig. 3a-d shows the SEM images carbonized material, activated carbon and synthesized carbon nanomaterial. Fig. 4 shows TEM image of the as-synthesized CNS which is in correlation with SEM results. Observations show that the

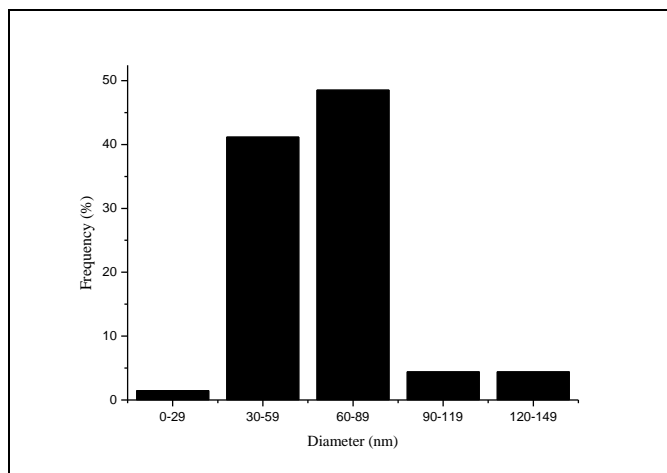


Fig. 2. Nanosphere particle size distribution

CNS are perfect spheres with smooth surfaces. Several agglomerates of the spheres and also bead-like accretions are present in both SEM and TEM. The size distribution obtained from the CNS obtained makes them a potential candidate for biomedical applications [26] and for use in heat transfer applications when dispersed in working fluids for enhanced thermal conductivity [27].

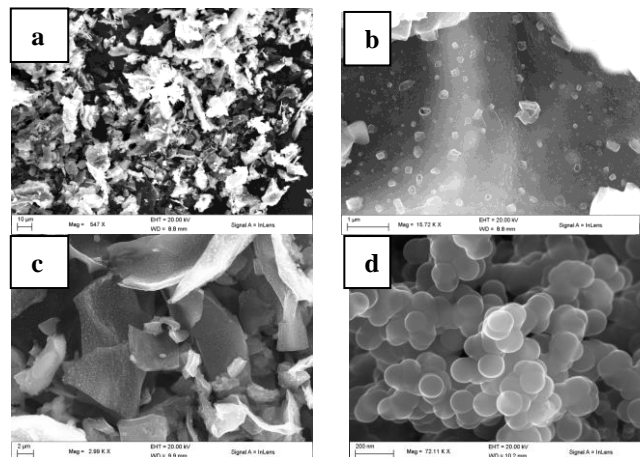


Fig. 3. (a and b) SEM images of carbonized coconut fibre at 600°C under different magnifications. (c) SEM image of activated carbon, physically activated under CO₂ for 30 mins at 800°C (d) SEM image of carbon nanosphere at 1100°C under ethanol vapour

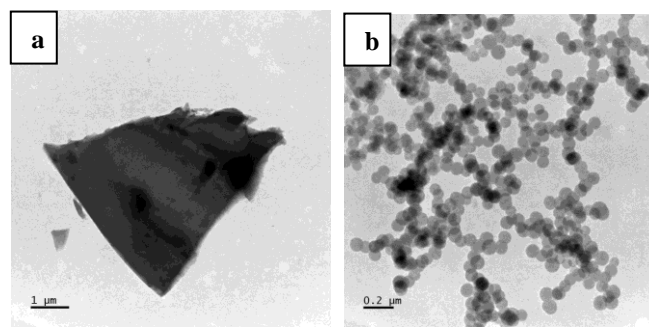


Fig. 4. (a): TEM image of carbonized coconut fibre (b) TEM image of as-synthesized carbon nanospheres.

B. Elemental Composition Analysis

The elemental composition of carbonized coconut fibre, activated carbon and CNS synthesized over ethanol vapour was revealed by EDX analysis shown in Fig 5a-5c. Carbonized coconut fibre contains mostly carbon (87.80%), oxygen (9.66%), magnesium (0.15%), chlorine (0.48%), and potassium (1.91%). Activated carbon elemental analysis contains carbon (87.40%), oxygen (5.36%) and other materials in trace quantities. The elemental composition of CNS has 98.59 % of carbon which confirms the purity of the nanomaterials produced. These results prove that treatment with ethanol vapour at 1100 °C formed well rounded carbon nanospheres. Table 1 shows elemental composition of carbonized CF, activated ACF and CNS. Decrease in oxygen is due to the rise in temperature from 600 °C for carbonized CF to 800 °C for activated CF and finally 1100°C for nanosphere production. The increase in temperature results in oxygen removal and an increment value of carbon.

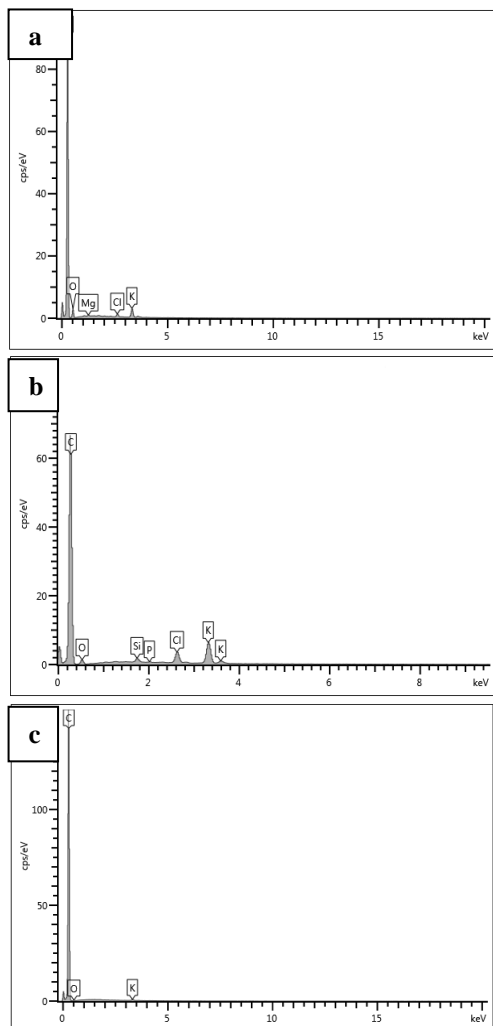


Fig. 5. (a) EDX of carbonized coconut fibre at 600 °C (b) EDX of coconut fibre activated carbon (c) EDX of CNS

C. Structural Analysis

The crystallinity and graphitization degree is studied using XRD analysis. Fig. 6 presents the XRD pattern in which the two Bragg diffraction peaks at 30.34° and 50.44° can be assigned as typical graphite (003) and (101) planes [28]. The d-spacing calculated is 0.342 nm which is close to graphite 3R given as 0.340 nm. The broadening peaks suggest a low graphitization degree and the possibility of the presence of amorphous carbon. These results fall in the range of authors [24] and [29] with d-spacing of 0.33nm and 0.36 nm respectively. No other peaks of are visible in the XRD pattern, which could be due to the high purity of the product. Fig. 5 confirms the purity of the material with a well-defined presence of carbon (98.59%).

The functional groups present in the carbon nanospheres synthesized were analyzed using FTIR analysis (Fig. 7). A peak at 3437 cm⁻¹ can be assigned to the O-H stretching vibrations including hydroxyl functional group [30]. 2787 cm⁻¹ to O-H acids, 2100 cm⁻¹ to C=C stretching in alkyne, the peaks at 1798 to the stretching vibration of C=O in carboxyl group [31] and 1743 can be attributed to C=C stretching vibrations. At 1210 cm⁻¹ the vibration can be assigned to C-C bond. The aromatic C-H bend at 805 cm⁻¹ suggests the presence of aromatic ring [32] while the unsaturated C=C groups indicates that a carbonization and

TABLE I
 ELEMENTAL COMPOSITION OF CARBONIZED CF, ACTIVATED CF AND CNS

	Carbonized CF	Activated CF	CNS
Carbon	87.80%	87.40%	98.59%
Oxygen	9.66%	5.36%	1.08%

activation process occurred while the presence of a hydroxyl group improves the rate of hydrophobicity and stability of the CNS in aqueous solution.

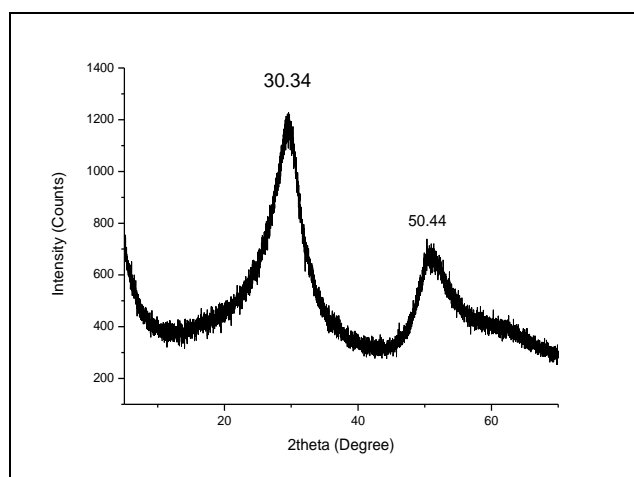


Fig. 6. XRD pattern of carbon nanospheres synthesized at 1100 °C

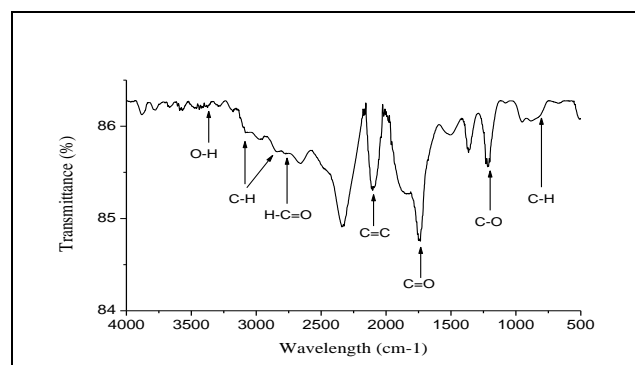


Fig. 7. FTIR spectra of CNS

IV. THERMAL STABILITY

The thermal stability of the material was studied through TGA in Fig. 8. The curve shows a single decomposition phase between 350°C and 1000°C. The curve shows that the material is fairly stable in an inert atmosphere with a small weight loss of about 5% which can be seen before 350°C. This could be as a result of loss in moisture in the sample. At about 400°C, there is a sharp slope which may indicate the presence of lattice defects that enables oxygen to rapidly pass through the spheres thereby facilitating rapid oxidation. The samples are entirely burnt off at 1000°C.

V. CONCLUSION

A general time effective and cost effective strategy has been adopted for preparing carbon nanospheres from coconut fibre bio-based feedstock. This method is not only cheap, but non-toxic and sustainable. The synthesis method involves carbonizing, followed by physical activation and

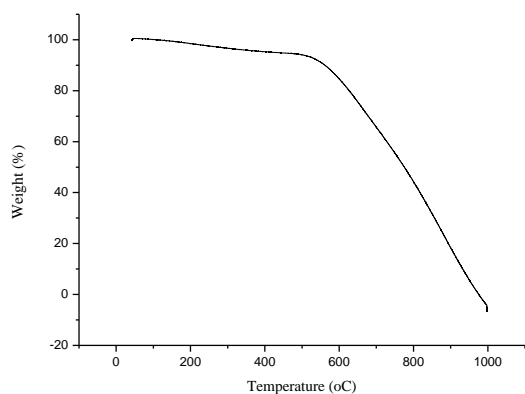


Fig. 8. TGA curve of as-synthesized carbon nanospheres

finally passing ethanol vapour through the activated carbon obtained. The carbonized coconut fibre and carbon nanospheres formation was investigated through XRD, SEM, TEM, EDX, FTIR and TGA analysis. SEM investigations confirms the production of carbon nanospheres with diameters between 30-150nm. The observations also show that the CNS are perfect spheres with smooth surfaces. Multiple conglomerates of the spheres are observed and also bead-like lumps are observed in both SEM and TEM. The nanosphere obtained can be used in Lithium-ion batteries, heat transfer fluids and medical field for drug delivery.

ACKNOWLEDGMENT

The financial assistance of the National Research Foundation (NRF) towards this research is hereby acknowledged. Opinions expressed and conclusions arrived at, are those of the author and are not necessarily to be attributed to the NRF.

REFERENCES

[1] S. A. Bello, J. O. Agunsoye, J. A. Adebisi, F. O. Kolawole, and S. B. Hassan, "Properties of coconut shell nanoparticles," *Journal of Science, Engineering and Technology*, vol. 12, pp. 63-79, June 2016 2016.

[2] M. Ali, "Coconut fibre: A versatile material and its applications in engineering," *Journal of Civil Engineering and Construction Technology*, vol. 2, pp. 189-197, 2011.

[3] I. Tan, A. Ahmad, and B. Hameed, "Preparation of activated carbon from coconut husk: optimization study on removal of 2, 4, 6-trichlorophenol using response surface methodology," *Journal of hazardous materials*, vol. 153, pp. 709-717, 2008.

[4] A. Nieto-Márquez, R. Romero, A. Romero, and J. L. Valverde, "Carbon nanospheres: synthesis, physicochemical properties and applications," *Journal of Materials chemistry*, vol. 21, pp. 1664-1672, 2011.

[5] H.-s. Qian, F.-m. Han, B. Zhang, Y.-c. Guo, J. Yue, and B.-x. Peng, "Non-catalytic CVD preparation of carbon spheres with a specific size," *Carbon*, vol. 42, pp. 761-766, 2004.

[6] Y. Z. Jin, C. Gao, W. K. Hsu, Y. Zhu, A. Huczko, M. Bystrzejewski, *et al.*, "Large-scale synthesis and characterization of carbon spheres prepared by direct pyrolysis of hydrocarbons," *Carbon*, vol. 43, pp. 1944-1953, 2005.

[7] J.-Y. Miao, D. W. Hwang, K. V. Narasimhulu, P.-I. Lin, Y.-T. Chen, S.-H. Lin, *et al.*, "Synthesis and properties of carbon nanospheres grown by CVD using Kaolin supported transition metal catalysts," *Carbon*, vol. 42, pp. 813-822, 2004.

[8] M. Ibrahim Mohammed, R. Ismaeel Ibrahim, L. H. Mahmoud, M. A. Zablouk, N. Manweel, and A. Mahmoud, "Characteristics of carbon nanospheres prepared from locally deoiled asphalt," *Advances in Materials Science and Engineering*, vol. 2013, 2013.

[9] X. Yu, J. Lu, C. Zhan, R. Lv, Q. Liang, Z.-H. Huang, *et al.*, "Synthesis of activated carbon nanospheres with hierarchical porous structure for high volumetric performance supercapacitors," *Electrochimica Acta*, vol. 182, pp. 908-916, 2015.

[10] Y. Wang, F. Su, C. D. Wood, J. Y. Lee, and X. S. Zhao, "Preparation and characterization of carbon nanospheres as anode materials in lithium-ion secondary batteries," *Industrial & Engineering Chemistry Research*, vol. 47, pp. 2294-2300, 2008.

[11] N. Katcho, P. Zetterström, E. Lomba, J. Marco, E. Urones-Garrote, D. Avila-Brandé, *et al.*, "Structure of carbon nanospheres prepared by chlorination of cobaltocene: Experiment and modeling," *Physical Review B*, vol. 77, p. 195402, 2008.

[12] P. Zhang, Z.-A. Qiao, and S. Dai, "Recent advances in carbon nanospheres: synthetic routes and applications," *Chemical Communications*, vol. 51, pp. 9246-9256, 2015.

[13] A. A. Arie, H. Kristianto, M. Halim, and J.-K. Lee, "Biomass Based Carbon Nanospheres as Electrode Materials in Lithium Ion Batteries," *ECS Transactions*, vol. 66, pp. 13-19, 2015.

[14] H. Kristianto, C. D. Putra, A. A. Arie, M. Halim, and J. K. Lee, "Synthesis and Characterization of Carbon Nanospheres Using Cooking Palm Oil as Natural Precursors onto Activated Carbon Support," *Procedia Chemistry*, vol. 16, pp. 328-333, 2015.

[15] X.-W. Chen, O. Timpe, S. B. Hamid, R. Schlögl, and D. S. Su, "Direct synthesis of carbon nanofibers on modified biomass-derived activated carbon," *Carbon*, vol. 47, pp. 340-343, 2009.

[16] J. Zhu, J. Jia, F. L. Kwong, D. H. L. Ng, and S. C. Tjong, "Synthesis of multiwalled carbon nanotubes from bamboo charcoal and the roles of minerals on their growth," *biomass and bioenergy*, vol. 36, pp. 12-19, 2012.

[17] H. Li, X. He, Y. Liu, H. Yu, Z. Kang, and S.-T. Lee, "Synthesis of fluorescent carbon nanoparticles directly from active carbon via a one-step ultrasonic treatment," *Materials Research Bulletin*, vol. 46, pp. 147-151, 2011.

[18] J. O. Alves, C. Zhuo, Y. A. Levendis, and J. A. Tenório, "Catalytic conversion of wastes from the bioethanol production into carbon nanomaterials," *Applied Catalysis B: Environmental*, vol. 106, pp. 433-444, 2011.

[19] K. Shi, J. Yan, E. Lester, and T. Wu, "Catalyst-Free Synthesis of Multiwalled Carbon Nanotubes via Microwave-Induced Processing of Biomass," *Industrial & Engineering Chemistry Research*, vol. 53, pp. 15012-15019, 2014.

[20] A. Melati and E. Hidayati, "Synthesis and characterization of carbon nanotube from coconut shells activated carbon," in *Journal of Physics: Conference Series*, 2016, p. 012073.

[21] H. Marsh and F. R. Reinoso, *Activated carbon*: Elsevier, 2006.

[22] R. Kumar, R. K. Singh, and D. P. Singh, "Natural and waste hydrocarbon precursors for the synthesis of carbon based nanomaterials: Graphene and CNTs," *Renewable and Sustainable Energy Reviews*, vol. 58, pp. 976-1006, 2016.

[23] J. Guo, B. Gui, S.-x. Xiang, X.-t. Bao, H.-j. Zhang, and A. C. Lua, "Preparation of activated carbons by utilizing solid wastes from palm oil processing mills," *Journal of Porous Materials*, vol. 15, pp. 535-540, 2008.

[24] A. Nath, D. D. Purkayastha, M. Sharon, and C. R. Bhattacharjee, "Catalyst free low temperature synthesis and antioxidant activity of multiwalled carbon nanotubes accessed from ghee, clarified butter of cow's milk," *Materials Letters*, vol. 152, pp. 36-39, 2015.


[25] M. L. Sekirifa, M. Hadj-Mahammed, S. Pallier, L. Baameur, D. Richard, and A. H. Al-Dujaili, "Preparation and characterization of an activated carbon from a date stones variety by physical activation with carbon dioxide," *Journal of Analytical and Applied Pyrolysis*, vol. 99, pp. 155-160, 2013.

[26] M. Doorley, S. R. Mishra, M. Laradji, R. K. Gupta, and K. Ghosh, "Carbon Nanospheres: "Green" Synthesis, Characterization, and Growth Kinetics," in *MRS Proceedings*, 2007, pp. 1054-FF12-41.

[27] M. Mehrali, S. T. Latibari, M. Mehrali, T. M. I. Mahlia, and H. S. C. Metselaar, "Effect of carbon nanospheres on shape stabilization and thermal behavior of phase change materials for

- thermal energy storage," *Energy Conversion and Management*, vol. 88, pp. 206-213, 2014.
- [28] P. Debye and P. Scherrer, "Interference on inordinate orientated particles in x-ray light. III," *Physikalische Zeitschrift*, vol. 18, pp. 291-301, 1917.
- [29] A. D. Faisal and A. A. Aljubouri, "Synthesis and Production of Carbon Nanospheres Using Noncatalytic CVD Method."
- [30] A. N. Mohan and B. Manoj, "Synthesis and characterization of carbon nanospheres from hydrocarbon soot," *Int. J. Electrochem. Sci*, vol. 7, pp. 9537-9549, 2012.
- [31] M. H. Joula and M. Farbod, "Synthesis of uniform and size-controllable carbon nanospheres by a simple hydrothermal method and fabrication of carbon nanosphere super-hydrophobic surface," *Applied Surface Science*, vol. 347, pp. 535-540, 2015.
- [32] P. Bhagat, K. Patil, D. Bodas, and K. Paknikar, "Hydrothermal synthesis and characterization of carbon nanospheres: a mechanistic insight," *RSC Advances*, vol. 5, pp. 59491-59494, 2015.

Synthesis of Carbon Nanotubes and Nanospheres from Coconut Fibre and the Role of Synthesis Temperature on Their Growth

GLORIA A. ADEWUMI ^{1,3} FREDDIE INAMBAO,¹
ANDREW ELOKA-EBOKA,¹ and NEERISH REVAPRASADU²

1.—Discipline of Mechanical Engineering, School of Engineering, University of KwaZulu-Natal, Howard College, Durban 4001, South Africa. 2.—University of Zululand, X1001, Kwadlangezwa 3886, South Africa. 3.—e-mail: adewumigloria@gmail.com

Carbon nanotubes (CNT) and carbon nanospheres were successfully synthesized from coconut fibre-activated carbon. The biomass was first carbonized then physically activated, followed by treatment using ethanol vapor at 700°C to 1100°C at 100°C intervals. The effect of synthesis temperature on the formation of the nanomaterials was studied using scanning electron microscopy (SEM), transmission electron microscopy (TEM), energy dispersive x-ray spectrometry, x-ray diffraction (XRD), Fourier transform infrared microscopy (FTIR) and thermogravimetric analysis. SEM analysis revealed that nanospheres were formed at higher temperatures of 1000°C and 1100°C, while lower temperatures of 800°C and 900°C favored the growth of CNT. At 700°C, however, no tubes or spheres were formed. TEM and FTIR were used to observe spectral features, such as the peak positions, intensity and bandwidth, which are linked to some structural properties of the samples investigated. All these observations provided facts on the nanosphere and nanotube dimensions, vibrational modes and the degree of purity of the obtained samples. The TEM results show spheres of diameter in the range 50 nm to 250 nm while the tubes had diameters between 50 nm to 100 nm. XRD analysis reveals the materials synthesized are amorphous in nature with a hexagonal graphite structure.

Key words: Carbon nanotubes, carbon nanospheres, SEM, bio-based precursors

INTRODUCTION

The excellent physical properties of carbon nanotubes (CNT) and carbon nanospheres (CNS) render them useful in many applications, such as emitters for electrons,^{1–4} materials for battery electrodes,⁵ rechargeable cells for lithium-ion batteries^{6–17} and working fluids for heat transfer applications. The development of carbon nanotechnology, which offers a future in wide applications is attracting increasing interest from an extensive range of fields,

including energy technology,¹⁸ electronic devices,¹⁹ and drug delivery in the medical field.^{20–22} Because of these applications, there is a growing interest in research aimed at producing nanomaterials from renewable and non-toxic precursors.^{23–30}

In general, synthesis temperature is a parameter affecting the final morphology, yield^{24,31} and purity³² of nanomaterials. Studies investigating the effect of temperature on the parameters of growth of CNTs have revealed 800°C to 1000°C as the optimum temperature favouring the highest yield of carbon nanotubes.^{32,33} The effect of temperature on the synthesis of CNTs using nickel substrates generated results, which indicate the growth of multi-walled CNT at lower temperature and nickel

(Received October 24, 2017; accepted March 20, 2018)

thickness.³⁴ The adjustment of the temperature between 700°C to 900°C produced fundamental outcomes in the CNT structure grown, which showed that higher temperatures promote core-shell configuration while lower temperatures enhance the formation of CNTs. Toussi et al.³⁵ showed that when the temperature of synthesis is lower than 750°C, CNT formation was lower; however, CNT formation was higher for temperatures greater than 900°C. The ideal temperature for CNT growth reported by Toussi et al.³⁵ was 800°C and 900°C, with the optimum growth temperature being 850°C. Shamsudin et al.³⁶ obtained an optimum growth of ~ 99.99% at 900°C. Apart from high temperature synthesis, carbon nanotubes can also be prepared from carbonaceous solids at lower temperature (450°C).³⁷

In this paper, we present results obtained from the synthesis of carbon nanomaterials from coconut fibre at temperatures between 700°C to 1100°C in the absence of an external catalyst or substrate using ethanol vapour treatment. The activated carbon from the coconut fibre has two functions, to act as a catalyst and also as a substrate for carbon nanomaterial growth.

EXPERIMENTAL PROCEDURE

Coconut fibre (CF) was obtained from coconut farmers in Oyo State, Nigeria. They were cleaned, cut into small sizes and dried in air for a period of 3 months. The CF were inserted into a heat resistant quartz tube and placed in a horizontal tube furnace (model MTF 12/38/400). Temperature effect on the development of nanomaterials was studied by treating activated carbon derived from CF with ethanol vapour at 700°C, 800°C, 900°C, 1000°C and 1100°C for 60 min. An aerosol was generated from ethanol using an ultrasonic air humidifier (Model GMH-200) operating at 50 Hz. Argon gas was passed through the aerosol mist and its function was to create an inert atmosphere for the reaction and to transport the aerosol droplets into the reactor chamber. The aerosol line was closed at the desired temperature, and the argon gas was allowed to flow thereby cooling the system.

Material Characterization

The synthesized nanomaterials were characterized with respect to their morphologies before and after the nanomaterial formation. The surface morphology and elemental composition of the nanomaterials were estimated using a field emission gun scanning electron microscope (Zeiss, Germany Model: Ultra Plus, FEGSEM) equipped with an energy dispersive x-ray spectrometer (EDX). The microstructure and the phase identification of the samples were studied further by transmission electron microscopy (TEM) using a JEOL 1400 TEM and high resolution transmission electron microscopy using a JEOL HRTEM 2100. The sample

preparation was carried out by placing a drop of dilute solution of nanoparticles on formvar-coated Cu grids (150 meshes) for TEM. The samples were left to dry completely at room temperature and viewed at an accelerating voltage of 100 kV (TEM). The images were digitally captured using a Mega-view III camera; stored and measured using Soft Imaging Systems iTEM software (TEM) and Gatan camera. The sample (a very fine powder) for XRD analysis was prepared by utilising the back loading preparation method. The sample was then analyzed with a PANalytical Empyrean Diffractometer (made in the Netherlands) with an X'Celerator detector and Co-K α radiation. The generator setting was 40 kV (voltage) and 40 mA (current). The coconut fibre carbon nanomaterials obtained were directly dispersed in 95% ethanol. After sonicating for 15 min, the samples were placed onto carbon coated copper grids and dried for the TEM investigation. Infrared spectra was carried out on a Perkin Elmer Product FT-IR Spectrum 100 Series. The thermal stability of as-synthesized materials was studied using thermogravimetric analysis (TGA), simultaneous thermal analyzer (STA) 6000 | PerkinElmer.

RESULTS AND DISCUSSION

Morphology and Particle Size Distribution

The increased furnace temperature enhances the collision frequency of the catalysts contained in the CF activated carbon leading to the formation of different structures as seen from Fig. 1. The CF activated carbon and synthesized nanomaterials obtained in the 700°C to 1100°C temperature range with 100°C increments were characterized by SEM and TEM. Figure 1a is a SEM image of physically activated CF carried out in the presence of CO₂ at 800°C for 30 min. The SEM micrographs from Fig. 1b to f reveal carbon sheets, CNT and CNS. From the SEM image, it is observed that at 700°C no nanomaterials were formed. At that temperature, sheet-like structures are observed, which suggests that the temperature of synthesis (700°C) was too low to trigger carbon nanomaterial growth. The sheets seen are similar to the sheets seen in the SEM image of CF activated carbon (Fig. 1a).

The particle size distribution (Fig. 2) shows the nanosphere diameters and the nanotube diameters measured using a cross-sectional view of the array from the TEM results (Fig. 3). The measurements were taken from a minimum of 30 TEM images for each sample. At 800°C there is a tube-like morphology with the particle size distribution ranging from 40 nm to 120 nm. Although carbon nanotubes are formed at this temperature, the structure of the tubes is not well defined.

A more defined carbon nanotube structure is seen at 900°C (Fig. 1c). The corresponding particle size distribution (Fig. 3b) shows tubes of diameter ranging from 40 nm to 90 nm. At higher temperatures of 1000°C and 1100°C, carbon nanospheres are formed

Synthesis of Carbon Nanotubes and Nanospheres from Coconut Fibre and the Role of Synthesis Temperature on Their Growth

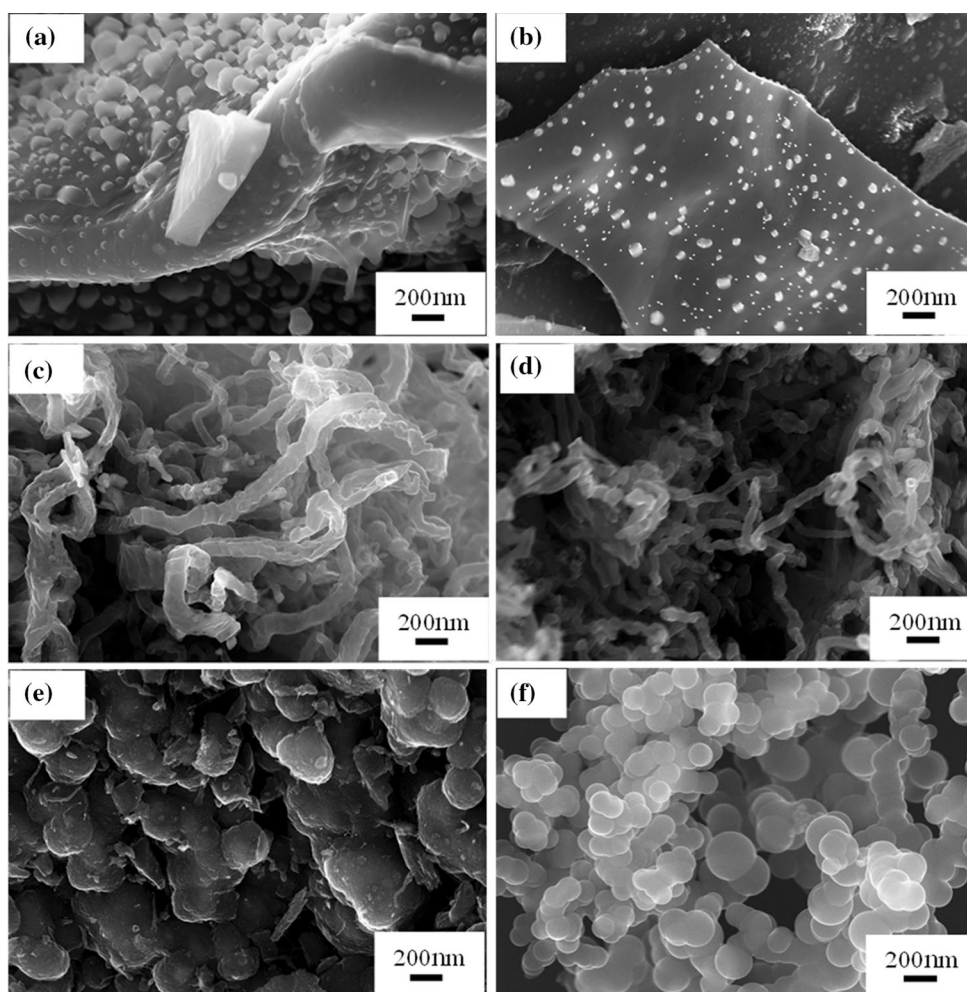


Fig. 1. SEM micrographs of (a) CF activated carbon, nanomaterials synthesized at (b) 700°C, (c) 800°C, (d) 900°C, (e) 1000°C, and (f) 1100°C.

(Fig. 2e and f). The nanospheres formed at 1000°C have rough surfaces with some degree of impurities. Those formed at 1100°C are highly agglomerated. The SEM micrographs of all the samples at the different temperatures show a clear change in the structure of materials synthesized.

The lack of the carbon nanomaterial growth at 700°C suggests that this temperature is not high enough for the CF activated carbon to metamorphose into tubes or spheres. When ethanol vapour is introduced, the condition in the tube containing CF activated carbon is changed thereby triggering the growth of carbon nanotubes or nanospheres on activated carbon. It was observed that lower temperatures (800°C to 900°C) favour the growth of multiwall CNTs while higher temperatures (1000°C to 1100°C) were suitable for the formation of nanospheres. The HRTEM and selected area electron diffraction (SAED) rings of the nanotubes are shown in Fig. 4. Figure 4a and c shows multiwall nanotubes with d-spacing to be about 0.33 nm. The SAED rings in Fig. 4b and d shows ring patterns which indicates crystallinity and graphitic nature of

the nanotubes. The brightest area of the rings in both Fig. 4b and d corresponds to the 002 reflection of hexagonal graphite while the next continuous ring seen in the diffraction pattern corresponds to the 110 reflection of hexagonal graphite. From Fig. 4d, there is no uniformity in the intensity of the brightness across the first ring, with two bright spots occurring at opposite positions across the ring. The brighter portions are the result of orientation in the nanotubes, which suggests some degree of disorderliness. The diffraction rings show that the samples display both crystalline and amorphous carbon structures.

The EDX analysis of CF activated carbon is shown in Table I. From the table, carbon content in samples is observed to be high for all synthesis temperatures, with the highest yield obtained at synthesis temperatures of 900°C and 1000°C. These temperatures have a high yield of carbon nanomaterials because the synthesis temperature is sufficient and also due to the burnout of amorphous carbon. On the contrary, the oxygen content has been observed to decrease, which is in line with

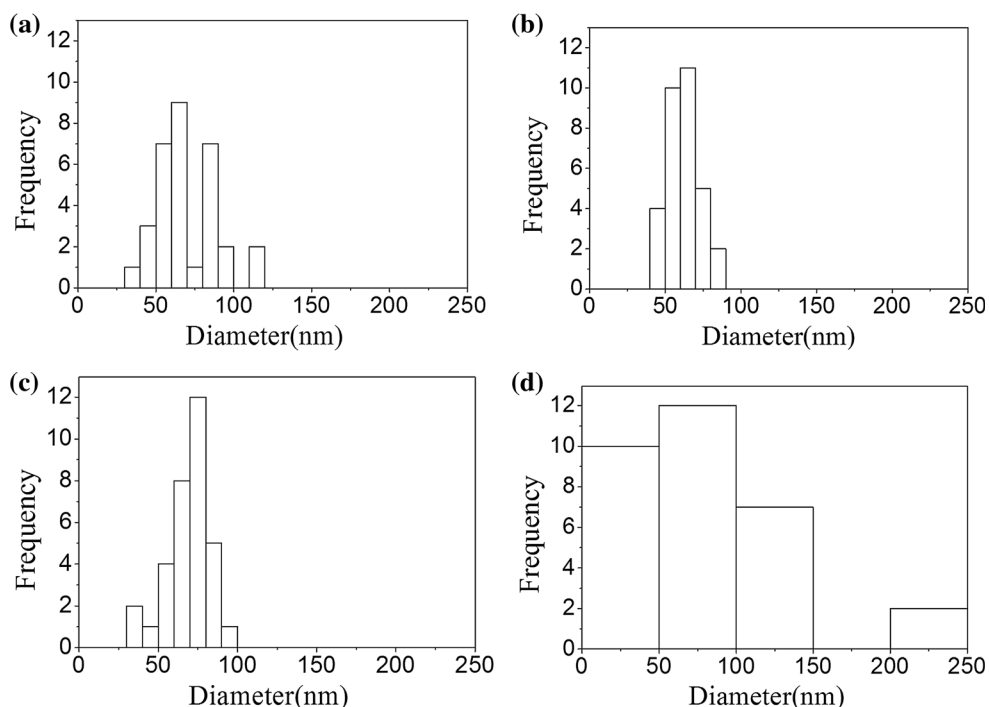


Fig. 2. Particle size distribution of nanomaterials synthesized at (a) 800°C, (b) 900°C, (c) 1000°C, and (d) 1100°C.

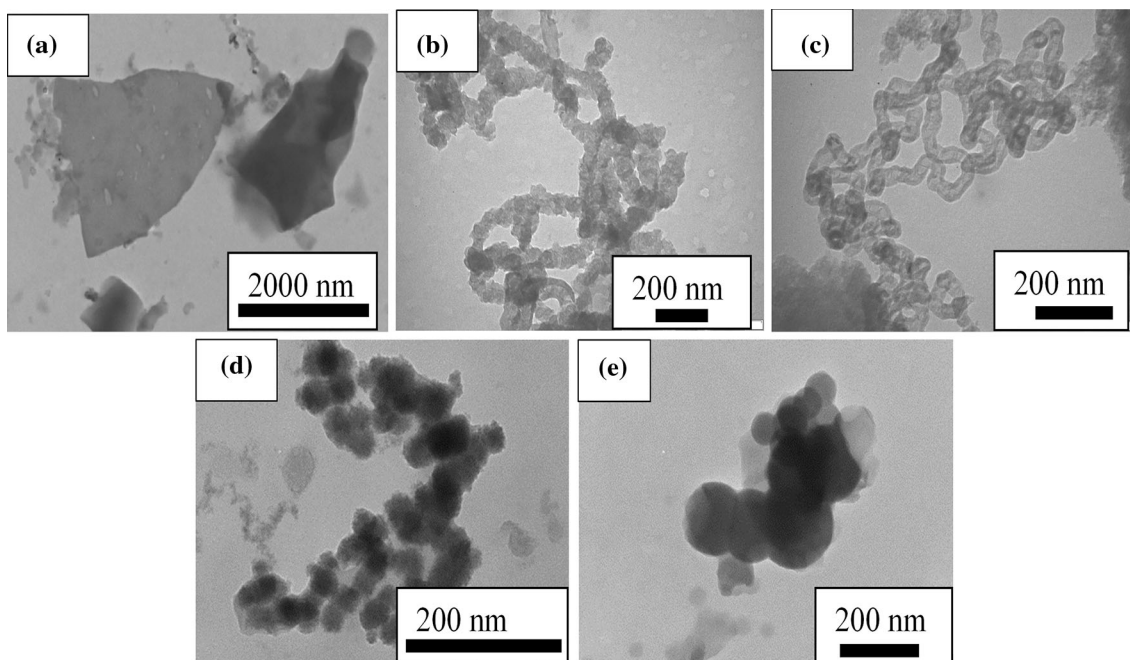


Fig. 3. TEM micrographs of nanomaterials synthesized at (a) 700°C, (b) 800°C, (c) 900°C, (d) 1000°C, and (e) 1100°C.

previous results.³⁸ The elements contained in the CF activated carbon includes carbon (C), oxygen (O), potassium (K) and chlorine (Cl), which are typically elements found in plants. The presence of O in all the samples can be ascribed to the physical activation of the bio-char which was carried out

using CO₂ and also from moisture. The presence of silicon (Si) is due to the quartz tube in which the reaction took place. An increase in Si is observed as temperature of synthesis increased and this is from the reaction of the materials with the silica glass tube used in the furnace.

Synthesis of Carbon Nanotubes and Nanospheres from Coconut Fibre and the Role of Synthesis Temperature on Their Growth

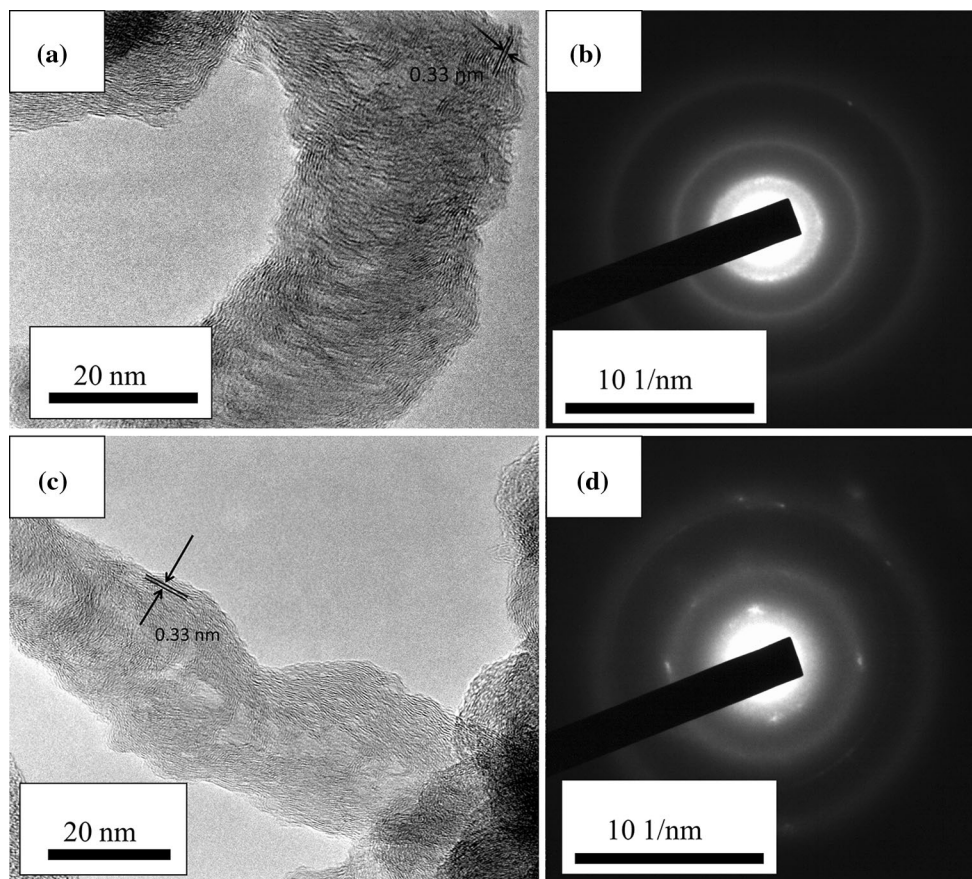


Fig. 4. (a) HRTEM of CNT produced at 800°C, (b) SAED at 800°C, (c) HRTEM of CNT produced at 900°C and (d) SAED at 900°C.

Table I. EDX analysis of coconut fibre activated carbon, and materials at the various synthesis temperature by atomic%

Element	Coconut fibre AC	Materials synthesized at 700°C	Materials synthesized at 800°C	Materials synthesized at 900°C	Materials synthesized at 1000°C	Materials synthesized at 1100°C
C	88.7	89.8	92.6	95.6	96.2	91.6
O	10.0	10.2	7.3	4.1	3.3	7.5
Si	–	–	–	–	0.3	0.6
K	1.0	–	0.1	0.3	0.2	0.3
Cl	0.3	–	–	–	–	–
Total	100	100	100	100	100	100

FTIR Characterization of Coconut Fibre Nanomaterials

The functional elements absorbed by the materials were characterized using FTIR. Figure 5a to f presents the comparison spectra in the range of 500 cm^{-1} to 4000 cm^{-1} of (a) activated carbon, nanomaterials synthesized from coconut fibre at 700°C, 800°C, 900°C, 1000°C and 1100°C for 60 min. All five samples show peaks corresponding to functionalities including hydroxyl (3440 cm^{-1}), carbonyl (1717 cm^{-1}) and unsaturated C=C (1576 cm^{-1}). The FTIR spectra from all the six

samples indicates matching vibrational modes but with different intensities and energy shifts.

The activated carbon (Fig. 5a) shows a broad peak at 3440 cm^{-1} , which is assigned to the -OH stretching vibration of the surface hydroxyl groups. It shows the presence of bonded hydroxide in the activated carbon sample which permits silicon carbide to be bonded to itself or another material with an oxide layer. This is confirmed in the EDX results of materials synthesized at 1000°C and 1100°C, which can be seen to contain 0.3% and 0.6% of silica, respectively. The materials synthesized at 900°C are carbon nanotubes, and it can

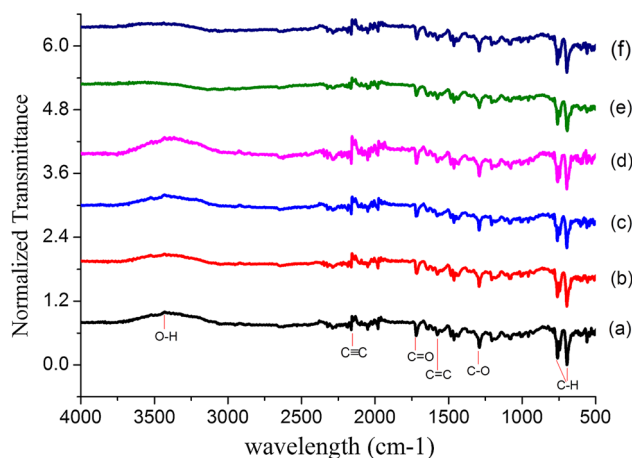


Fig. 5. FTIR results for (a) activated carbon, materials synthesized at (b) 1100°C, (c) 1000°C, (d) 900°C, (e) 800°C, and (f) 700°C.

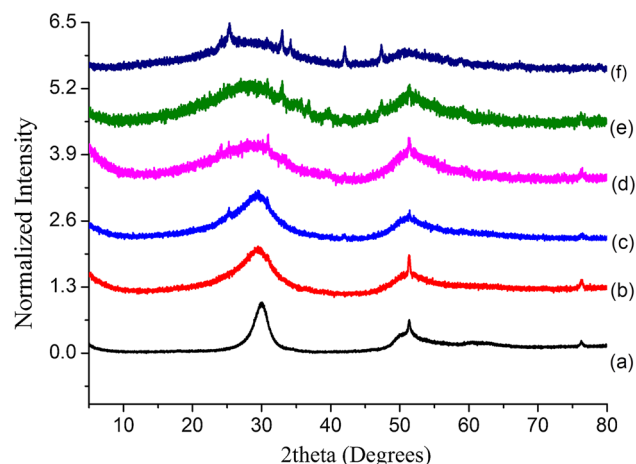


Fig. 6. XRD patterns of (a) synthetic CNT, Materials synthesized at (b) 1100°C, (c) 1000°C, (d) 900°C, (e) 800°C, and (f) 700°C.

be observed that the broadened -OH peak is more intense at this point and diminishes for the materials synthesized at 700°C and 800°C, which is associated with the presence of amorphous carbon.³⁹ A peak at 2165 cm^{-1} can be assigned to the alkyne $\text{C}\equiv\text{C}$ stretch. This peak has the highest intensity at 900°C. The peak at 1717 cm^{-1} can be assigned to the ester groups $\text{C}=\text{O}$ and $-\text{C}-\text{O}-\text{C}-$ stretching respectively.⁴⁰ A peak at 1293 cm^{-1} can be assigned to the single bond $\text{C}-\text{O}$. A peak at 693 cm^{-1} and 762 cm^{-1} , which is an out-of-plane deformation can be assigned to the aromatic bend of $\text{C}-\text{H}$. The in-plane graphitic $\text{C}-\text{C}$ bond makes them remarkably strong and rigid against axial strains.

XRD Analysis

The phases of minerals present in the nanomaterials synthesized at different temperatures are analysed from XRD patterns as seen in Fig. 6 below. The results of the materials synthesized at 1100°C, 1000°C, 900°C, and 800°C show two major broad peaks at (002) and (011), which signify a hexagonal graphite structure. The (002) peak is located at $2\theta = 30^\circ$ while the (011) peak is found at $2\theta = 51^\circ$. These values are in line with results obtained from the studies carried out by other studies.^{32,37} The XRD pattern of the synthetic CNT are similar to the materials synthesized at 6(b), 6(c), 6(d), and 6(e). The Miller indices represented on each pattern are based on the hexagonal lattice constant of graphite. The broadened peaks suggest a low graphitization degree and the presence of amorphous carbon. The d-spacings in Fig. 6b, c, d, and e are all calculated as 0.33 nm, closely matching the d-spacing (0.34 nm) for synthetic CNT which was purchased commercially.

TGA Analysis

The thermal stability of the synthesized materials at various temperatures was carried out in the

presence of nitrogen gas at a heating rate of $10^\circ\text{C}/\text{min}$ and shown in Fig. 7. The initial small weight loss at 200°C for all the samples is from the volatilization of moisture, loss of functional groups and other non-carbon materials. The decomposition of the nanotubes synthesised at 800°C started at approximately 270°C , which was due to the presence of amorphous carbon from low synthesis temperature.³⁹ However, for nanotubes prepared at 900°C , the onset degradation temperature begins at 360°C , which is as a result of less amorphous carbon from a longer time of reaction and this result in the production of more superior nanotubes. As the temperature increased the thermal stability of the nanotubes also increased from 99.87% for nanotubes synthesized at 800°C to 94.83% for nanotubes produced at 900°C . At 1000°C and 1100°C , the temperature of synthesis is high enough and so there is very little amorphous carbon present, which has been burnt off. For nanospheres synthesized at 1000°C and 1100°C , however, the thermal stability improved from 100% decomposition to 90.2%, respectively. These results were in agreement with the SEM and EDX results.

CONCLUSIONS

Carbon nanospheres and nanotubes have been successfully synthesized by passing ethanol vapour through activated carbon obtained from coconut fibre at 700°C to 1100°C at 100°C increments. The process did not involve the use of an external catalyst or substrates. At 700°C no nanomaterials were formed indicating a low temperature of synthesis. At 800°C and 900°C , nanotubes were formed in which the EDX results reveal carbon content of 92.6% and 95.6%, respectively, while temperatures at 1000°C and 1100°C favoured the growth of nanospheres with carbon contents of 96.2% and 91.6%, respectively.

Synthesis of Carbon Nanotubes and Nanospheres from Coconut Fibre and the Role of Synthesis Temperature on Their Growth

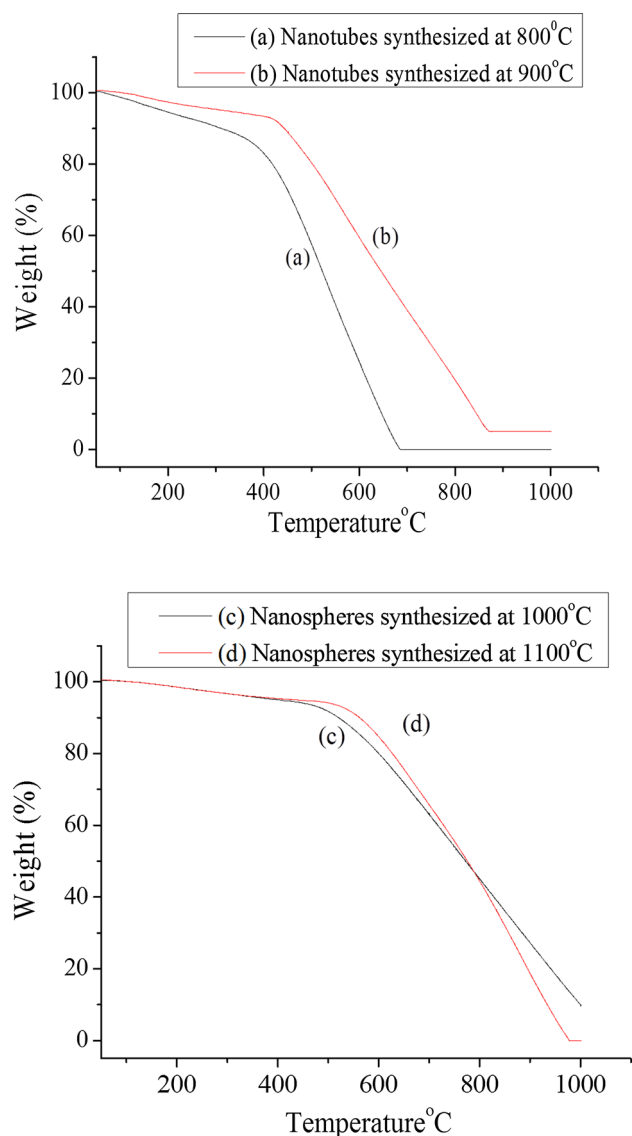


Fig. 7. TGA analysis of nanomaterials synthesized at (a) 800°C, (b) 900°C, (c) 1000°C, and (d) 1100°C.

ACKNOWLEDGEMENTS

The financial assistance of the National Research Foundation (NRF) towards this research is hereby acknowledged.

REFERENCES

1. X. He, H. Li, Y. Liu, H. Huang, Z. Kang, and S.-T. Lee, *Colloids Surf. B* 87, 326 (2011).
2. H. Li, X.D. He, Y.Y. Liu, H. Huang, S. Lian, S.T. Lee, and Z.H. Kang, *Carbon* 49, 605 (2011).
3. H. Li, X. He, Y. Liu, H. Yu, Z. Kang, and S.-T. Lee, *Mater. Res. Bull.* 46, 147 (2011).
4. Z. Ma, H. Ming, H. Huang, Y. Liu, and Z. Kang, *New J. Chem.* 36, 861 (2012).
5. J.S. Sagu, U. Wijayantha, K. Gamage, M. Bohm, S. Bohm, and T.K. Rout, *Adv. Eng. Mater.* 18, 1059 (2016).
6. Y. Ding, H. Alias, D. Wen, and R.A. Williams, *Int. J. Heat Mass Transf.* 49, 240 (2006).

7. P. Estellé, *Mater. Lett.* 138, 162 (2015).
8. S. Halefadi, P. Estellé, B. Aladag, N. Doner, and T. Maré, *Int. J. Therm. Sci.* 71, 111 (2013).
9. S. Halefadi, T. Maré, and P. Estellé, *Exp. Therm. Fluid Sci.* 53, 104 (2014).
10. B. Jo and D. Banerjee, *Mater. Lett.* 122, 212 (2014).
11. M.-S. Liu, M. Ching-Cheng Lin, I.T. Huang, and C.-C. Wang, *Int. Commun. Heat Mass Transf.* 32, 1202 (2005).
12. L. Lu, Z.-H. Liu, and H.-S. Xiao, *Sol. Energy* 85, 379 (2011).
13. T. Maré, S. Halefadi, S. Van Vaerenbergh, and P. Estellé, *Int. Commun. Heat Mass Transf.* 66, 80 (2015).
14. R. Sadri, G. Ahmadi, H. Togun, M. Dahari, S.N. Kazi, E. Sadeghinezhad, and N. Zubir, *Nanoscale Res. Lett.* 9, 151 (2014).
15. R. Saidur, K.Y. Leong, and H.A. Mohammad, *Renew. Sustain. Energy Rev.* 15, 1646 (2011).
16. X.-Q. Wang and A.S. Mujumdar, *Int. J. Therm. Sci.* 46, 1 (2007).
17. Y. Wang, F. Su, C.D. Wood, J.Y. Lee, and X.S. Zhao, *Ind. Eng. Chem. Res.* 47, 2294 (2008).
18. D. Antiohos, M. Romano, J. Chen, and J.M. Razal, *Syntheses and Applications of Carbon Nanotubes and Their Composites*, ed. S. Suzuki (Rijeka: InTech, 2013), <https://doi.org/10.5772/51784>.
19. L.-M. Peng, Z. Zhang, and S. Wang, *Mater. Today* 17, 433 (2014).
20. H. He, L.A. Pham-Huy, P. Dramou, D. Xiao, P. Zuo, and C. Pham-Huy, *BioMed Res. Int.* 2013, 1 (2013).
21. V. Amenta and K. Aschberger, *WIREs Nanomed. Nanobiotechnol.* 7, 371 (2015).
22. W. Shao, P. Arghya, M. Yiyong, L. Rodes, and S. Prakash, *Syntheses and Applications of Carbon Nanotubes and Their Composites*, ed. S. Suzuki (Rijeka: InTech, 2013), <https://doi.org/10.5772/51785>.
23. K. Shi, J. Yan, E. Lester, and T. Wu, *Ind. Eng. Chem. Res.* 53, 15012 (2014).
24. J.O. Alves, J.A.S. Tenório, C. Zhuo, and Y.A. Levendis, *J. Mater. Res. Technol.* 1, 31 (2012).
25. H.M. Al-Swaidan, A. Ahmad, in *3rd International Conference on Chemical, Biological and Environmental Engineering*, (2011), pp. 25–31.
26. T.A. Hassan, V.K. Rangari, V. Fallon, Y. Farooq, S. Jeelani, in *Proceedings of the Nanotechnology Conference*, (2010), pp. 278–281.
27. S.S. Shams, L.S. Zhang, R. Hu, R. Zhang, and J. Zhu, *Mater. Lett.* 161, 476 (2015).
28. N.A. Fathy, *RSC Adv.* 7, 28535 (2017).
29. P. Gonugunta, S. Vivekanandhan, A.K. Mohanty, and M. Misra, *World J. Nano Sci. Eng.* 2, 148 (2012).
30. X.-W. Chen, O. Timpe, S.B.A. Hamid, R. Schlögl, and D.S. Su, *Carbon* 47, 340 (2009).
31. I. Abdullahi, N. Sakulchaicharoen, and J.E. Herrera, *Diam. Relat. Mater.* 41, 84 (2014).
32. N. Jeong, Y. Seo, and J. Lee, *Diam. Relat. Mater.* 16, 600 (2007).
33. M.S. Shamsudin, N.A. Asli, S. Abdullah, S.Y.S. Yahya, and M. Rusop, *Adv. Condens. Matter Phys.* 2012, 1 (2012).
34. D. Lopez, I. Abe, and I. Pereyra, *Diam. Relat. Mater.* 52, 59 (2015).
35. S.M. Toussi, A. Fakhru'l-Razi, A. Suraya, in *IOP Conference Series: Materials Science and Engineering*, vol. 17 (IOP Publishing, 2011), p. 012003.
36. M. Shamsudin, N. Asli, S. Abdullah, S. Yahya, and M. Rusop, *Adv. Condens. Matter Phys.* 2012, 420619 (2012).
37. Y. Jiang and C. Lan, *Mater. Lett.* 157, 269 (2015).
38. S. Alam, B. Seema, and F.K. Bangash, *J. Chem. Soc. Pak.* 31, 46 (2009).
39. G. Allaadini, S.M. Tasirin, and P. Aminayi, *J. Alloys Compd.* 647, 809 (2015).
40. O.-K. Park, H.-S. Chae, G.Y. Park, N.-H. You, S. Lee, Y.H. Bang, D. Hui, B.-C. Ku, and J.H. Lee, *Compos. B* 76, 159 (2015).

CHAPTER 4: VISCOSITY AND STABILITY OF GREEN NANOFLUIDS FROM COCONUT FIBRE CARBON NANOPARTICLES

Adewumi, G.A., Inambao, F.L., Sharifpur, M and Meyer J. Investigation of the Viscosity and Stability of Green Nanofluids from Coconut Fibre Carbon Nanoparticles: Effect of Temperature and Mass Fraction. *International Journal of Applied Engineering Research* ISSN 0973-4562 Volume 13, Number 10 (2018) pp. 8336-8342. (Published)

Investigation of the Viscosity and Stability of Green Nanofluids from Coconut Fibre Carbon Nanoparticles: Effect of Temperature and Mass Fraction

Gloria A Adewumi,^a Professor Freddie Inambao,^a Mohsen Sharifpur^b and Josua P Meyer^b

^a*Discipline of Mechanical Engineering, School of Engineering, University of KwaZulu-Natal, Howard College, 4041 South Africa.*

^b*Department of Mechanical and Aeronautical Engineering, University of Pretoria, Pretoria, 0002, South Africa.
inambaof@ukzn.ac.za; adewumigloria@gmail.com*

Abstract

This study entails the experimental measurements of the viscosity of 60:40% ethylene glycol (EG) and water (W) nanofluids containing nanoparticles obtained from coconut fibre. Furthermore, the effects of temperature and mass fraction of the synthesised nanoparticles on the relative viscosity of the green nanofluid was studied. The morphology of the prepared nanofluids was obtained using transmission electron microscope (TEM) while stability was determined by zeta potential, viscosity and UV spectroscopy measurements of nanofluids for 720 min. The nanofluids prepared were very stable for more than 720 min. The results of characterisation show that the average diameters of the spheres are between 30 nm to 60 nm. Also the results of experiments showed that with increase in temperature, the viscosity decreased. In addition, when the mass fraction was increased, there was an enhancement in viscosity of up to 50%.

Keywords: Coconut Fibre, Viscosity, Green Nanofluid, Green Precursor, Stability.

INTRODUCTION

Fluids with solid nanometer sized particles are called nanofluids and are an innovative class of fluids which have novel characteristics different from the base fluids. The base fluids used are usually conventional heat transfer fluids which are used for heat transfer applications. Nanofluids are becoming popular because they are high energy absorbing materials and they have the ability to skip the intermediate heat transfer state [1]. In addition, they have overall enhanced heat transfer efficiency. Previous base fluids used include: ethylene glycol, water, glycol, propylene glycol and oil. The dispersion of nanoparticles in these base fluids have proven to result in a corresponding improvement in the thermo-physical properties of the fluids [1-8].

The study of viscosity and stability of fluids is important in applications relating to flow of fluids as the knowledge of viscosity is used in determining the pumping power required which can in turn affect the efficiency of the system. A study on the viscosity of MWCNT based high temperature nanofluids shows a significant increase by doping MWCNT in alkali carbonate eutectic. The increase in viscosity was reported to be likely due to the aggregation of the nanotubes [2] which

increases the effective volume of the nanotubes [3]. The nanofluids in the study by [3] behaved as a shear thinning material at high particle content and as a Newtonian fluid at lower particle content.

With the on-going studies on nanoparticles and their applications, the issue of their effects on humans, animals and the environment is an issue of concern. Good as they may sound, adverse effects such as the ability to penetrate through skin cells in humans and animals are possible. It can also be absorbed into the lungs through inhalation which can lead to inflammation [9]. Exposure to this class of materials is somewhat unavoidable as they are part of our daily lives. They are present in the atmosphere, creams and liquids. According to a study conducted by Nowack and Bucheli [10], the oxides in metal nanoparticles are able to generate reactive oxygen species and this increases their toxicity. Cytotoxicity and genotoxicity are terms which refer to the death of cells which is also an adverse effect of nanoparticle reaction with human and animal cells [11].

Bio-based nanofluids are beginning to gain research focus because of their low toxicity and availability of the bio-precursors used. They are sourced from nature and are environmental friendly. Recent research has proven that plant and fruit parts after being synthesised can be dispersed in base fluids to produce nanofluids with enhanced thermo-physical properties. A composite containing agricultural waste materials and graphene was synthesised through simultaneous activation and the results yielded high electrical and thermal conductivities of 6.47 % increase at 40 °C and 787.5 % respectively [12]. Bio-nanofluids were also synthesised by [13, 14] in which clove buds were used to prepare carbon nanotubes and covalently functionalised nanoplatelets based nanofluids. The study was reported to have good potential for heat transfer applications. However, the natural convection heat transfer coefficient of nanofluids obtained from mango bark nanoparticles dispersed in water was found to deteriorate [15]. For the same mango bark nanoparticle based nanofluid, the thermal conductivity measurements showed a minor enhancement with the viscosity results showing an exponentially decreasing trend. Kallamu et al. [16] and Awua et al. [17] conducted an experimental study on the viscosity of nanofluids by using a two-step method that involved the dispersion of banana fibre-based nanoparticles and palm kernel fibre-based nanoparticles respectively obtained from ball-

milling into a suitable base fluid. The viscosity obtained from both authors was reported to be higher compared to the base fluid which increased with an increase in the volume fraction.

Several of the bio-nanofluids reviewed showed an enhancement in viscosity when compared to the base fluid which is not a good property in nanofluid flow and heat transfer applications. Viscosity is a crucial parameter in fluid flow which determines pumping power and pressure. Therefore, an ideal heat transfer fluid should possess lower viscosity and an increased thermal conductivity. The method of synthesis of these nanoparticles could be a contributing factor to their ineffective viscosity for heat transfer application. However, they may be ideal in applications relating to lubrication.

The present study aimed to investigate the influence of temperature and mass concentration on the viscosity of a new class of green nanofluids in which carbon nanospheres synthesised from a bio-based source, namely, coconut fibre was dispersed in 60:40 EG/W. The stability at different mass fractions was also studied.

MATERIALS AND METHODS

Carbon nanosphere synthesis from coconut fibre and its characterisation

Coconut fibre (CF) was obtained from local farmers in Oyo State, Nigeria. It was cleaned, cut into small sizes and dried in air for over three months. The CF was inserted into a heat resistant quartz tube and placed in a horizontal tube furnace (model MTF 12/38/400). Aerosol was generated from ethanol using an ultrasonic air humidifier (Model GMH-200) operating at 50 Hz. Nitrogen gas was passed through the aerosol mist at a flow rate of 200 mL/min; its function was to create an inert atmosphere for the reaction and to transport the aerosol droplets into the reactor chamber. The exhaust from the reactor was vented directly into the extraction system of the fume cupboard. The aerosol line was closed at the desired temperature, and the nitrogen gas was allowed to flow thereby cooling the system. The experimental procedure and characterisation has been described in our previous study [18] and the setup is presented in Fig. 1.



Figure 1. Experimental setup

Nanofluid preparation

The nanofluid was prepared by using a two-step method which involves the direct dispersal of nanoparticles in a suitable base fluid. A pre-calculated mass of the nanospheres corresponding to the desired weight fraction was weighed using a digital weighing balance (Highland HCB 1002, maximum 1000g, precision 0.001g from Adam equipment). The mixture of the nanospheres, gum arabic (GA) and 60:40 ethylene glycol/water (EG/W) was magnetically stirred using a hotplate stirrer (Lasec from Benchmark Scientific Inc., model-H4000-HSE) and sonicated with a 20 kHz, 700 Watts, QSonica ultrasonic processor. The nanofluid was kept in a programmable temperature bath (LAUDA ECO RE1225 Silver temperature bath) the whole time during sonication and the temperature was maintained at 15 °C.

Dry carbon nanospheres obtained from the synthesis of CF, ethylene glycol (Merck (Pty) Ltd), GA acquired from Fluka Analytical and deionised water was used for the nanofluid preparation. The nanotubes were dispersed in a base fluid consisting of 60:40% EG/DW in the weight concentration of 0.04 wt%, 0.08 wt% and 0.5wt% and 1 wt%. It was stirred with a magnetic stirrer for 2 h after which it was ultrasonicated for another 2 h. The diameters of the nanospheres are between 30 nm and 65 nm with the highest occurrence between 45 nm and 50 nm (Fig. 2).

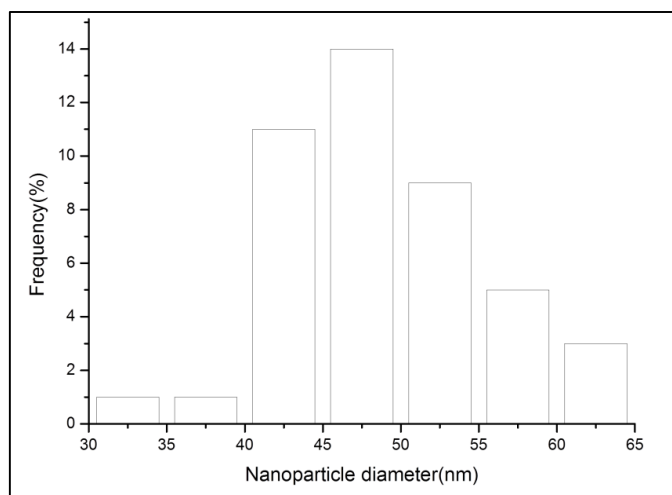


Figure 2. Particle size distribution of CNS

Viscosity and stability measurements

The instrument used for measuring viscosity is a piece of equipment known as a sine-wave vibroviscometer SV-10 from A&D Company Ltd., Japan. The cup used for measurement is connected to an adjustable temperature bath for effective sample temperature control. The viscometer uses a tuning-fork vibration technique to measure viscosity of fluids. The viscometer was calibrated using 99.5 % glycerol with manufacturer-stated viscosity of 1412 mPa.s at 20 °C. The viscosity was measured at a temperature range of 15 °C to 60 °C. The stability of the fluids was carried out by using zeta potential, viscosity measurements at a constant temperature for 700 min, and a UV Spectrometer.

NANOFLUID VISCOSITY

Existing models

Several models and relationships have been proposed to relate viscosity with parameters of nanofluids like mass concentration, temperature and morphology of nanoparticles. Pioneering work on the relationship between the viscosity of nanofluids and base fluids was carried out by Einstein [19]. He proposed a model which took into consideration fluids containing particles with a volume percentage of less than 1%.

$$\mu_{nf} = (1 + 2.5\phi)\mu_{bf} \quad (1)$$

Where: μ_{nf} is the nanofluid viscosity, μ_{bf} is the base fluid viscosity and ϕ is the volume fraction.

A particle volume fraction of up to 4 % in base fluid was proposed by Brinkman [20]. This was derived from Einstein's model:

$$\mu_{nf} = \mu_{bf} \left(\frac{1}{(1-\phi)^{2.5}} \right) \quad (2)$$

Batchelor [21] studied the effect of Brownian motion on fluids with spherical particles dispersed. His results were:

$$\mu_{nf} = \mu_{bf} (1 + 2.5\phi + 6.5\phi^2) \quad (3)$$

Selvakumar and Dhinakaran [22] recently developed a model to explain nanofluid viscosity by considering the phenomena of particle clustering and interfacial layer formation. This model is reported to be valid through all volume particle fractions:

$$\mu_{eff} = \mu_{bf} \left(1 - \frac{\phi_{ecs}}{\phi_m} \right)^{[\eta]\phi_m} \quad (4)$$

Where: μ_{eff} is effective viscosity, μ_{bf} is the base fluid viscosity, ϕ_{ecs} is the effective volume fraction of cluster spheres and ϕ_m is the maximum particle volume fraction which is usually taken as 0.605.

A correlation was developed by Sundar et al. [23] from experimental results obtained by putting into consideration the effects of temperature on the viscosity of nanofluids. This was developed to close the gap in the limitation of Einstein model:

$$\mu_{nf} = \mu_{bf} A e^{B\phi} \quad (5)$$

Where: A = 1.1216 and B = 77.56 (60:40 EG/W nanofluid).

Aberoumand et al. [24] have also considered the effect of temperature and volume fraction in their study.

$$\frac{\mu_{nf}}{\mu_{bf}} = (1.15 + 1.061\phi - 0.5442\phi^2 + 0.1181\phi^3) \quad (6)$$

RESULTS AND DISCUSSION

XRD and nanofluid stability

Fig. 3 shows the XRD pattern of the nanospheres obtained from CF. It shows two major broad peaks at (002) and (011) which signify a hexagonal graphite structure. The (002) peak is located at $\theta = 30^\circ$ while the (011) peak is found at $\theta = 51^\circ$.

The d-spacing is calculated as 0.33 nm. The stability of the green nanofluid was determined using zeta potential and viscosity at a constant temperature (20 °C) for 700 min.

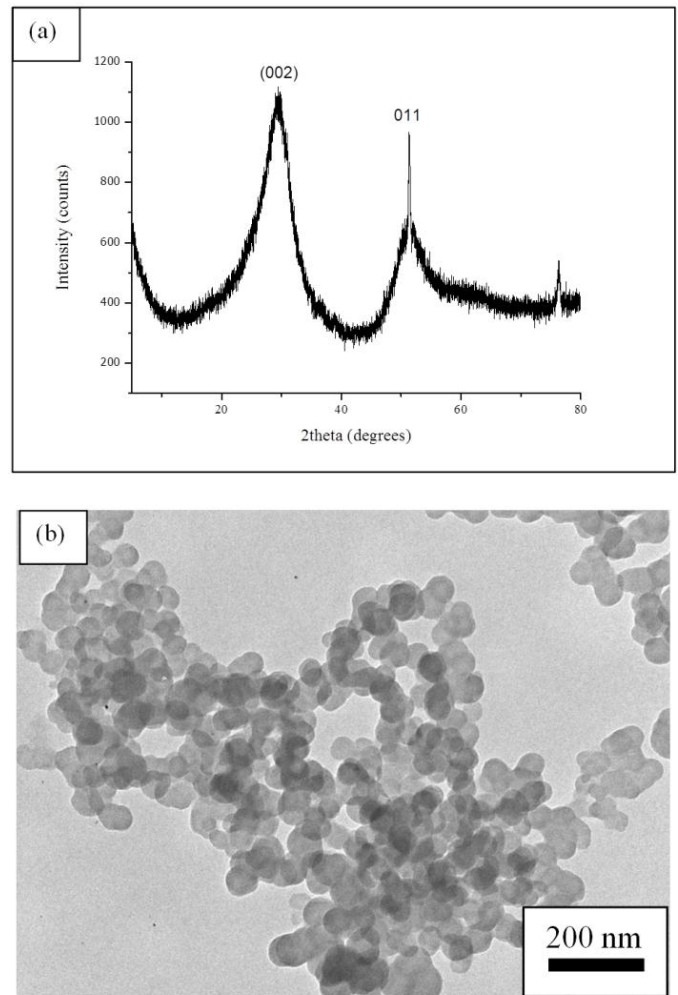


Figure 3. (a) XRD pattern. (b) TEM results

Nanofluid stability is a key parameter in nanofluid preparation and its subsequent application. A nanofluid with poor stability cannot be utilised in heat transfer applications and applications involving fluid flow. The stability of a nanofluid is affected by the surface charge present in the nanoparticles, while the index of the surface charge present is referred to as zeta potential. Fig. 4 shows a photograph of the nanofluids taken after one week. From Fig. 4(a), it is evident that there were complete sedimentations and the nanofluids displayed poor stability when the nanofluids were kept for one week for nanofluids with 1:1, 1:2, 1:2.5, and 1:3 of CNS/GA. However a good stability can be seen for nanofluid containing 1:3.5 CNS/GA. The zeta potential was measured for 0.04 wt%, 0.08 wt%, 0.5 wt% and 1 wt% dispersed in 60:40 EG/W and the obtained values were 84.8 mV, 130 mV, 126 mV and 120 mV respectively.

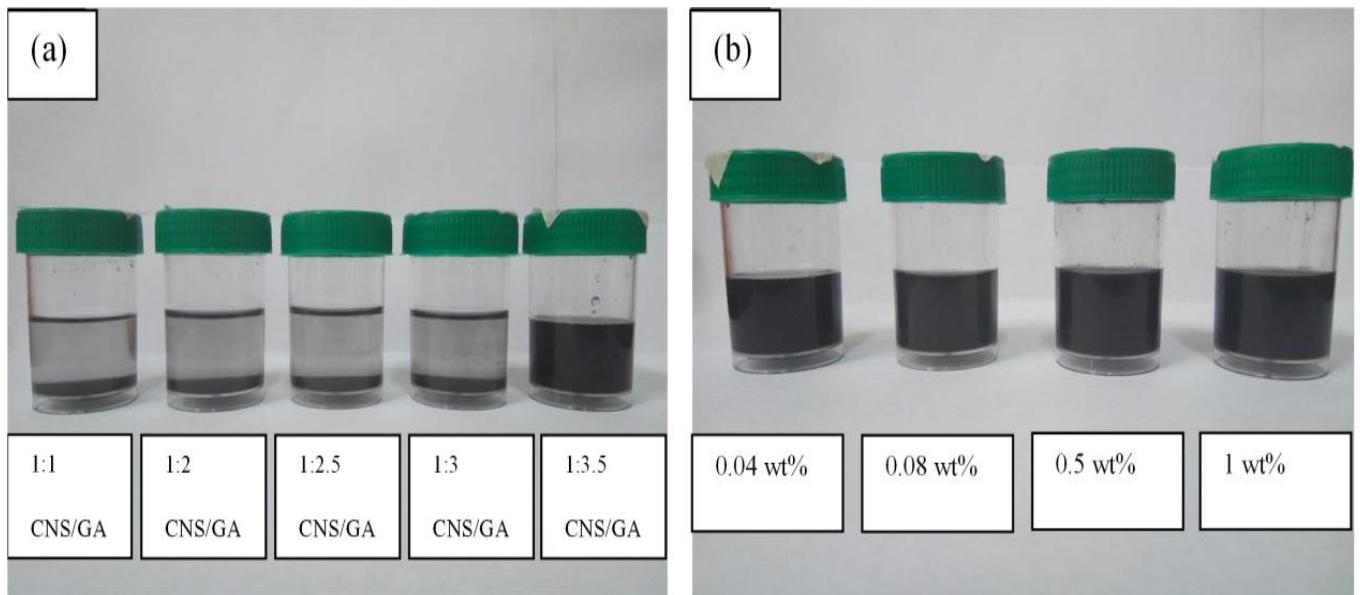


Figure 4. Photos of nanofluid: (a) After one week (b) After one week (1:3.5 CNS/GA)

Colloidal stability of the prepared nanofluids were further tested by measuring the viscosity at 20 °C for 720 min. Fig. 5 is the result of the observation from nanofluids which shows that the viscosity values were hardly changed for the whole duration. This is an indication that the fluids were stable for more than 720 min which is more than sufficient time to take the viscosity measurements. It was therefore determined that a ratio of 1:3.5 CNS/GA gave a good stability and this ratio was maintained throughout this study.

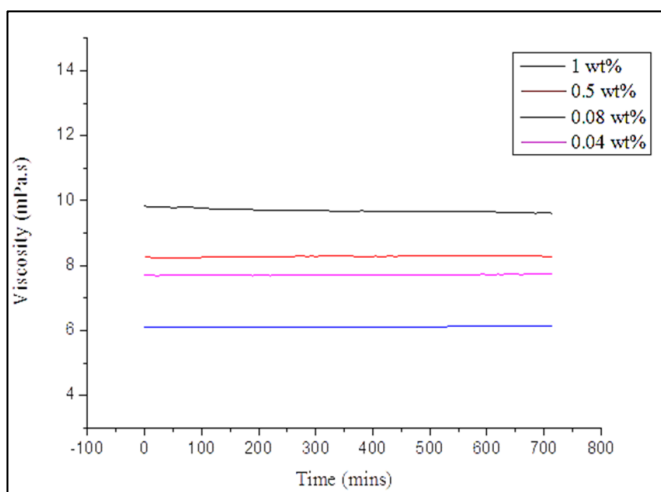


Figure 5 Stability test using viscosity at a constant temperature for 720 min

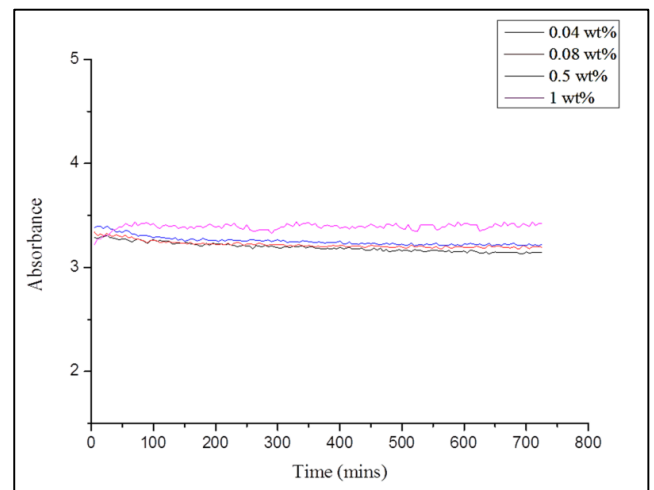


Figure 6. Stability test using UV spectroscopy at a constant temperature for 720 min

Nanofluid viscosity

Effect of temperature and mass fraction

In order to ensure minimal error in results, the viscometer was calibrated using deionised water at 25 °C. The measured value of deionised water at 25 °C is 0.883 mPa.s, which closely matches that of the theoretical value. The relative deviation is 0.7% which is of the same order as the degree of data uncertainty. Viscosity at various temperatures was measured from 15 °C to 60 °C for four different weight fractions (0.04 wt%, 0.08 wt%, 0.5 wt% and 1 wt%). The results are presented in Fig. 6. The results show that an increase or decrease in temperature has a significant impact on the viscosity value. The viscosity is seen to decrease as the temperature increases. This effect has been attributed to a decrease in intermolecular forces

arising from micro-convection [24]. This is in agreement with results from Sundar et al. [23] and Singh et al. [8] validating the theory that dispersing nanoparticles in a base fluid leads to a resistance between fluid layers which results in increased viscosity, which occurs in all the fluids at different mass fractions. Results from Fig. 7 indicate that the nanofluid with the mass concentration of 1 wt% had the highest viscosity compared with nanofluids of lower mass fractions. There is a similar trend in viscosity at various mass fractions which indicates a consistency in the obtained values.

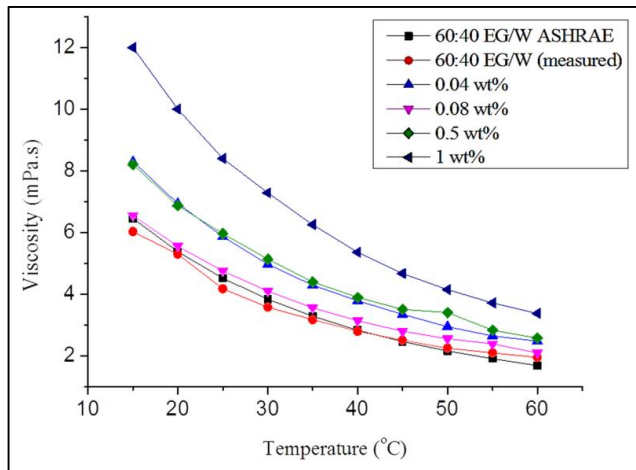


Figure 7. Nanofluid viscosity as a function of temperature

The relative viscosity presented in Fig. 8 indicates an almost constant value at all temperatures. These results are in line with those obtained in [3]. However, nanofluids with 1 wt% nanoparticles display a higher viscosity while it is interesting to note that nanofluids with 0.08 wt% have the lowest relative viscosity. The results show an increase in relative viscosity with an increase in nanoparticle concentration which is in contrast with studies carried out by Attari et al. where at the same mass fraction, an increase in temperature reduced the viscosity ratio of the nanofluids prepared.

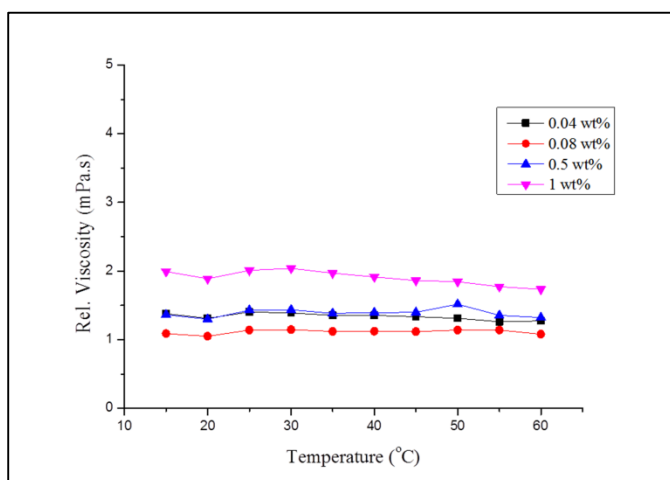


Figure 8. Nanofluid relative viscosity as a function of temperature

From Fig. 8, an enhancement in relative viscosity is observed for increasing mass fraction at all temperatures. At 0.08 wt% there is a drop in viscosity and it begins to improve again at higher mass fractions.

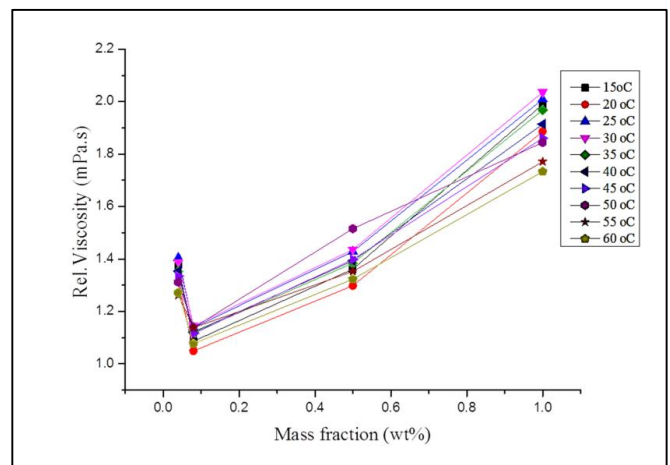


Figure 9. Nanofluid relative viscosity as a function of mass fraction

PROPOSED CORRELATION

A correlation for viscosity was proposed based on forty data points as given in Fig. 9. The various correlations at different mass concentrations are plotted in Fig 10. The figure shows very good relationship between the correlations and the obtained results.

Mass concentration 0.04 wt%,

$$\mu = 6E - 08T^5 - 1E - 05T^4 + 0.0007T^3 - 0.014T^2 - 0.1798T + 12.43 \quad (R^2 = 1) \quad (7)$$

Mass concentration 0.08 wt%,

$$\mu = -5E - 08T^5 + 1E - 05T^4 - 0.0007T^3 + 0.0262T^2 - 0.6664T + 12.526 \quad (R^2 = 1) \quad (8)$$

Mass concentration 0.5 wt%,

$$\mu = -3E - 08T^5 + 5E - 06T^4 - 0.0003T^3 + 0.0146T^2 - 0.5587T + 14.127 \quad (R^2 = 0.9983) \quad (9)$$

Mass concentration 1 wt%

$$\mu = 9E - 08T^5 + 2E - 05T^4 - 0.0015T^3 + 0.0643T^2 - 1.6087T + 25.961 \quad (R^2 = 0.9999) \quad (10)$$

The experimental values obtained from this study can be estimated from the correlations proposed at different mass concentrations. The following correlation can only predict viscosity of CF-based 60:40 EG/W based nanofluids at mass fractions of 0.04 wt%, 0.08 wt%, 0.5 wt% and 1 wt%. The following correlation was also evaluated based on the experimental data for relative viscosity of the prepared nanofluids at 20 °C:

$$\mu_{nf} = 0.2127\phi^2 - 0.8861\phi + 1.9561 \quad (11)$$

With polynomial goodness of fit $R^2 = 0.9961$

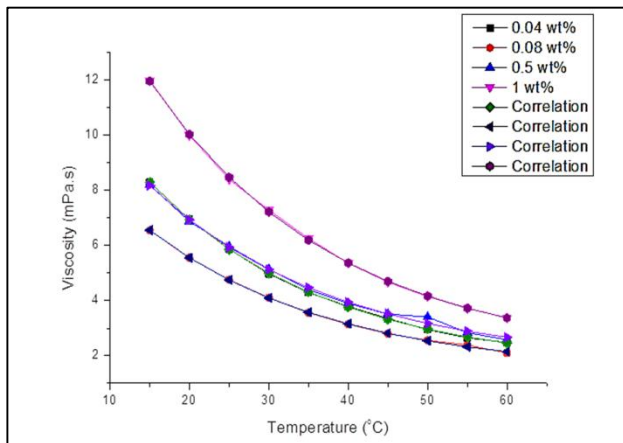


Figure 10. Correlations obtained compared with results

CONCLUSION

In this article, the viscosity and stability of green nanofluids prepared from CF was investigated. The base fluid used was 60:40 ethylene glycol/water and GA was the surfactant used. The results of TEM analysis and particle size distributions show spherical carbon nanoparticles with diameters of between 30 nm and 65 nm. Stability analysis was carried out using visual analysis, zeta potential, viscosity values for a period of 720 min, and UV-Vis spectroscopy. The results indicate a very stable fluid with high zeta potential values. It can also be depicted from the values obtained that addition of these green nanoparticles in 60:40 EG/W have a significant effect on the nanofluids' viscosity which is a function of temperature and nanoparticle mass fraction. The viscosity of the nanofluids at different mass fractions decreases with an increase in temperature, while the relative viscosity remains fairly constant with an increase in temperature. An increase in mass fraction enhances the viscosity of nanofluids at all temperatures under study. Empirical correlations have been developed to predict the viscosity of nanofluids at different temperatures and mass fractions.

ACKNOWLEDGEMENTS

The financial assistance of the National Research Foundation (NRF) South Africa (Grant number 109819) towards this research is hereby acknowledged. Opinions expressed and conclusions arrived at are those of the author and are not necessarily to be attributed to the NRF.

REFERENCES

[1] R. A. Taylor, P. E. Phelan, T. P. Otanicar, C. A. Walker, M. Nguyen, S. Trimble and R. Prasher, "Applicability of nanofluids in high flux solar collectors," *Journal of Renewable and Sustainable Energy*, vol. 3, no. 2, p. 023104, 2011.

[2] B. Jo and D. Banerjee, "Viscosity measurements of multi-walled carbon nanotubes-based high temperature nanofluids," *Materials Letters*, vol. 122, pp. 212-215, 2014.

[3] S. Halelfadl, P. Estellé, B. Aladag, N. Doner, and T. Maré, "Viscosity of carbon nanotubes water-based nanofluids: Influence of concentration and temperature," *International Journal of Thermal Sciences*, vol. 71, pp. 111-117, 2013.

[4] Y. Ding, H. Alias, D. Wen, and R. A. Williams, "Heat transfer of aqueous suspensions of carbon nanotubes (CNT nanofluids)," *International Journal of Heat and Mass Transfer*, vol. 49, no. 1-2, pp. 240-250, 2006.

[5] S. Halelfadl, T. Maré, and P. Estellé, "Efficiency of carbon nanotubes water based nanofluids as coolants," *Experimental Thermal and Fluid Science*, vol. 53, pp. 104-110, 2014.

[6] L. Syam Sundar, E. Venkata Ramana, M. K. Singh, and A. C. M. Sousa, "Thermal conductivity and viscosity of stabilized ethylene glycol and water mixture Al₂O₃ nanofluids for heat transfer applications: An experimental study," *International Communications in Heat and Mass Transfer*, vol. 56, pp. 86-95, 2014.

[7] H. Cheng, W. T. Ma, W. Hu, J. F. Wu, J. Xiao, Z. B. Chen, Q. J. Zhang & N. M. Wereley, "Carbon nanotubes suspended in ethylene glycol yield nanofluids with enhanced heat transfer properties," *WIT Trans. Eng. Sci*, vol. 83, pp. 73-80, 2014.

[8] N. Singh, G. Chand, and S. Kanagaraj, "Investigation of Thermal Conductivity and Viscosity of Carbon Nanotubes–Ethylene Glycol Nanofluids," *Heat Transfer Engineering*, vol. 33, no. 9, pp. 821-827, 2012/07/01 2012.

[9] M. Sajid, M. Ilyas, C. Basheer, M. Tariq, M. Daud, N. Baig, F. Shehzad, "Impact of nanoparticles on human and environment: review of toxicity factors, exposures, control strategies, and future prospects," *Environmental Science and Pollution Research*, journal article vol. 22, no. 6, pp. 4122-4143, March 01 2015.

[10] B. Nowack and T. D. Bucheli, "Occurrence, behavior and effects of nanoparticles in the environment," *Environmental pollution*, vol. 150, no. 1, pp. 5-22, 2007.

[11] B. A. Jamuna and R. V. Ravishankar, "Environmental Risk, Human Health, and Toxic Effects of Nanoparticles," in *Nanomaterials for Environmental Protection*: John Wiley & Sons, Inc, 2014, pp. 523-535.

[12] H. Yarmand, S. Gharekhani, S. F. S. Shirazi, A. Amiri, E. Montazer, H. K. Arzani, R. Sadri, M. Dahari, S. Kazi, "Nanofluid based on activated hybrid of biomass carbon/graphene oxide: synthesis, thermo-physical and electrical properties," *International*

Communications in Heat and Mass Transfer, vol. 72, pp. 10-15, 2016.

- [13] R. Sadri, M. Hosseini, S. N. Kazi, S. Bagheri, Ali H. Abdelrazek, G. Ahmadi, N. Zubir, R. Ahmad and N. I. Z. Abidin. "A facile, bio-based, novel approach for synthesis of covalently functionalized graphene nanoplatelet nano-coolants toward improved thermo-physical and heat transfer properties," *Journal of Colloid and Interface Science*, 509, pp. 140-152, 2017.
- [14] R. Sadri, M. Hosseini, S. N. Kazi, S. Bagheri, N. Zubir, K. H. Solangi, T. Zaharinie, A. Badarudin, "A bio-based, facile approach for the preparation of covalently functionalized carbon nanotubes aqueous suspensions and their potential as heat transfer fluids," *Journal of Colloid and Interface Science*, vol. 504, pp. 115-123, 2017.
- [15] A. B. Solomon, M. Sharifpur, J. P. Meyer, J. Ibrahim, and B. Immanuel, "Convection heat transfer with water based mango bark nanofluids," Paper presented at the 13th International Conference on Heat Transfer, Fluid Mechanics and Thermodynamics, Portoroz, Slovenia on 17-19 July 2017.
- [16] U. M. Kallamu, J. Ibrahim, M. Sharifpur, and J. Meyer, "Experimental Investigation on Viscosity Of Nanofluids Prepared From Banana Fibre-Nanoparticles," 12th International Conference on Heat Transfer, Fluid Mechanics and Thermodynamics (HEFAT 2016), Costa del Sol, Spain, 2016, 2016.
- [17] J. Awua, J. Ibrahim, A. Kwagheger, M. Sharifpur, and J. Meyer, "Investigation into thermal conductivity of palm kernel fibre nanofluids with mixture of ethylene glycol/water as base fluid," 12th International Conference on Heat Transfer, Fluid Mechanics and Thermodynamics (HEFAT 2016), Costa del Sol, Spain, 2016, 2016.
- [18] G. A. Adewumi, N. Revaprasadu, A. C. Eloka-Eboka, F. L. Inambao, and C. Gervas "A Facile Low-cost Synthesis of Carbon Nanosphere from Coconut Fibre," in *Proceedings of the World Congress on Engineering and Computer Science*, vol. 2. pp. 577-582, 2017
- [19] A. Einstein, "Eine neue bestimmung der moleküldimensionen," *Annalen der Physik*, vol. 324, no. 2, pp. 289-306, 1906.
- [20] H. Brinkman, "The viscosity of concentrated suspensions and solutions," *The Journal of Chemical Physics*, vol. 20, no. 4, pp. 571-571, 1952.
- [21] G. Batchelor, "The effect of Brownian motion on the bulk stress in a suspension of spherical particles," *Journal of Fluid Mechanics*, vol. 83, no. 1, pp. 97-117, 1977.
- [22] R. D. Selvakumar and S. Dhinakaran, "Effective viscosity of nanofluids—A modified Krieger–Dougherty model based on particle size distribution (PSD) analysis," *Journal of Molecular Liquids*, vol. 225, pp. 20-27, 2017.
- [23] L. S. Sundar, E. V. Ramana, M. K. Singh, and A. C. Sousa, "Thermal conductivity and viscosity of stabilized ethylene glycol and water mixture Al₂O₃ nanofluids for heat transfer applications: an experimental study," *International Communications in Heat and Mass Transfer*, vol. 56, pp. 86-95, 2014.
- [24] S. Aberoumand, A. Jafarimoghaddam, M. Moravej, H. Aberoumand, and K. Javaherdeh, "Experimental study on the rheological behavior of silver-heat transfer oil nanofluid and suggesting two empirical based correlations for thermal conductivity and viscosity of oil based nanofluids," *Applied Thermal Engineering*, vol. 101, pp. 362-372, 2016.

CHAPTER 5: ELECTRICAL CONDUCTIVITY OF CARBON NANOSPHERE-BASED GREEN NANOFUIDS

Adewumi, G.A., Inambao, F.L., Sharifpur, M. and Meyer J. Investigation into the Electrical Conductivity of Carbon Nanosphere-Based Green Nanofluids. *Transactions on Engineering Technologies: World Congress on Engineering and Computer Science*, 2017. (Under Review)

INVESTIGATION INTO THE ELECTRICAL CONDUCTIVITY OF CARBON NANOSPHERE-BASED GREEN NANOFUIDS

Gloria Adedayo Adewumi¹, Freddie Inambao², Mohsen Sharifpur³ and Josua Meyer⁴

Gloria A Adewumi,^{*a} Freddie Inambao,^a Mohsen Sharifpur^b and Josua P Meyer^b

- a. Discipline of Mechanical Engineering, School of Engineering, University of KwaZulu-Natal, Howard College, 4041 South Africa
- b. Department of Mechanical and Aeronautical Engineering, University of Pretoria, Pretoria, 0002, South Africa.

(Corresponding author: Gloria Adewumi, Address: 280 Sphiwe Zuma Avenue, Glenmore, South Africa, 4001. email: adewumigloria@gmail.com tel: +27749423154)

Abstract

Electrical conductivity measurements of green nanofluids prepared from carbon nanospheres dispersed in 60:40 ethylene glycol and water (60:40 EG/W) based nanofluids have been studied. In order to investigate the effect of temperature and volume concentration on the electrical conductivity of the nanofluids, the temperature was varied from 15 °C to 60 °C and volume fractions of 0.04, 0.1, 0.12, and 0.2 vol% were used. The results show that the electrical conductivity is greatly enhanced with an increase in temperature and volume fraction. The highest enhancement is seen at 0.2 vol% with 1 470 % increase in electrical conductivity. The high conductivity enhancement indicates a potential for cooling applications.

Keywords: Activated carbon, Carbon nanospheres, Coconut fibre, Electrical conductivity, Green nanofluids, Green nanoparticles, Temperature, Volume concentration.

5.1 Introduction

Synthesis of nanoparticles from “green” bio-precursors has environmental advantages over other conventional methods because of their low-costs and low-toxicity [1, 2]. Nanomaterials synthesized from plants already have their surfaces functionalized; an advantage which is absent in synthetic nanomaterials, and this enables them to have better dispersability and stability in base-fluids and subsequently enhanced properties [3]. A detailed review by Buzea,

et al. [4] outlines the numerous effects of nanoparticle exposure on the human body and environment. These effects can be reduced by investing more into “green” nanotechnology.

A study by Kumar et al. [5] investigated the use of natural sources such as fossil hydrocarbons, waste natural products and botanical hydrocarbon precursors as a means of synthesizing carbon nanomaterials and graphene. It was revealed that those based on fossil hydrocarbons are mostly expensive and not readily accessible. In addition, a lot of the liquid and gaseous fossil hydrocarbons are explosive or toxic in nature and are not acceptable due to atmospheric pollution and its negative effect on human health. On the other hand, carbon nanomaterials derived from carbon based natural precursors have the advantage of producing scalable amounts, they are safe to use in the environment, are cheap, and allow for fast production techniques.

Thermophysical properties of fluids are those properties that vary with temperature and yet do not have any impact on the chemical structure of the fluid. Just like other thermo-physical properties, electrical conductivity of fluids needs to be enhanced as this can improve the overall working efficiency of their applications relating to cooling, such as in proton electron membranes (PEM) [6]. They can also improve the life span of the electrodes used in metallic cathodes and nozzles [7]. To deal with emission issues, PEM fuel cells are starting to be used in place of batteries as they are light-weight, quiet, have exceptional storage density and possess high fuel energy efficiency [8]. The life span of electrodes is influenced by the electrical conductivity of the liquids flowing through them.

The concept of electrical conductivity arises from the movement of ions in a medium. When an electric field is applied to the medium or nanofluids, the central ion will be attracted and the result is an asymmetric field from a formerly symmetric field [9].

From Stokes law, the hydrodynamic force needed for the movement of a spherical body with radius r and a velocity through a fluid with viscosity μ is given as [9]:

$$F_s = 6\pi\mu r v \quad (1)$$

For microscopic particles with relatively same size as the base fluid, the hydrodynamic drag force on an ion moving under the influence of a chemical potential gradient is [9]:

$$-F_d = 6\pi\mu r_i v_i \quad (2)$$

Where r_i and v_i is the radius and velocity of i ion respectively. The Navier-Stokes equation is given as [9]:

$$D_i = \frac{kT}{6\pi\mu r_i} \quad (3)$$

Where D_i , k and T are the diffusion coefficient of the ion, thermal conductivities and temperatures respectively. When there is movement of ions in a solution, the local solvent molecules are dragged along. For electric current to be created in a fluid, the positive and negative ions move in opposite directions under the influence of an electromagnetic force (e.m.f). This results in an electrophoretic effect with a counter-current velocity v_e [9]. If the number of positive ions is denoted as n_{+ve} and the number of negative ions as n_{-ve} both having drift velocities of v_{+ve} and v_{-ve} respectively with charge q_{+ve} and q_{-ve} respectively, then the current density J will be [10]:

$$J = n_{+ve}q_{+ve}v_{+ve} - n_{-ve}q_{-ve}v_{-ve} \quad (4)$$

Equation (4) can also be written as:

$$J = \frac{nq^2\tau_f E}{m} \quad (5)$$

Where τ_f , E , and m are the mean free time, electric field and mass respectively. From Ohms law, the electrical conductivity σ is:

$$\sigma = \frac{J}{E} \quad (6)$$

Combining equation (5) and equation (6):

$$\sigma = \frac{nq^2\tau_f}{m} \quad (7)$$

The electrical conductivity in nanofluids can be assumed to be governed by the number of ions present per unit of volume and their respective drift velocities [10].

From past research [7, 11-14], conclusions can be made that the electrical conductivity of nanofluids depend on temperature, volumetric concentration and particle diameter. Increasing the volumetric concentration increases the conducting pathway and therefore increases the electrical conductivity. Similarly, increasing the temperature of the nanofluids will result in a decrease in viscosity thereby enhancing the mobility of ions in the nanofluids. In addition, the numbers of ions are increased due to molecular dissociation, resulting in enhanced electrical

conductivity [11]. The interface effect was considered by [15] as a factor that could enhance the electrical conductivity in carbon nanotubes as the electrical conductivity of complex CNTs in their study decreased rapidly with increasing interfacial layer thickness depending on the percolation threshold.

Coconut fibre (CF) is obtained from the pericarp of coconut fruit and a coconut is made up of 33 % to 35 % of husk. Presently, CF are being used as fuel in the processing of coconut-based products, as a fibre source for manufacturing ropes and mats and as a fuel for domestic application [16]. To benefit from this plentiful and low-cost agricultural waste, CF has been transformed into a carbon nanomaterial in the present study. The conversion of CF into carbon nanomaterials will function as an important raw material obtained from agricultural waste as they are bacteria and fungi resistant. Carbon is a group 14 element that is distributed very widely in nature. It also has a remarkable ability to bond with several other elements as a result of its polyvalent properties creating structures with distinct properties. Recent research has turned carbon into nanoscale, resulting in carbon nanospheres, carbon nanotubes and carbon nanofibres. Heptagonal and pentagonal pairing of carbon atoms can result in the creation of carbon nanospheres. The graphite sheets in nanospheres occur as waving flakes instead of closed shells which take the form of a sphere, hence having several open ends at the surface, and thus establishing carbon nanospheres (CNS) as suitable materials for catalytic and adsorption application [17].

Laboratory fabrication of carbon nanospheres involve methods such as chemical vapour deposition (CVD) [18-21], hydrothermal treatment [22], pyrolysis of polymers [23], ultrasonic treatments and chlorination of cobaltocene [24]. Generally, chemical vapour deposition (CVD) occurs when rare earth metal oxides or metal oxides are used as catalysts which results in a need for purification of the synthesized carbon spheres in order to get rid of the catalyst. This makes the process limited to a small scale [25]. Various sources of biomass are being used for the production of nanomaterials derived from carbon [26, 27] because of their low toxicity and availability. These biomasses are often first carbonized, and then activated before being converted to carbon nanomaterials using different methods [28-33]. The method of activation used can either be physical (thermal), chemical or a combination of both physical and chemical processes [16]. The physical process involves the use of CO₂, steam or air and takes place at higher temperatures while the chemical process which is one-step, takes place at lower temperatures and involves the co-carbonization of a parent feedstock with a suitable chemical compound.

To the best of the authors' knowledge, there has been no study carried out on the behavior of electrical conductivity of green nanofluids from CF-based nanospheres. In this study, the authors present the results from the dispersion of already synthesized carbon nanospheres from coconut fibre in 60:40 ethylene glycol/water (EG/W) and finally electrical conductivity measurements. The effect of volume concentration and temperature on the electrical conductivity was also reported.

5.2 Experimental Method

5.2.1 Materials and Stable Nanofluid Preparation

Nanoparticles used in this study were synthesized from CF. They were first carbonized followed by physical activation in the presence of CO₂ and then treated with ethanol vapour at 800 °C. The procedure is outlined in our previous study of the synthesis procedure in [34]. A known weight of the nanoparticles were measured using a digital weight balance (RADWAG model: AS 220.R2 Max: 220 g Min: 10 mg) and dispersed in 60:40 EG/W (Merck (Pty) Ltd), gum arabic (GA) acquired from Fluka Analytical and deionized water was used for the nanofluid preparation. The nanotubes were dispersed in a base fluid consisting of 60%:40% EG/W in the volume fractions of 0.04 %, 0.1 %, 0.12 % and 0.2 % respectively. The mixture of the nanoparticles, GA and 60:40 ethylene glycol/water (EG/W) was magnetically stirred using a hotplate stirrer (Lasec from Benchmark Scientific Inc., model-H4000-HSE) and sonicated with a 20 kHz, 700 Watts, QSonica ultrasonic processor. The nanofluid was kept in a programmable temperature bath (LAUDA ECO RE1225 Silver temperature bath) the whole time of sonication and the temperature maintained at 15 °C.

The nanospheres are in the size range of 10 nm to 150 nm and the size with the highest occurrence is 60 nm to 89 nm. From Fig. 1, nanospheres of diameter in the range 60 nm to 89 nm constituted almost 50 % (48.5 %) while nanospheres of diameter 30 nm to 59 nm constituted 41 %. This shows uniformity in the size range of the nanospheres. The particle size distribution and morphology of the green nanoparticles is given in Fig 5.1. The morphology indicates smooth round nanospheres with some degree of aggregation due to strong Van der Waals forces. These aggregates can lead to reduced stability and electrical conductivity, hence the need to break the agglomerates.

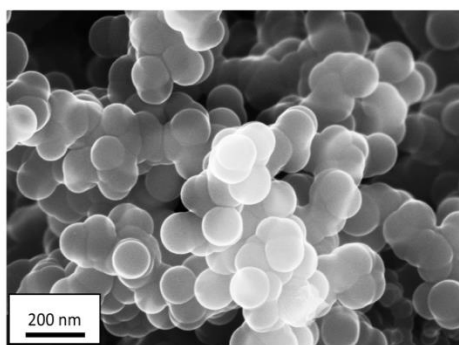
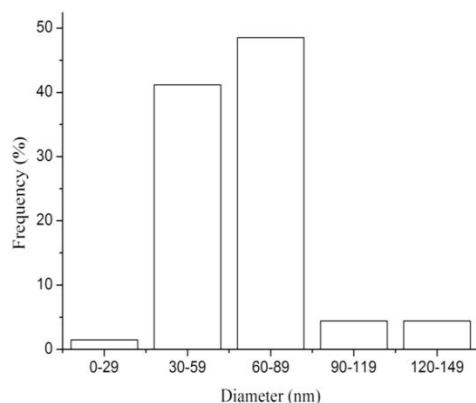


Fig. 5.1. Nanosphere particle size distribution

5.3 Measurement of Electrical Conductivity

A CON700 conductivity meter was used to measure electrical conductivity (EUTECH instruments). The CON700 conductivity meter is comprised of an electrode with a nominal cell constant of $k = 1.0$, built-in temperature sensor, and 1 meter cable. The electrode design offers fast temperature response and reduces air entrapment, ensuring accurate, repeatable, and stable readings. Measurements were taken at temperatures ranging from 15 °C to 60 °C at 5 °C intervals. This temperature control was done using a temperature control bath. The conductivity meter was initially calibrated at room temperature with a 1413 μS standard fluid from the supplier.

5.4 Results and Discussion

5.4.1 XRD and Stability of Nanofluid

The graphitization and crystallinity of the synthesized nanospheres was studied using XRD analysis. Fig. 5.2 is the XRD results which shows two Bragg diffraction peaks at 30.34° and 50.44° . These peaks can be assigned to typical graphite (003) and (101) planes [35]. The d-

spacing calculated is 0.342 nm which is close to graphite 3R given as 0.340 nm. The broadening peaks suggest a low graphitization degree and the possibility of the presence of amorphous carbon. These results fall in the range of values from authors [36] and [37] who found d-spacing of 0.33 nm and 0.36 nm respectively. No other peaks are visible in the XRD pattern, which could be due to the high purity of the product.

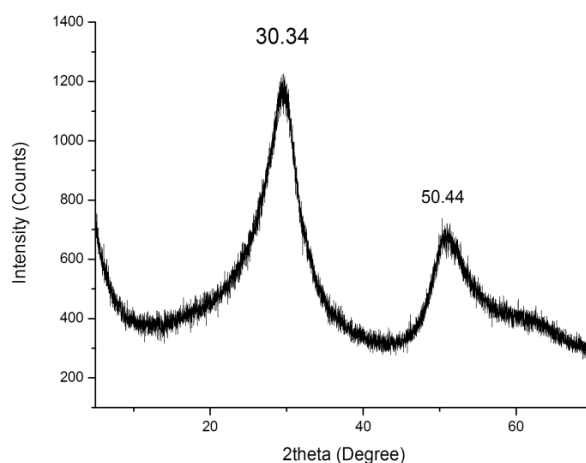


Fig. 5.2. XRD pattern of carbon nanospheres synthesized at 1100 °C

Fig. 5.3 confirms the purity of the material with a well-defined presence of carbon (98.59 %) with a trace of oxygen and potassium.

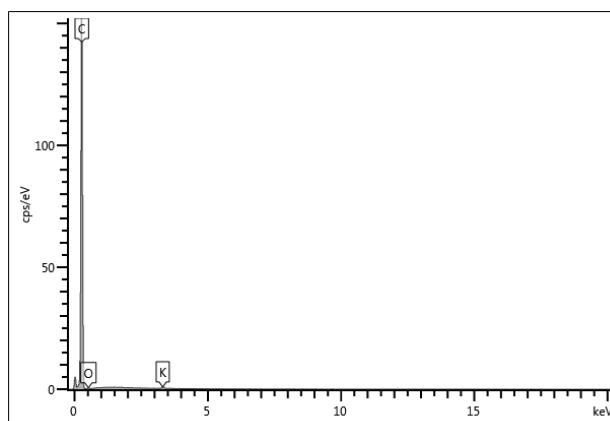


Fig. 5.3. EDX of CNS

The stability of the green nanofluid was determined by observing the viscosity at a constant temperature (20 °C) for 720 min. Fig. 5.4 is the result of the observation from stability of nanofluids which shows that the viscosity values were hardly changed for the whole duration. This is an indication that the fluids were stable for more than 720 min which is more than

sufficient time to take the electrical conductivity measurements. It was therefore determined that a ratio of 1:3.5 CNS/GA gave a good stability and this ratio was maintained throughout this study.

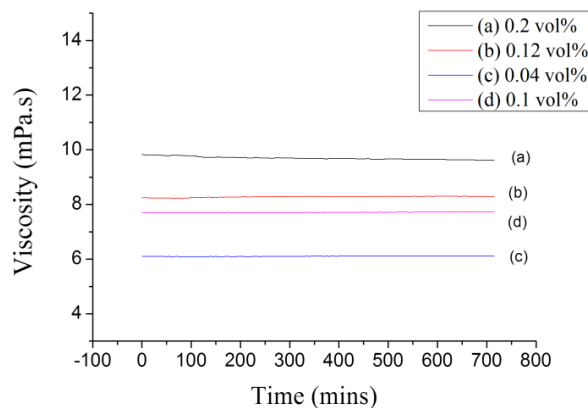


Fig. 5.4. Stability test using viscosity at a constant temperature for 720 min

5.4.2 Electrical Conductivity Evaluation

Temperature effects on the electrical conductivity of prepared green nanofluids from coconut fibre nanosphere are shown in Fig. 5.5. The results indicate the dependence of electrical conductivity on temperature. From Fig.5. 6 the effect of the nanosphere volume concentration on the electrical conductivity is reported. The result reveals that an increase in the nanosphere loading impacted greatly on the electrical conductivity as this led to a change in the ionic configuration [38].

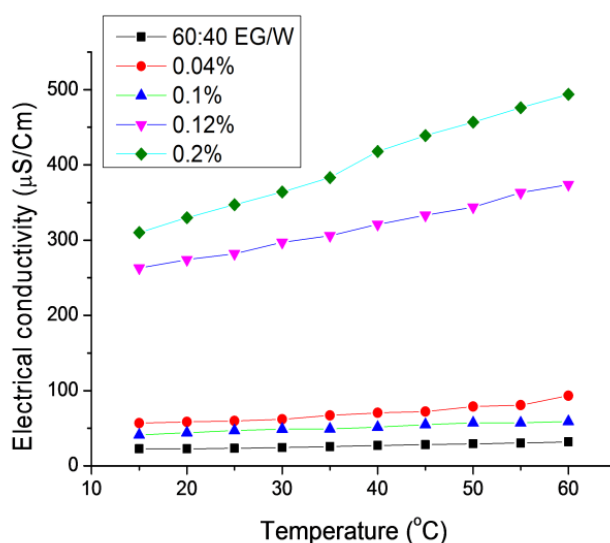


Fig. 5.5. Electrical conductivity at different temperatures for different volume concentrations

At 0.2 % volume fraction, the highest electrical conductivity was observed at all temperatures. This is in line with results from recent studies on nanofluids electrical conductivity [38]. With an increase in particle volume concentration, the availability of conducting pathways is increased in the nanofluids, consequently leading to a rise in electrical conductivity.

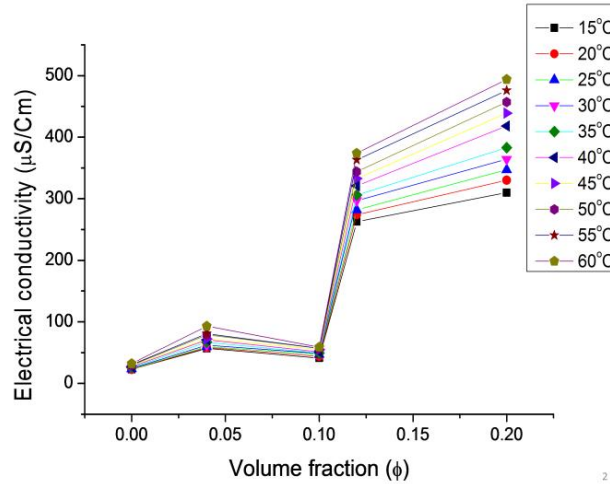


Fig. 5.6. Electric conductivity at various mass fractions

The electrophoretic mobility in nanofluids is also increased when it is stable thereby reducing equivalent particulate masses resulting in an increased electrical conductivity [12]. It is therefore safe to say increasing the temperature of nanofluids reduces the equivalent particulate masses and increases the electrophoretic mobility. The enhancement in electrical conductivity was calculated based on equation 3 [13]:

$$\frac{\sigma_{nf} - \sigma_{bf}}{\sigma_{bf}} \times 100 \tag{8}$$

Where σ_{nf} is the nanofluids electrical conductivity and σ_{bf} is the base fluid electrical conductivity. From Fig. 5.7 and Fig. 5.8, the percentage enhancement in electrical conductivity increases with an increase in temperature and volume fraction. At 0.04 vol% an enhancement of about 100 % is seen while an enhancement of 1 470 % is observed at 55 °C for 0.2 vol%.

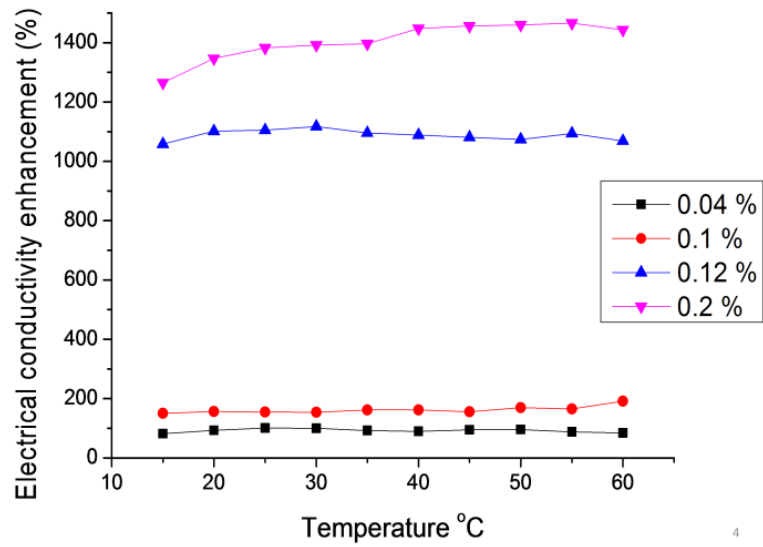


Fig. 5.7. Electrical conductivity enhancements at various temperatures for different volume concentrations

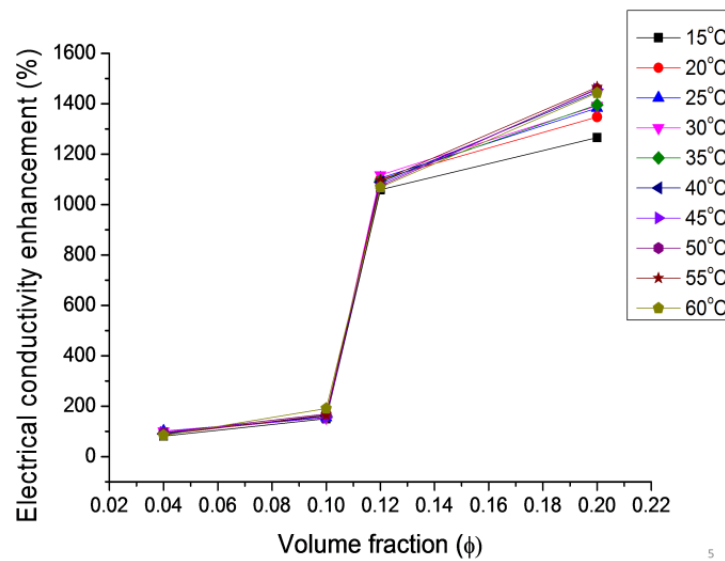


Fig. 5.8. Electrical conductivity enhancement at different volume fractions

5.5 Conclusion

This study presents the results on the electrical conductivity behavior of green nanospheres synthesized from coconut fibre dispersed in 60:40 EG/W and 1:3.5 nanosphere/GA. The measurement of electrical conductivity was varied with volume concentration and temperature. The results obtained show an improved electrical conductivity with increase in temperature and volume concentration. At 0.2 vol%, a maximum electrical conductivity of 1 470% was

achieved at a temperature of 55 °C. The results presented show the potentials of carbon nanosphere-based green nanofluids as heat transfer fluid for cooling applications. Due to its less toxic nature, it can also be used in applications where human contact is required.

Acknowledgement

The financial assistance of the National Research Foundation (NRF) towards this research is hereby acknowledged.

References

- [1] B. Orhevba, M. Umaru, I. A. Garba, B. Suleiman, M. U. Garba, and N. Ernest, Synthesis of Composite Biomass Briquettes as Alternative Household Fuel for Domestic Application, Lecture Notes in Engineering and Computer Science: Proceedings of the World Congress on Engineering and Computer Science 2016, WCECS 2016, October 19-21, 2016, San Francisco, USA, pp 696-700.
- [2] J. D. Bayani, J. R. M. D. Pena, and E. R. Magdaluyo Jr, Infrared Spectra and Mechanical Properties of Corn Oil-based Polyurethane Reinforced with Silica Nanoparticles from Rice Husk Ash, Lecture Notes in Engineering and Computer Science: Proceedings of the World Congress on Engineering 2016, WCE 2016, June 29 - July 1, 2016, London, U.K., pp 998-1002.
- [3] V. Makarov *et al.*, "'Green' Nanotechnologies: Synthesis of Metal Nanoparticles Using Plants," *Acta Naturae (англоязычная версия)*, vol. 6, no. 1 (20), 2014.
- [4] C. Buzea, I. I. Pacheco, and K. Robbie, "Nanomaterials and Nanoparticles: Sources and Toxicity," *Biointerphases*, vol. 2, no. 4, pp. MR17-MR71, 2007.
- [5] R. Kumar, R. K. Singh, and D. P. Singh, "Natural and Waste Hydrocarbon Precursors for the Synthesis of Carbon Based Nanomaterials: Graphene and CNTs," *Renewable and Sustainable Energy Reviews*, vol. 58, pp. 976-1006, 2016.
- [6] M. R. Islam, B. Shabani, and G. Rosengarten, "Electrical and Thermal Conductivities of 50/50 Water-ethylene Glycol Based TiO₂ Nanofluids to be Used as Coolants in PEM Fuel Cells," *Energy Procedia*, vol. 110, pp. 101-108, 2017.
- [7] H. Konakanchi, R. Vajjha, D. Misra, and D. Das, "Electrical Conductivity Measurements of Nanofluids and Development of New Correlations," *Journal of Nanoscience and Nanotechnology*, vol. 11, no. 8, pp. 6788-6795, 2011.
- [8] J. W. Pratt, L. E. Klebanoff, K. Munoz-Ramos, A. A. Akhil, D. B. Curgus, and B. L. Schenkman, "Proton Exchange Membrane Fuel Cells for Electrical Power Generation On-Board Commercial Airplanes," *Applied Energy*, vol. 101, pp. 776-796, 2013.
- [9] S. I. Smedley, *The Interpretation of Ionic Conductivity in Liquids*. Springer Science & Business Media, 2012.
- [10] H. Semat and R. Katz, "Physics, Chapter 28: Electrical Conduction in Liquids and Solids," 1958. Robert Katz Publications.
- [11] I. Nurdin and Satriananda, "Investigation on Electrical Conductivity Enhancement of Water Based Maghemite (γ -Fe₂O₃) Nanofluids," *International Journal of Materials Science and Applications*, Journal vol. 6, pp. 32-36, 2017, Art. no. 1.
- [12] M. Zawrah, R. Khattab, L. Girgis, H. El Daidamony, and R. E. A. Aziz, "Stability and Electrical Conductivity of Water-Base Al₂O₃ Nanofluids for Different Applications," *HBRC Journal*, vol. 12, no. 3, pp. 227-234, 2016.

- [13] T. T. Baby and S. Ramaprabhu, "Investigation of Thermal and Electrical Conductivity of Graphene Based Nanofluids," *Journal of Applied Physics*, vol. 108, no. 12, p. 124308, 2010.
- [14] M. Kole and T. Dey, "Investigation of Thermal Conductivity, Viscosity, and Electrical Conductivity of Graphene Based Nanofluids," *Journal of Applied Physics*, vol. 113, no. 8, p. 084307, 2013.
- [15] K. Yan, Q. Xue, Q. Zheng, and L. Hao, "The Interface Effect of the effective Electrical Conductivity of Carbon Nanotube Composites," *Nanotechnology*, vol. 18, no. 25, p. 255705, 2007.
- [16] I. Tan, A. Ahmad, and B. Hameed, "Preparation of Activated Carbon from Coconut Husk: Optimization Study on Removal of 2, 4, 6-trichlorophenol using Response Surface Methodology," *Journal of Hazardous Materials*, vol. 153, no. 1, pp. 709-717, 2008.
- [17] A. Nieto-Márquez, R. Romero, A. Romero, and J. L. Valverde, "Carbon Nanospheres: Synthesis, Physicochemical Properties and Applications," *Journal of Materials Chemistry*, vol. 21, no. 6, pp. 1664-1672, 2011.
- [18] H.-s. Qian, F.-m. Han, B. Zhang, Y.-c. Guo, J. Yue, and B.-x. Peng, "Non-Catalytic CVD Preparation of Carbon Spheres with a Specific Size," *Carbon*, vol. 42, no. 4, pp. 761-766, 2004.
- [19] Y. Z. Jin *et al.*, "Large-Scale Synthesis and Characterization of Carbon Spheres Prepared by Direct Pyrolysis of Hydrocarbons," *Carbon*, vol. 43, no. 9, pp. 1944-1953, 2005.
- [20] J.-Y. Miao *et al.*, "Synthesis and Properties of Carbon Nanospheres Grown by CVD Using Kaolin Supported Transition Metal Catalysts," *Carbon*, vol. 42, no. 4, pp. 813-822, 2004.
- [21] M. Ibrahim Mohammed, R. Ismaeel Ibrahim, L. H. Mahmoud, M. A. Zablouk, N. Manweel, and A. Mahmoud, "Characteristics of Carbon Nanospheres Prepared from locally Deoiled Asphalt," *Advances in Materials Science and Engineering*, vol. 2013, 2013.
- [22] X. Yu *et al.*, "Synthesis of Activated Carbon Nanospheres with Hierarchical Porous Structure for high Volumetric Performance Supercapacitors," *Electrochimica Acta*, vol. 182, pp. 908-916, 2015.
- [23] Y. Wang, F. Su, C. D. Wood, J. Y. Lee, and X. S. Zhao, "Preparation and Characterization of Carbon Nanospheres as Anode Materials in Lithium-Ion Secondary Batteries," *Industrial & Engineering Chemistry Research*, vol. 47, no. 7, pp. 2294-2300, 2008.
- [24] N. Katcho *et al.*, "Structure of Carbon Nanospheres Prepared by Chlorination of Cobaltocene: Experiment and Modeling," *Physical Review B*, vol. 77, no. 19, pp. 195402, 2008.
- [25] P. Zhang, Z.-A. Qiao, and S. Dai, "Recent Advances in Carbon Nanospheres: Synthetic Routes and Applications," *Chemical Communications*, vol. 51, no. 45, pp. 9246-9256, 2015.
- [26] A. A. Arie, H. Kristianto, M. Halim, and J.-K. Lee, "Biomass Based Carbon Nanospheres as Electrode Materials in Lithium Ion Batteries," *ECS Transactions*, vol. 66, no. 11, pp. 13-19, 2015.
- [27] H. Kristianto, C. D. Putra, A. A. Arie, M. Halim, and J. K. Lee, "Synthesis and Characterization of Carbon Nanospheres Using Cooking Palm Oil as Natural Precursors onto Activated Carbon Support," *Procedia Chemistry*, vol. 16, pp. 328-333, 2015.

- [28] X.-W. Chen, O. Timpe, S. B. Hamid, R. Schlögl, and D. S. Su, "Direct Synthesis of Carbon Nanofibers on Modified Biomass-Derived Activated Carbon," *Carbon*, vol. 47, no. 1, pp. 340-343, 2009.
- [29] J. Zhu, J. Jia, F. L. Kwong, D. H. L. Ng, and S. C. Tjong, "Synthesis of Multiwalled Carbon Nanotubes from Bamboo Charcoal and the Roles of Minerals on Their Growth," *Biomass and Bioenergy*, vol. 36, pp. 12-19, 2012.
- [30] H. Li, X. He, Y. Liu, H. Yu, Z. Kang, and S.-T. Lee, "Synthesis of Fluorescent Carbon Nanoparticles Directly from Active Carbon Via a one-Step Ultrasonic Treatment," *Materials Research Bulletin*, vol. 46, no. 1, pp. 147-151, 2011.
- [31] J. O. Alves, C. Zhuo, Y. A. Levendis, and J. A. Tenório, "Catalytic Conversion of Wastes from the bioethanol Production into Carbon Nanomaterials," *Applied Catalysis B: Environmental*, vol. 106, no. 3, pp. 433-444, 2011.
- [32] K. Shi, J. Yan, E. Lester, and T. Wu, "Catalyst-Free Synthesis of Multiwalled Carbon Nanotubes via Microwave-Induced Processing of Biomass," *Industrial & Engineering Chemistry Research*, vol. 53, no. 39, pp. 15012-15019, 2014.
- [33] A. Melati and E. Hidayati, "Synthesis and Characterization of Carbon Nanotubes from Coconut Shells Activated Carbon," in *Journal of Physics: Conference Series*, 2016, vol. 694, no. 1, p. 012073: IOP Publishing.
- [34] G. A. Adewumi, N. Revaprasadu, A. C. Eloka-Eboka, F. Inambao, and C. Gervas, A Facile Low-cost Synthesis of Carbon Nanosphere from Coconut Fibre, Lecture Notes in Engineering and Computer Science: Proceedings of The World Congress on Engineering and Computer Science 2017, WCECS 2017, 25 October - 27 October, 2017, San Francisco, USA, pp. 577-582.
- [35] P. Debye and P. Scherrer, "Interference on Inordinate Orientated Particles in X-Ray Light. III," *Physikalische Zeitschrift*, vol. 18, pp. 291-301, 1917.
- [36] A. Nath, D. D. Purkayastha, M. Sharon, and C. R. Bhattacharjee, "Catalyst Free Low Temperature Synthesis and Antioxidant Activity of Multiwalled Carbon Nanotubes Accessed from Ghee, Clarified Butter of Cow' S Milk," *Materials Letters*, vol. 152, pp. 36-39, 2015.
- [37] A. D. Faisal and A. A. Aljubouri, "Synthesis and Production of Carbon Nanospheres Using Noncatalytic CVD Method." *International Journal of Advanced Research*, vol. 2, no. pp. 586-91, 2016
- [38] S. A. Adio, M. Sharifpur, and J. P. Meyer, "Investigation into Effective Viscosity, Electrical Conductivity, and pH of γ -Al₂O₃-Glycerol Nanofluids in Einstein Concentration Regime," *Heat Transfer Engineering*, vol. 36, no. 14-15, pp. 1241-1251, 2015.

CHAPTER 6: THERMAL CONDUCTIVITY OF NANOFLUIDS PREPARED FROM BIOBASED NANOMATERIALS

Adewumi, G.A., Inambao, F.L., Sharifpur, M. and Meyer J. Thermal Conductivity of Nanofluids Prepared from Biobased Nanomaterials Dispersed in 60:40 Ethylene Glycol/Water Base Fluid, *Submitted to NANOSMAT Africa Conference, 2018 Capetown South Africa.*

THERMAL CONDUCTIVITY OF NANOFLUIDS PREPARED FROM BIOBASED NANOMATERIALS DISPERSED IN 60:40 ETHYLENE GLYCOL/WATER BASE FLUID

Gloria A Adewumi,^{*a} Freddie Inambao,^a Mohsen Sharifpur^b and Josua P Meyer^b

c. Discipline of Mechanical Engineering, School of Engineering, University of KwaZulu-Natal, Howard College, 4041 South Africa

d. Department of Mechanical and Aeronautical Engineering, University of Pretoria, Pretoria, 0002, South Africa.

(Corresponding author: Gloria Adewumi, Address: 280 Sphiwe Zuma Avenue, Glenmore, South Africa, 4001. email: adewumigloria@gmail.com tel: +27749423154)

Abstract

In the present study, experimental investigation on thermal conductivity of green nanofluids prepared from coconut fibre-based nanoparticles and suspended in 60:40 ethylene glycol (EG) water (W) mixture was carried out. The measurement of thermal conductivity was conducted at 15 °C to 60 °C at mass fractions of 0.04 wt%, 0.08 wt%, 0.5 wt% and 1 wt%. The results show deterioration in thermal conductivity with an increasing temperature. Also the deterioration increased as the mass fraction increased.

Keywords: Thermal Conductivity; Green Nanofluids; Mass Fraction; Bio-based nanomaterials

6.1 Introduction

Cooling and heat addition are two processes that must occur in industrial applications, therefore methods to meet these needs must be addressed. The conventional methods for heat removal include the use of conventional solid-liquid suspensions and use of extended surfaces.

These methods however have some limitations which are listed as follows:

- a. Rapid settling of particles;
- b. Non-applicability in microsystems due to channel clogging; and
- c. Drop in pressure and pumping power.

With the advent of miniaturization, micro-scale devices such as heat exchangers used in microchannels and micropumps have emerged bringing forth new requirements for more advanced fluids for heat transfer [1]. Nanofluids are suspensions containing nano-metered particles suspended in known heat transfer fluids like ethylene glycol, water, propylene glycol and oil. Dispersion of these particles in the base fluids has been reported to reduce pumping power and prevent channel clogging [2].

Since the discovery of nanofluids by Choi at Argonne Lab [2], new developments in the field of nanofluids preparation and enhancements have been made in proposing new mechanisms behind enhanced thermal properties of nanofluids. A linear rise in thermal conductivity of ethylene glycol/water (EG/W) base fluids have been observed with the addition of carbon nanotubes (CNT) in increasing concentrations [3-5]. TiO₂ nanoparticles were also dispersed in EG/W base fluids and an increase in thermal conductivity was reported with an increase in concentration [6]. A similar pattern of linear increase was observed for CNT/Water nanofluids [7-9]. The effect of volume fraction and temperature on nanofluid thermal conductivity has been studied by several authors [5, 9, 10] in order to know their behaviour when subjected to various temperatures. A general trend was noted in their results which demonstrates an increase in thermal conductivity when temperature is increased [10] which was attributed to the increase in Brownian motion [5, 9].

Recently, the research community has drawn attention to the safety of nanomaterials in relation to humans who are in contact with them, and their impact on the environment. Due to the small size of nanoparticles, which is similar to biological proteins, they are easily adsorbed into the surface of tissues and blood in the human body. Even though this can be an advantage during drug delivery, they can also pass to the lungs when inhaled and may lead to lung inflammation and heart problems [11]. An extensive study on the pros and cons of nanoparticles has been published by [12] where it was established that nanoparticles behaved in a similar manner to ultrafine particles and may have similar side effects as ultrafine particles when inhaled. During synthesis of nanomaterials, the various precursors used may contain or release some toxic chemicals which may be deposited on human skin both intentionally and unintentionally. Through their disposal, they can also be deposited in water and land, and can also come in contact with the environment through transportation from production facilities to other locations where they will be used for research and other applications. In light of these safety concerns, more research focus should be channelled into the synthesis of nanomaterials which have lower risks of toxicity for humans and the environment.

In this study, the thermal conductivity of a new class of green nanofluids prepared from coconut fibre bio-based precursors suspended in 60:40 EG/W base fluid and 1:3.5 nanoparticle to gum arabic as surfactant has been investigated considering the effect of volume fraction and temperature. The results from this study will be applicable in thermal management and in heat transfer applications.

6.2 Theory

The phenomena of heat conduction deals with the transfer of heat arising from vibration of molecules which occurs even when the fluid is at equilibrium. The effective thermal conductivity k_{eff} can generally be expressed as a function of the base fluid thermal conductivity k_{bf} , nanoparticles thermal conductivity k_p and nanoparticle volume concentration φ . This can be written mathematically as [1]:

$$k_{eff} = f(k_{bf}, k_p, \varphi) \quad (1)$$

The Maxwell equation for thermal conductivity of fluid mixtures with low particle-volume concentrations effectively models equation (1) and is given as [1]:

$$k_{eff} = k_{bf} + 3\varphi \frac{k_p - k_{bf}}{2k_{bf} + k_p} k_{bf} \quad (2)$$

From Maxwell's equation, particle interactions due to their shape was neglected and the study focused on dilute suspension of spherical particles. This model under-predicts the thermal conductivity of nanofluids because it does not take into consideration geometry, temperature and surface area of nanoparticles. This limitation led to a model by Hamilton and Crosser [13] in which particle shape was considered:

$$k_{eff} = k_f \left(\frac{k_f + (n-1)k_f + (n-1)\varphi(k_p - k_f)}{k_p + (n-1)k_f - \varphi(k_p - k_f)} \right) \quad (3)$$

Where the empirical shape factor is denoted as n . This model also had limitations due to its lack of consideration of temperature and particle size on the nanofluids thermal conductivity. Maxwell's model was modified by Mehta et al. [14] by including the effect of particle size and temperature on the thermal conductivity of nanofluids through incorporation of the influence of Brownian motion and micro-convection heat transfer:

$$\frac{q_{eff}}{q_f} = \left[\frac{k_p + 2k_f + 2(k_p - k_f)\varphi}{k_p + 2k_f - (k_p - k_f)\varphi} \right] + \frac{k_p k_p}{k_f \alpha_m \mu d_p \left(\frac{6\varphi}{\pi} \right)^{1/3}} \quad (4)$$

Where q_{eff} is the effective heat flux, q_f is the nanofluids heat flux, α_m is the thermal diffusivity, d_p is the average particle diffusivity and μ is the dynamic viscosity.

Another model considering the impact of Brownian motion on thermal conductivity was studied by [15]. The result is an equation for thermal conductivity in nanofluid suspension

containing some modes of energy transportation such as: thermal diffusion of nanoparticles in fluids, thermal interactions of dynamic nanoparticles, base fluid molecules and the thermal conductivity of the base fluid [15]. The effective thermal conductivity is [15]:

$$k_{eff} = k_{bf}(1 - \varphi) + k_p\varphi + h\delta_T \quad (5)$$

Where δ_T and h is the boundary layer thickness and heat transfer coefficient respectively for a flow past of nanoparticles.

In general, transfer of heat in nanofluids results from two prominent factors, namely, conduction in base fluids and nanoparticles, and micro-convection from Brownian motion of nanoparticles.

6.3 Experimental

6.3.1 Preparation of Stable Nanofluids

Nanoparticles prepared from the ethanol treatment of coconut fibre activated carbon were used for the preparation of the nanofluids. The process of carbon nanosphere synthesis has been reported in our previous study [16, 17]. From the synthesis, a spherical morphology was obtained (Fig. 1) which was suspended in a base fluid containing 60:40 ethylene glycol/water base fluid using the conventional two-step method. A known weight of the nanoparticles corresponding to 0.04 wt%, 0.08 wt%, 0.5 wt% and 1 wt% was measured using a digital weighing balance. In order to get a stable nanofluid, gum arabic was used as surfactant which was based on the study by Sadri et al. [9]. The mixture was stirred using a magnetic hotplate stirrer (Lasec from Benchmark Scientific Inc., model-H4000-HSE). After stirring the mixture was then vibrated using a 20 kHz, 700 Watts, QSonica ultrasonic processor. Sonication took place in a constant temperature water bath (LAUDA ECO RE1225 Silver temperature bath) at 15 °C to maintain the temperature of sonication.

6.3.2 Thermal Conductivity Measurements

KD2 Pro (Decagon, USA) makes use of the transient hot-wire method to measure the thermal conductivity of nanofluids. Calibration of the thermal conductivity meter was carried out using standard glycerine with known thermal conductivity of 0.282 W/m.K at 20 °C. A KS-1 sensor probe of 60 mm in length was used for measurement of nanofluids enclosed in insulation with a read time of 10 minutes which was aimed at lowering errors from contact resistance. Also, free convection errors were reduced by the low heat of the KS-1 needle. Changes in

temperature while taking measurements were corrected by means of a linear drift term. To optimise measurement precision, readings were taken eight times at each mass concentration to ensure accuracy in measurement within 5 %. Repeatability of measurements was ensured by taking thermal conductivity of 60:40 EG/W) at 15 °C to 60 °C and the results obtained were compared with ASHRAE [24]. The error in the setup was established by comparing the experimental value of thermal conductivity of distilled water with its standard value. The experiments with distilled water were conducted three times to check the repeatability of the results, and the accuracy of the measurement is found to be within 10 mW/m.K.

6.4 Results and Discussion

6.4.1 Morphology and Stability of Nanofluids

Figure 6.1 shows the analysis of the nanoparticles using particle size distribution and transmission electron microscope (TEM). From the figure, the diameters of the particles ranged from about 30 nm to 100 nm with the highest distribution of particles at 75 nm. Figure 6.2 presents the results of XRD of the carbon nanoparticles. The peaks present correspond to hexagonal graphitic structure of carbon [18] as reported in [16]. There is also the presence of amorphous carbon due to the broadened peaks as shown in the diffractogram.

The stability of nanofluids is essential for their effective use in heat transfer applications. An unstable nanofluid will result in clogged pipes and an overall inefficient nanofluid. The percentage of gum arabic used as surfactant is 3.5 % with respect to the nanoparticles. This ratio brought about an excellent stability in the nanofluids. Recently the use of ultra violet (UV) spectroscopy to study the stability of nanofluids has been studied by several researchers [19-23]. By using this technique, the rate at which incident light is absorbed by nanoparticles is measured. A linear relationship exists between the sedimentation time absorbance which allows the stability of nanofluids to be determined from the time of sedimentation. This is in accordance with Beer Lamberts law:

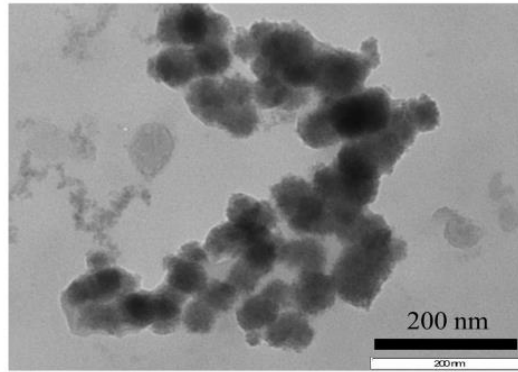
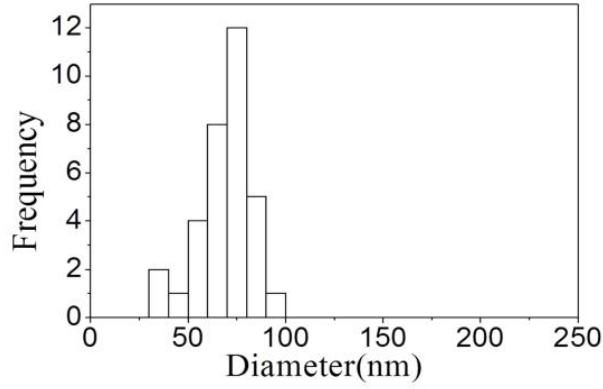
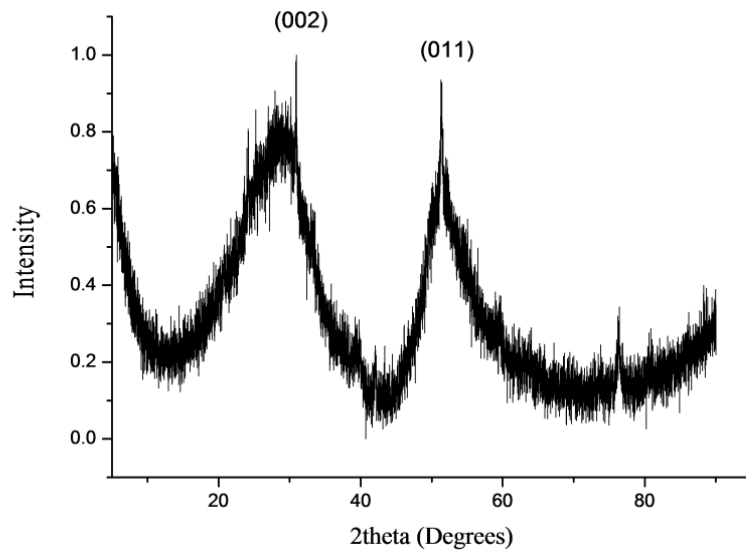


Fig. 6.1. Particle size distribution and TEM image of green nanoparticles synthesized from bio-based precursor and used in the present study

$$A = \log_2 \left[\frac{I_0}{I} \right] = \varepsilon CL \quad (1)$$

Where: I is the final intensity of light; I_0 is the initial intensity of light; ε is the molecular absorptivity; L is the sample path length and C is the concentration.

Figure 6.3 shows the UV-Vis spectroscopy indicating the absorbance of the different mass fractions of the nanofluid with a sedimentation time of 800 minutes. The outcomes confirm the stability of the nanofluid for the period of observation. With these results, the thermal conductivity measurements could be carried out with no concerns regarding particle settlement or agglomeration.



2

Fig. 6.2. X-ray diffractogram of nanoparticles

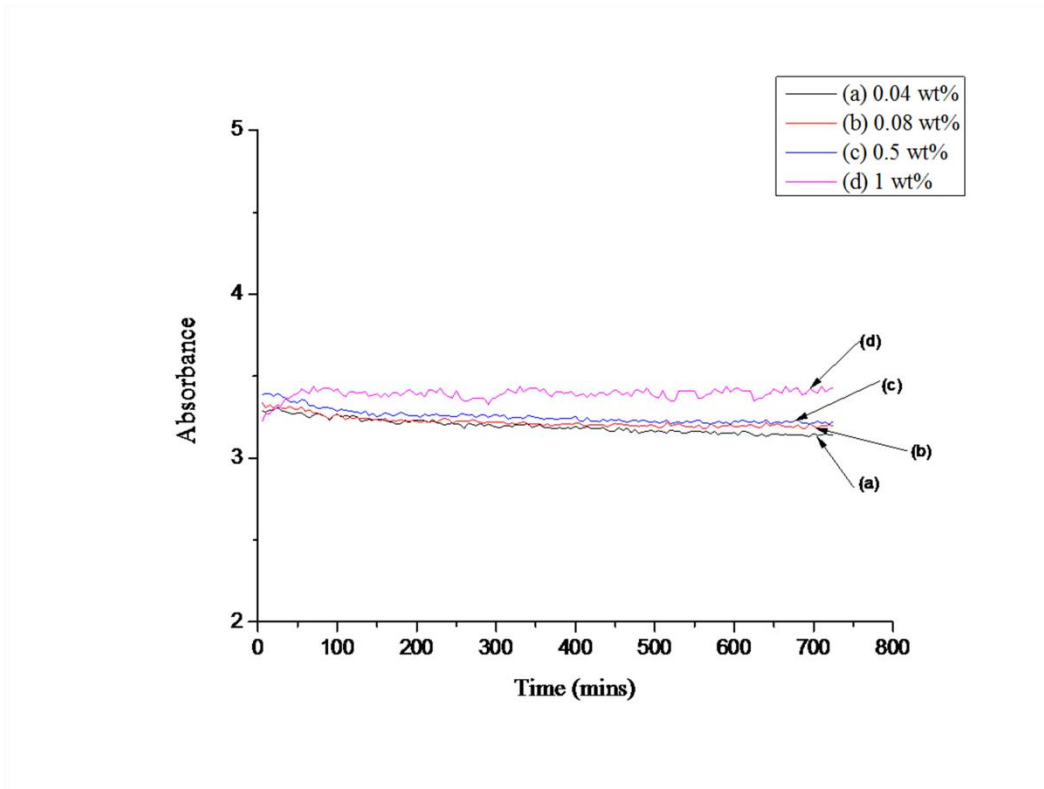


Fig. 6.3. UV-Vis spectroscopy for stability analysis of nanofluids

6.5 Measurement of Thermal Conductivity

To establish and confirm the accuracy of the measuring device, the measured thermal conductivity of the 60:40 EG/W base fluid was compared with results from the ASHRAE handbook [24]. The results are presented in Fig. 6.4. The results from measurement show good agreement with the ASHRAE values.

Thermal conductivity of the nanofluids was measured at mass fractions of 0.04 wt%, 0.08 wt%, 0.5 wt% and 1 wt% all with a nanoparticle to surfactant ratio of 1:3.5. While past studies have shown an enhancement in thermal conductivity of nanofluids compared to known heat transfer fluids, the results presented in Fig. 6.5 indicate deterioration in thermal conductivity of the prepared green nanofluids with an increase in temperature for all mass fractions. Therefore, it can be assumed that the thermal conductivity of the nanofluid is inversely proportional to the temperature and directly proportional to the mass fraction as there was an increase in thermal conductivity with an increase in mass fraction at all temperatures (Fig. 6.6). A similar result has been published by Altan et al. [25] where a deterioration in thermal conductivity was observed in aqueous magnetite nanofluids. The deterioration in the study was attributed to an incompatibility between the base fluid and the nanoparticles. In addition, the presence of thermal boundary resistance could be a source of deterioration in thermal conductivity in nanofluids.

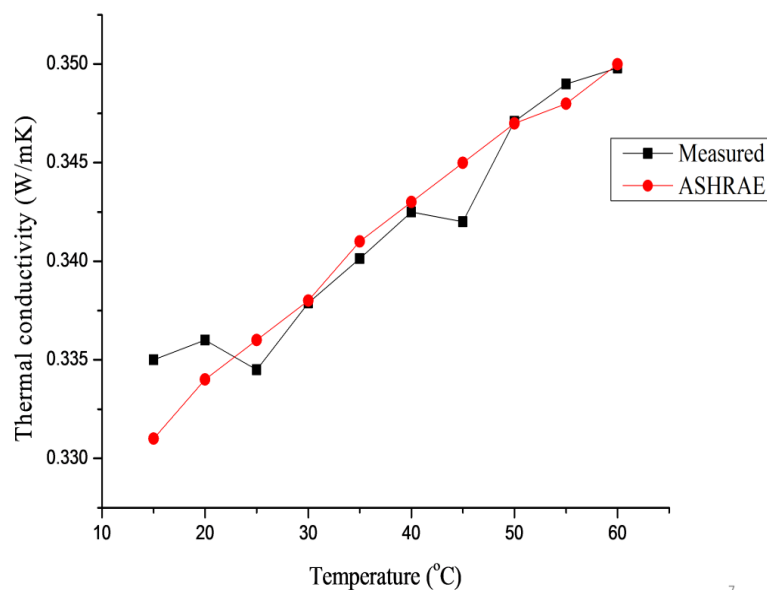


Fig. 6.4. Comparison of measured data and ASHRAE

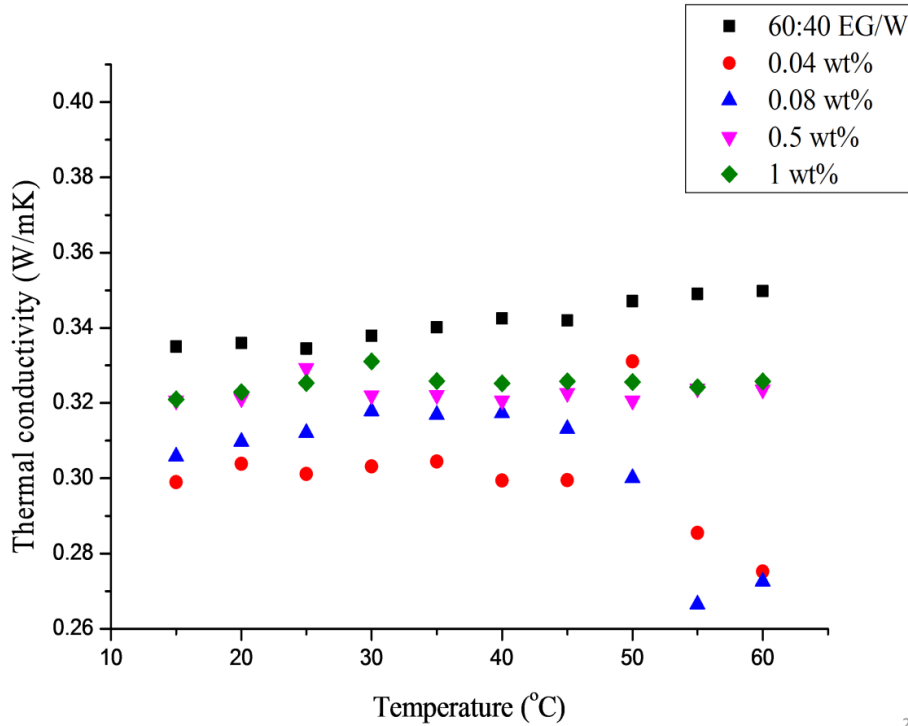


Fig. 6.5. Thermal conductivity at different mass fractions

In the present study, the nanofluid is a composite fluid comprising the green nanoparticles, gum arabic, ethylene glycol and water. An interruption is caused between the particles interface, gum arabic and ethylene glycol/water. Inconsistencies in mass density which occur at the junction between dissimilar materials, creates an impedance mismatch [26]. There is an interruption of phonons between the interface layers of dissimilar mass segments which represents the fundamental reason behind the thermal resistance. An elevated jump takes place when there is an increase in length of the phonons with a denser mass segment thereby resulting in a decrease in thermal conductivity and heat flux.

Based on the above theories, the decline in thermal conductivity cannot only be dependent on the thermal boundary resistance as other factors such as purity of the nanoparticles, inconsistent size of nanoparticles and ratio of surfactant or a combination of all these factors could contribute to the decline.

In summary, the overall decrease in thermal conductivity of the prepared green nanofluids cannot really be explained as other references in literature have reported an enhancement in thermal conductivity of nanofluids relative to the base fluid. These findings show that there is still more research to be carried out in this area. The thermal conductivity of the green

nanoparticles dispersed in other base fluids together with the effect of thermal boundary resistance on the thermal conductivity of this new class of nanofluids needs to be studied.

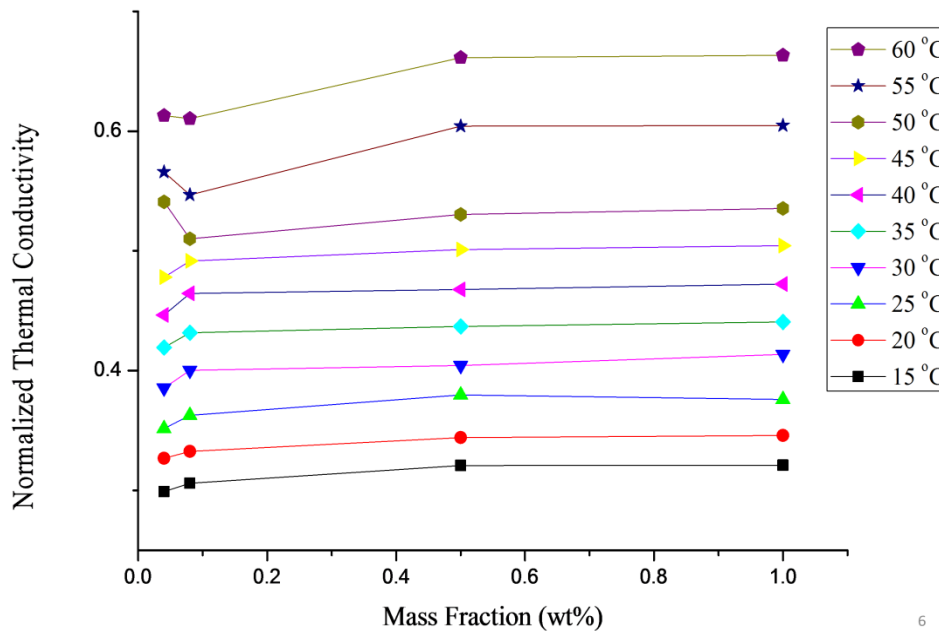


Fig. 6.6. Temperature effect on thermal conductivity of prepared nanofluids

6.6 Conclusion

The effect of temperature and mass fraction on the thermal conductivity of nanospheres synthesized from coconut fibre and suspended in a mixture of 60:40 EG/W nanofluids has been reported. The results show deterioration in thermal conductivity as temperatures increase for all mass fractions and this deterioration increased as the mass fraction increased. This decrease has been attributed to factors such as a high thermal boundary resistance, ratio of surfactant and inconsistent size of the nanoparticles.

In conclusion, the results from the present study point to the fact that a lot of research still has to be carried out in order to tailor this new class of nanofluids to specific applications.

References

- [1] S. K. Das, S. U. Choi, W. Yu, and T. Pradeep, *Nanofluids: Science and Technology*. John Wiley & Sons, 2007.
- [2] S. U. Choi and J. A. Eastman, "Enhancing Thermal Conductivity of Fluids with Nanoparticles," Argonne National Lab., IL (United States) 1995.
- [3] N. Singh, G. Chand, and S. Kanagaraj, "Investigation of Thermal Conductivity and Viscosity of Carbon Nanotubes–Ethylene Glycol Nanofluids," *Heat Transfer Engineering*, vol. 33, no. 9, pp. 821-827, 2012/07/01 2012.

- [4] W. Rashmi *et al.*, "Stability and Thermal Conductivity Enhancement of Carbon Nanotube Nanofluid Using Gum Arabic," *Journal of Experimental Nanoscience*, vol. 6, no. 6, pp. 567-579, 2011.
- [5] M.-S. Liu, M. Ching-Cheng Lin, I. T. Huang, and C.-C. Wang, "Enhancement of Thermal Conductivity with Carbon Nanotube for Nanofluids," *International Communications in Heat and Mass Transfer*, vol. 32, no. 9, pp. 1202-1210, 2005.
- [6] M. R. Islam, B. Shabani, and G. Rosengarten, "Electrical and Thermal Conductivities of 50/50 Water-ethylene Glycol Based TiO₂ Nanofluids to be Used as Coolants in PEM Fuel Cells," *Energy Procedia*, vol. 110, pp. 101-108, 2017.
- [7] M. Xing, J. Yu, and R. Wang, "Experimental Study on the Thermal Conductivity Enhancement of Water Based Nanofluids Using Different Types of Carbon Nanotubes," *International Journal of Heat and Mass Transfer*, vol. 88, pp. 609-616, 2015.
- [8] Y. Ding, H. Alias, D. Wen, and R. A. Williams, "Heat Transfer of Aqueous Suspensions of Carbon Nanotubes (CNT Nanofluids)," *International Journal of Heat and Mass Transfer*, vol. 49, no. 1-2, pp. 240-250, 2006.
- [9] R. Sadri *et al.*, "An Experimental Study on Thermal Conductivity and Viscosity of Nanofluids Containing Carbon Nanotubes," *Nanoscale Research Letters*, vol. 9, no. 1, p. 151, 2014.
- [10] T. Maré, S. Halelfadl, S. Van Vaerenbergh, and P. Estellé, "Unexpected Sharp Peak in Thermal Conductivity of Carbon Nanotubes Water-Based Nanofluids," *International Communications in Heat and Mass Transfer*, vol. 66, pp. 80-83, 2015.
- [11] P. C. Ray, H. Yu, and P. P. Fu, "Toxicity and Environmental Risks of Nanomaterials: Challenges and Future Needs," *Journal of Environmental Science and Health, Part C*, vol. 27, no. 1, pp. 1-35, 2009/02/17 2009.
- [12] M. R. Gwinn and V. Vallyathan, "Nanoparticles: Health Effects—Pros and Cons," *Environmental Health Perspectives*, vol. 114, no. 12, p. 1818, 2006.
- [13] R. L. Hamilton and O. Crosser, "Thermal Conductivity of Heterogeneous Two-Component Systems," *Industrial & Engineering Chemistry Fundamentals*, vol. 1, no. 3, pp. 187-191, 1962.
- [14] S. Mehta, K. P. Chauhan, and S. Kanagaraj, "Modeling of Thermal Conductivity of Nanofluids by Modifying Maxwell's Equation Using Cell Model Approach," *Journal of Nanoparticle Research*, vol. 13, no. 7, pp. 2791-2798, 2011.
- [15] S. P. Jang and S. U. Choi, "Role of Brownian Motion in the Enhanced Thermal Conductivity of Nanofluids," *Applied Physics Letters*, vol. 84, no. 21, pp. 4316-4318, 2004.
- [16] G. A. Adewumi, F. Inambao, A. Eloka-Eboka, and N. Revaprasadu, "Synthesis of Carbon Nanotubes and Nanospheres from Coconut Fibre and the Role of Synthesis Temperature on Their Growth," *Journal of Electronic Materials*, 2018. <https://doi.org/10.1007/s11664-018-6248-z>
- [17] G. A. Adewumi, N. Revaprasadu, A. C. Eloka-Eboka, F. Inambao, and C. Gervas, "A Facile Low-cost Synthesis of Carbon Nanosphere from Coconut Fibre," in *Lecture Notes in Engineering and Computer Science: Proceedings of The World Congress on Engineering and Computer Science San Francisco, USA, 2017*, vol. 2, pp. 577-582, USA, 2017.
- [18] U. Hofmann and D. Wilm, "Ueber die Kristallstruktur von Kohlenstoff Zeitschrift fuer Elektrochemie," *J. Elektrochem.*, vol. 42, pp. 504-522, 1936.
- [19] Y.-j. Hwang *et al.*, "Stability and Thermal Conductivity Characteristics of Nanofluids," *Thermochimica Acta*, vol. 455, no. 1-2, pp. 70-74, 2007.

- [20] M. Pastoriza-Gallego, C. Casanova, R. Páramo, B. Barbés, J. Legido, and M. Piñeiro, "A Study on Stability and Thermophysical Properties (Density and Viscosity) of Al₂O₃ in Water Nanofluid," *Journal of Applied Physics*, vol. 106, no. 6, p. 064301, 2009.
- [21] M. K. Abdolbaqi, W. Azmi, R. Mamat, K. Sharma, and G. Najafi, "Experimental Investigation of thermal Conductivity and Electrical Conductivity of Bioglycol–Water Mixture Based Al₂O₃ Nanofluid," *Applied Thermal Engineering*, vol. 102, pp. 932-941, 2016.
- [22] M. Sharif, W. Azmi, A. Redhwan, N. Zawawi, and R. Mamat, "Improvement of Nanofluid Stability Using 4-Step UV-Vis Spectral Absorbency Analysis," vol. 4, no. 2, pp. 233-247 2017.
- [23] M. Hadadian, E. K. Goharshadi, and A. Youssefi, "Electrical conductivity, thermal conductivity, and rheological properties of graphene oxide-based nanofluids," *Journal of Nanoparticle Research*, vol. 16, no. 12, p. 2788, December 11 2014.
- [24] American Society of Heating, Refrigerating and Air-Conditioning Engineers, Handbook, Atlanta, GA, USA, 2009.
- [25] C. L. Altan, B. Gurten, N. A. Sommerdijk, and S. Bucak, "Deterioration in Effective Thermal Conductivity of Aqueous Magnetic Nanofluids," *Journal of Applied Physics*, vol. 116, no. 22, p. 224904, 2014.
- [26] P. Patel and P. Gajjar, "Interface Thermal Resistance and Thermal Conductivity in Composites—an abrupt Junction Thermal Diode Model," *Physics Letters A*, vol. 378, no. 34, pp. 2524-2528, 2014.

CHAPTER 7: CONCLUSION AND FUTURE WORK

7.1 Conclusion

The aim of this study was to investigate the thermophysical properties (electrical conductivity and viscosity) of green nanofluids prepared from dispersing coconut fibre nanomaterials in 60:40 EG/W. In order to achieve this, carbon nanotubes and carbon nanospheres were synthesized from coconut fibre and then dispersed in 60:40 EG/W base-fluid. The results obtained have been presented in a number of publications and conference proceedings.

Chapter 2 is an extensive review of the thermal conductivity and viscosity of bio-based carbon nanotubes. The review covers past studies carried out on both thermal conductivity of individual carbon nanotubes and nanofluids containing carbon nanotubes. Synthesis parameters have been shown to have a direct impact on the shape and morphology of as-grown CNTs. The parameters include precursor, synthesis time, temperature, diameter, among others. The inconsistent heat transfer properties such as thermal conductivity of CNTs are attributed to the various conditions such as temperature, diameter, length, and the morphology of growth of the CNTs. Past studies on viscosity also show that viscosity can be enhanced by increasing the CNT concentration and decreasing temperature. In addition, CNT water nanofluids act as non-Newtonian fluids since the dynamic viscosity varies accordingly with an increase in shear rate.

Chapter 3 is divided into two parts with both parts communicating results from the synthesis of carbon nanospheres and carbon nanotubes. The effect of synthesis temperature on the growth of carbon nanomaterials from coconut fibre charcoal using ethanol vapour treatment at 700 °C to 1100 °C at 100 °C increments was reported. The process of synthesis involved no use of toxic materials or catalysts or substrates. At 700 °C the low temperature did not favour the growth of carbon nanotubes or carbon nanospheres. At 800 °C and 900 °C, nanotubes were formed in which the EDX results reveal carbon content of 92.6 % and 95.6 % respectively while temperatures at 1000 °C and 1100 °C favoured the growth of nanospheres with carbon contents of 96.2 % and 91.6 % respectively.

In chapter 4, investigation of the stability and viscosity of the prepared nanofluids was presented, considering the effects of temperature and mass fraction. The base fluid used was 60:40 ethylene glycol/water and GA was the surfactant used. Stability analysis was carried out using visual analysis, zeta potential, viscosity values for a period of 720 min, and UV-Vis spectroscopy. The results indicate a very stable fluid with high zeta potential values. It can also

be depicted from the values obtained that addition of these green nanoparticles in 60:40 EG/W have a significant effect on the nanofluids' viscosity which is a function of temperature and nanoparticle mass fraction. The viscosity of the nanofluids at different mass fractions decreases with an increase in temperature, while the relative viscosity remains fairly constant with an increase in temperature. An increase in mass fraction enhances the viscosity of nanofluids at all temperatures under study. Empirical correlations have been developed to predict the viscosity of nanofluids at different temperatures and mass fractions.

Chapter 5 entails the measurement of electrical conductivity at varied concentration and temperature. The results obtained show an improved electrical conductivity with increase in temperature and volume concentration. At 0.2 vol%, a maximum electrical conductivity of 1 470 % was achieved at a temperature of 55 °C. The results presented show the potential of carbon nanosphere-based green nanofluids as heat transfer fluids for cooling applications. Due to its less toxic nature, it can also be used in applications where human contact is required.

Chapter 6, presents experimental investigations on the thermal conductivity measurements of the synthesized green nanoparticles dispersed in 60:40 EG/W, which was carried out at different volume fractions (0.04 wt% to 1 wt%). The results show that the thermal conductivity deteriorates which is unusual. This deterioration can possibly be attributed to high thermal boundary resistance, impurities in the precursor nanomaterials and a high nanoparticle to surfactant ratio. All these are assumptions and a more detailed study as to the reason for this deterioration should be studied in future work.

7.2 Future Work

While carrying out this research, several limitations were encountered. Further studies on the use of other bio-based precursors for the synthesis of nanoparticles are recommended. Also, other base fluids used in the preparation of the nanofluids should be considered to determine the effect of base fluid on the thermophysical properties of green nanofluids.

The thermal conductivity of the prepared nanofluids was observed to decrease with an increase in temperature. Further research on thermal conductivity should be carried out to determine the factors leading to this decrease.

Specific heat capacity and density of the nanofluids should also be studied in future work in order to calculate the theoretical heat transfer coefficient.

APPENDIX 1

Adewumi, G.A., Eloka-Eboka, A.C. and Inambao, F.L., 2016. A Review on Thermal Conductivity of Bio-Based Carbon Nanotubes. *In proceedings of World Academy of Science, Engineering and Technology: International Conference on Nanotechnology and Biotechnology*, Miami USA Mar 24-25, 2016, pp. 1633 1642.

A Review on Thermal Conductivity of Bio-Based Carbon Nanotubes

Gloria A. Adewumi, Andrew C. Eloka-Eboka, Freddie L. Inambao

Abstract—Bio-based carbon nanotubes (CNTs) have received considerable research attention due to their comparative advantages of high level stability, simplistic use, low toxicity and overall environmental friendliness. New potentials for improvement in heat transfer applications are presented due to their high aspect ratio, high thermal conductivity and special surface area. Phonons have been identified as being responsible for thermal conductivities in carbon nanotubes. Therefore, understanding the mechanism of heat conduction in CNTs involves investigating the difference between the varieties of phonon modes and knowing the kinds of phonon modes that play the dominant role. In this review, a reference to a different number of studies is made and in addition, the role of phonon relaxation rate mainly controlled by boundary scattering and three-phonon Umklapp scattering process was investigated. Results show that the phonon modes are sensitive to a number of nanotube conditions such as: diameter, length, temperature, defects and axial strain. At a low temperature (<100K) the thermal conductivity increases with increasing temperature. A small nanotube size causes phonon quantization which is evident in the thermal conductivity at low temperatures.

Keywords—Carbon nanotubes, phonons, thermal conductivity, umklapp process.

I. INTRODUCTION

SINCE their discovery in 1991, research on carbon nanotubes (CNTs) has emerged, branching open new discoveries and opportunities. CNTs have wonderful heat and electrical transfer properties which makes them a sort of wonder material. The diversity in property which is an advantage stems from their abilities to be rolled up in different tube axis based on different helicities [1] and this is determined by a vector, called a chiral vector which discriminates CNTs into “zigzag”, “armchair”, and “chiral” forms. Carbon nanotubes are one-dimensional cylinders and can be single or multiple layers of carbon. Nanotubes with a single layer are called single wall carbon nanotubes (SWCNTs) while carbon nanotubes with more than one wall are called multi-wall carbon nanotubes (MWCNTs) [2]. The diameters of the tubes are in the range of a few nanometers (0.4nm-1.4nm) and a length in micrometers, which confers high aspect ratios [1]. MWCNTs are easier to synthesize when

compared to SWCNT because they can be grown from most hydrocarbons at a low temperature (600-900°C). SWCNTs are usually synthesized by incorporating transition metals in catalytic amounts in the arc-discharge process while being able to grow from selected hydrocarbons [1]. Earlier studies determined that CNT immersed in suitable base fluids had the ability to reduce erosion and clogging which is seen in micro particles and this has led to significant energy savings and high efficiency in micro-channels [1], [3], [4]. The knowledge of the thermal conductivity of CNTs is very useful in the design of microelectromechanical systems (MEMS) and nanoelectromechanical systems (NEMS) used for efficient thermal transport system in electrical, mechanical and chemical applications, solar energy systems and central air conditioning systems. It is also necessary in the development of molecular theories in nanofluids and nanofluid mixtures [5]. Low thermal conductivity is a primary limitation in developing energy-efficient heat transfer fluids required for ultrahigh performance cooling [1]. Nanofluids however, are seen to have high thermal conductivities which depends not only on forces acting on nanoparticles but also on particle motion and interaction with turbulent eddies which leads to an astonishing reduction in heat exchanger pumping power [3]. After reviewing previous works, we find that the reported thermal conductivities of CNT is as high as 3000W/mK [6]. For bio-based CNT on the other hand, there is less literature available. Recently, the thermal conductivity of bio-based phase change (PCM) was enhanced by adding carbon nanotubes and the thermal conductivity reported is 0.557W/mK [7]. In comparison to tested carbon black, studies by [8] revealed a 36% in the thermal conductivity of carbonized ball milled lignin after synthesis by ball-milling. This review presents the various methods of synthesis of carbon nanoparticles and equally important, an investigation of the thermal conductivity measurements of MWCNT and SWCNT. The effects of temperature, length, substrate and diameter of the nanotubes have been analysed. The current trend towards miniaturization and the global need for a renewable and sustainable heat transfer source has motivated this study.

II. SYNTHESIS OF CARBON NANOPARTICLES

The tube diameter (d) and the helical angle θ are the two factors that describe the structure of a nanotube, not to forget the helical vector $C = na_1 + ma_2$ (where a_1 and a_2 are the graphene sheets). Tubes are characterized by (x,y) notation depending on how they are rolled. The diameter and helical

G. A. Adewumi is a doctoral candidate in Mechanical Engineering, University of Kwa Zulu-Natal, Howard College, Durban South Africa (Phone: +27749423154; e-mail: 213574188@stu.ukzn.ac.za).

A. C. Eloka-Eboka is a Postdoctoral Fellow in Mechanical Engineering Discipline at the University of KwaZulu-Natal, Howard College, Durban South Africa (Phone: +27617317515; e-mail: eloka-ebokaa@ukzn.ac.za).

F. L. Inambao is with the Discipline of Mechanical Engineering University of Kwa Zulu-Natal, Howard College, Durban South Africa (e-mail: inambaof@ukzn.ac.za).

angle of nanotubes can be found from x and y [1] and given in (1) and (2):

$$d = \frac{c}{\pi} = \frac{\sqrt{3r_{c-c}(y^2+xy+x^2)^{1/2}}}{\pi} \quad (1)$$

$$\theta = \tan^{-1} \frac{\sqrt{3m}}{(y+zx)} \quad (2)$$

where r_{c-c} : the c-c distance of the graphene layer (1.421Å), C: Length of the chiral vector

From a broad view, there exist three methods of synthesizing carbon nanotubes [1], [9], [10]:

- Formation of single-walled nanotubes (SWNT) by the incorporation of transition metals in catalytic amounts in the arc-discharge process;
- Laser evaporation which results in the formation of rope-like structures; and
- Chemical vapour deposition.

Bio-based carbon nanoparticles are a promising substitute for the metal based nanoparticles. Past studies on CNTs have shown increase in thermal conductivity, latent heat, thermal resistance, environmental friendliness, renewability and overall thermal efficiency [7], [8], [11]-[13]. The precursor used during synthesis is very important in controlling the morphology and yield of carbon nanoparticles. Precursors such as graphite powders, petroleum pitch, carbon rich polymers, and other types of hydrocarbons have been successfully used in synthesizing CNT and research is still ongoing in this area, [1], [14]-[18]. However due to toxicity and environmental hazards that can be caused, it is important to produce nanomaterials which are free from amorphous carbon. They should be obtained from green sources that would pose no harm to humans and the environment.

The authors in [19] reviewed greener routes used for nanoparticle production. Greener routes sourced from plant extracts and natural products used in past research were studied. These natural products, some of which were used as reductants and capping agents during synthesis have proven to assist with problems relating to environmental contamination, while using non-toxic solvents like water. Plant parts such as the leaf, roots, fruits, seeds and stem are being used for metal nanoparticle synthesis [19]-[23]. This is identified to be due to the presence of polyphenols because they are stable in acidic solutions and they also modulate the oxidative defense system in cells [24]. The bio-molecules present in plant are reported to reduce metal ions or act as capping agents to nanoparticles in a single-step green synthesis methods developed by [23]. The authors emphasized their advantages of being rapid, readily conducted at room temperature and easily scaled up. Micro-organisms have been used to produce nanoparticles but the rate at which synthesis occurred was found to be slow and only limited number of sizes and shapes are amenable compared to that of plant-based. The polyphenols present in tea extracts can act as both chelating and reducing agents which prevents agglomeration in nanoparticle formation and consequently leads to an increase in stability and longevity [19].

References [11] and [25] synthesized carbon nanoparticles from glucose and alkali or acid additives. However, the former carried out their experiments under ultra-sonication condition, while the latter utilized hydrothermal synthesis. From their results, the method based on ultrasonic synthesis was more efficient in terms of particle size agglomeration as the particle size obtained (5nm) as opposed to the particle sizes from [25] which was 70-100nm. Ultrasound has been known to generate alternating low-pressure and high-pressure waves in solution, leading to the formation and collapse of small vacuum bubbles [11]. Reference [12] has also applied a simple hydrothermal method using L-ascorbic acid as a carbon source. There were no acidic additives and there was no need for any surface modification. However, the addition of ethanol improved the surface state of the carbon nanoparticle. Gonugunta et al. [26] reported the synthesis of bio-based carbon nanoparticle using lignin as the carbon source. The freeze drying process was used in order to avoid lumps or aggregates formed from carbonization. It was observed that there was an increase in thermal stability with a corresponding increase in KOH. This was as a result of the influence of KOH on the particle size as lignin samples modified with KOH yielded ultrafine particles even though it forms agglomeration at higher concentrations of 15% [26]. To avoid the problem of lump formation (agglomeration) which usually arises from carbonization, thermal pyrolysis method was recently used by [27] to synthesize bio-based nanoparticles from coconut milk. The authors used the pyrolysis method because it does not involve any acid treatment or any surface passivating agent. The result however shows a large size range (20nm-50-nm) which could be due to non-homogeneity in the pyrolysis method adopted. Apart from the chemical methods used for synthesis, physical approaches are also being used for synthesis of nanoparticles [8], [17], [28], [29]. Physical methods include: ball milling and mechanical grinding. A bottom-up mechano-chemical approach using milling of inorganic precursors was also presented by [17]. Conventionally, ball milling is a top down approach because the particles are broken down into nanometer sized particles.

A. Effects of Synthesis Parameters on CNT Growth

The parameters involved in the synthesis of CNT play an important role on the final characteristics of the CNT structures. The influence of synthesis time on CNT yield from literature increases with increasing time [30]-[34]. This is evident from studies by [30], where at 2 minutes, short and isolated SWCNT with poor quality and high defects were obtained while CNTs with lesser defects were achieved for synthesis carried out in 30 minutes. Conversely, it has been observed that CNTs obtained after much longer synthesis time were likely to possess weaker crystallinity [32]. This report stated that increasing the reaction time of synthesis led to a constant inner diameter while the outer diameter increased. The effect of temperature on synthesis of CNT using nickel substrates generated results which indicate a major formation of multi-walled carbon nanotubes at lower temperature and nickel thickness [35]. The temperature was varied between

900°C, 800°C and 700°C and the fine tuning of the temperatures produced radical results in the CNT structure obtained. The study showed that higher temperatures promotes core-shell configuration and for decreasing temperature, the formation of CNT is enhanced. Toussi et al. [34] showed that when the temperature of synthesis is lower than 750°C, CNT formation was lesser; however CNT formation was higher for higher temperatures (>900°C). The best temperature for CNT growth by [34] occurred between 800°C and 900°C and the optimum growth temperature was at 850°C, while [36] obtained an optimum growth of ~99.99% at 900°C. Apart from synthesizing from high temperatures, carbon nanotubes can also be synthesized from carbonaceous solids at low temperature (450°C) [37].

In the chemical vapour deposition method (CVD) method, a hydrocarbon gas which is the carbon source is used together with a metal catalyst which acts as seed for the growth of CNTs. CVD takes place at a lower temperature (500-1000°C) [1]. Synthesis of CNTs is usually followed by purification, deposition and suspension in an organic solvent [2]. Using CVD method of synthesis allows more precision control of CNT orientation, lower cost and more defined product(s). Selecting a proper precursor, catalyst and suitable vapour pressure optimizes the yield of growth rate and quality of produced CNTs [38].

The choice of catalyst and substrate is important for the successive growth and desired orientation of CNTs [39]. The use of transition metals as catalyst for CNT synthesis have been reported by [40]-[42]. The most common transition metal catalysts used are Fe, Co, and Ni due to their high solubility and carbon diffusion rate. They are desirable due to high melting points and strong adhesion qualities. Higher quality nanotubes growth is obtained when Fe is used as catalyst during synthesis compared to Co and Ni. This has been attributed to its greater carbon solubility. Increasing the Fe loading decreased the quality of the nanotubes synthesized due to extensive agglomeration of the Fe particles. It was concluded that lower metal loading percentage is preferable for the growth of better quality CNTs with uniform diameters [43]. MgO and Mo have also been identified to be a suitable catalyst support for Fe as it produces nanotubes with better graphitisation, smaller and more uniform nanoparticles [40], [41]. A uniform diameter CNT was synthesized using Mn₁₂ as a catalyst precursor [44]. The diameter grown is 1.5±0.31nm and the result indicates that an adhesion strength exists which can determine the diameter of as-grown SWCNT needed for controlled synthesis [44]. Cheng et al. [45] revealed that the amount and dimension of the catalytic particles dispersed on the support was useful in controlling nanotube shape. A novel method of synthesis was reported by the authors using an improved floating catalyst approach produced by catalytically pyrolyzing benzene at 1100°C-1200°C [45].

Solid organo-metalloenes have been used due to their metal liberating qualities which catalyses hydrocarbon deposits efficiently [38], [46]. Alloy of metals also play a substantial role in catalysing the growth CNTs and through them a better yield of CNTs are derived [47]-[50]. As more

research continues on enhancing the growth of CNTs, noble metals have been discovered to effectively synthesize CNTs. However, they are most effective when their particle sizes are very small (<5nm) [38]. A robust and cost effective method of CNT synthesis was reported by [7], in which catalytic particles solution and carbon sources were atomized without the use of a special heating system. This method of synthesis proved more effective than thermal pyrolysis based catalytic vapour deposition (CVD) in which there is difficulty in controlling the quantity of particles entrained in carrier gas due to steep temperature gradient between furnaces. The method is also proved more effective than aerosol pyrolysis [7]. Catalytic pyrolysis involving annealing of carbonaceous solid containing cobalt has been used to synthesize MWCNT [37]. The cobalt is used as a catalyst to decompose carbonaceous solid, form carbon gas species and eventually growth of CNTs. Cobalt precursors however, have disadvantages which consist of the availability of high pressure to achieve adequate SWCNT yield to overcome equilibrium limitations at atmospheric pressure. The use of cobalt can also lead to the deposition of carbon at high temperatures and are hazardous [41]. This mentioned downside of cobalt and other transition metals motivated Abdullahi *et al.* [41] to use a systematic approach based on catalyst loading, pre-treatment and selection of the right operating conditions for the improvement of a monometallic catalytic system for the growth of SWCNT. High quality SWCNTs with high yield was achieved by using a 2 wt.% Fe-MgO catalyst with diameters ranging from 0.8-2.0nm.

Understanding the growth and controlling the diameter of CNT facilitates the study of fundamental properties and the exploration of new applications [10], [51]. The key role of a catalyst in defining the nanotube diameter produced by CVD is evident from the analysis of the diameter distribution which shows a close correlation between diameters of nanocluster catalyst and nanotubes [51]. This discovery was made when Cheung et al. prepared [51] iron nanoclusters having three distinct average diameters which were used to grow carbon nanotubes with similar average diameters. Diameter-controlled synthesis of SWCNT using Mn₁₂ cluster as a catalyst precursor by means of mist flow CVD has also been reported by [44]. The mist flow CVD was reported to be effective for the diameter controlled growth of SWCNTs. Site selective synthesis based on CVD is able to grow CNTs at controllable locations and with desired orientations on surfaces [10]. CVD are described to be effective in the preparation of hybrid materials based on CNT on different supports where surface located growth is required [39]. The study was on the utilization and comparison of natural nontronites and synthetic haematites as interface modification nanoparticles for local growth of CNT at required support.

III. THERMAL CONDUCTIVITY OF CARBON NANOTUBES

A. Thermal Conductivity in a Base Fluid

Thermal conductivity and heat transfer of nanofluids depends not only on the forces acting on nanoparticles, but

also on particle motion and interaction with turbulent eddies [4]. Convective heat transfer can be passively improved by altering the boundary conditions, flow geometry or by increasing the thermal conductivity of the base fluid [52]. Decrease in diameter of nanoparticles brings about a more uniform temperature distribution. However, there is a corresponding increase in cost and complexity of nanoparticle production [53]. Previous study reveals that the effective thermal conductivity of suspensions with spherical particles increases with the volume fraction of the particles and also increases with the ratio of the surface area to volume ratio of the particle [3]. It has also been pointed that since heat transfer takes place at the surface, nanoparticle with a wide surface area should be used. Compared to millimeter and micrometer sized particles suspensions, nanofluids possess better long term stability and rheological properties which makes them have higher thermal compatibility [54]. Carbon based nanoparticles are being used to enhance the thermal conductivity of their applications [7], [54]-[57]. The high conductivity, high aspect ratio of CNTs and also their special surface area is responsible in making them suitable for heat transfer purposes in nanofluids [54], [56]. The enhanced thermal conductivity is due to the nature of heat conduction in nanotube suspensions and an organized structure at the solid/liquid interface [54]. Brownian motion has also been suggested to be a major phenomenon in controlling a nanofluids thermal conductivity [54].

The study by [7] considered the preparation of thermal enhanced bio-based phase change materials (PCM) by using vacuum impregnation method with exfoliated graphite nanoplatelets. The results show a 375% increase in thermal conductivity. There was also an increase in the latent heat and thermal resistance. The thermal conductivity of ethylene glycol and synthetic engine oil were improved by dispersing multi-walled carbon nanotubes and was measured using the transient hot wire method [54]. The authors reported an increase in thermal conductivity with an increase in volume fraction. Thermal conductivity enhancements up to 12.4% was achieved for CNT-ethylene glycol suspensions at a volume fraction of 1 vol% when compared to CuO based nanoparticles. In addition, up to 30% enhancement in thermal conductivity was achieved for CNT-engine oil suspension with 2 vol%. These results clearly indicate that the enhanced thermal conductivity ratios increase with a corresponding increase in the volume fraction of CNTs and it is nearly non-linear [54].

B. Thermal Conductivity of Multi-Walled Carbon Nanotubes

The need to measure the intrinsic thermal properties and thermal conductivity of individual carbon nanotubes in order to get an accurate estimation prompted the study by [6] and [58]. The studies of the thermal properties of MWCNTs by taking bulk measurements had a disadvantage of yielding an ensemble average over different tubes in a sample. This is as a result of the existence of various tube-tube junctions which

can be an obstacle to thermal transport in bundle nanotubes [6]. These tube-tube interactions are primarily caused by van der Waals forces except for special instances when local charge introduce additional electrostatic fields [59]. The interaction between confined nanotubes in bundles can partially decrease their rotational and vibrational freedom, lead to extinguishing of phonon modes which also decrease the thermal conductivity [59]. To achieve high thermal conductivity in long MWCNT, it was proposed that the nanotubes should touch each other over less than 2-3% of their total length [59]. A micro-fabricated suspended device hybridized with MWCNT to probe thermal transport was developed by Kim et al [6]. A mechanical approach was used to place MWCNT on the device and this approach produced a nanotube device that can be used to measure the thermal conductivity of individual MWCNT. The thermal conductivity reported is over 3000W/mK at room temperature. On the other hand, [58] used a combination of electric fields with an alternating current (ac); direct current (dc) to place a single CNT across the electrodes for thermal conductivity measurements using $3-\omega$. This approach is based on selective deposition technique which has a benefit of permitting the control of single nanotube placement. The thermal conductivity was reported as 650 and 830 W/mK respectively. The technique is reported to operate on a narrow-band detection technique and is said to give better signal-to-noise ratio [60]. In order to produce reliable data on the thermal conductivity of various sizes of nanotubes, a novel measurement technique was developed based on the four-point-probe third-harmonic ($3-\omega$) method with assistance of a focused ion beam (FIB) for electric field supply [61]. As compared to the two point probe $3-\omega$ method used by [58], the accuracy of the measurement is significantly enhanced by eliminating the contact contribution in the measurement which was previously done by annealing the nanotube samples at 600°C. The measured value for the CNTs investigated by the authors [61] is 300 ± 20 W/mK. The variation in thermal conductivity is likely to depend on the type and size of carbon nanotube utilized which gives rise to different mean free paths of the energy carriers. The $3-\omega$ technique of measuring thermal conductivity recently used by [62], was employed to determine the thermal conductivity for a low temperature grown vertical MWCNT bundles. This is important because CNT bundles which are required to obtain a low electrical and heat resistance applications need to possess low thermal conductivity. The thermal conductivity reported was 1.7-3.5 W/mK. The disadvantage of this method is a low quality sample arising from a low growth temperature. Table I gives some of the thermal conductivity results from literature.

TABLE I
 THERMAL CONDUCTIVITY AND MEASUREMENT OF MWCNT FROM LITERATURE

Author	Thermal conductivity technique	Result
[63]	Pulsed photothermal reflectance	15W/mK
[59]	Equivalent circuit simulations and an experimental self-heating 3ω method	150W/mK
[62]	Vertical 3ω method	1.7-3.5W/mK
[58]	Horizontal 3ω method	650-830W/mK
[64]	Pulsed photothermal reflectance method	2586W/mK
[65]	Equilibrium molecular dynamics simulations	950W/mK (along the tube axis) 5.6W/mK (perpendicular to the tube)
[6]	Microfabricated suspended device	>3000W/mK

The notable technical difficulty in fabricating devices used by the authors from literature [6], [58], [60], [61], motivated the research by [66]. The authors estimated the thermal conductivity of an individual CNT from the obtained thermal diffusivity measurement of MWCNT array based on a laser flash technique. The following correlation was used to determine the thermal conductivity [66]:

$$\lambda = \alpha \rho C_p \quad (3)$$

where: C_p : Specific heat; ρ : Density; and α : Thermal diffusivity of CNT.

The thermal conductivity at room temperature was reported to be about 750W/mK and it increased smoothly with an increase in temperature. Measuring the thermal conductivity of a film of MWNTs using pulsed photo-thermal reflectance technique was used by [63] and [64]. This non-contact method is said to have an advantage of having no boundary scattering due to reservoir junction which has been observed in electrical junction [64]. The thermal conductivity for CNT bundle length of 10 – 50 μm and diameter 40-100 nm was measured and was found to be about 15W/mK [63] while [64] reported a thermal conductivity of 2586 W/mK for an individual CNT of length 2 μm and diameter 150nm. The high thermal conductivity of the individual MWCNT by [64] has been proposed to arise from the existence of ballistic flux of long-wave acoustic phonon, which originates from all the walls having equal contribution to thermal transport. These phonons enable heat transport in MWCNT, and are therefore an essential factor of the thermal conductivity. For novel materials for which quantitative measurements cannot be carried out, simulations involving molecular dynamics are applied. The need to understand the lattice thermal transport properties of carbon nanotubes for nano-electromechanical systems (NEMS) and microelectromechanical systems (MEMS) devices prompted the study by [65] and [67]. The MD approach is essential to observe the theoretical predictions of the thermal conductivity of CNT and the influence of various defects. One major concern of using MD however, is the size effect of the simulation box due to periodic boundary simulations [65]. The thermal conductivity is extracted from the Green-Kubo relationship in (4):

$$\Lambda(w) = \frac{1}{2\kappa_B T^2 V} \hat{C}_{jj}^q(\omega) \quad (4)$$

where κ_B : Boltzmann constant; V : Volume; T : Temperature of the sample; and \hat{C}_{jj}^q : Quantum canonical correlation function.

The thermal conductivity obtained was 950 W/mK along the tube axis and 5.6 W/mK in the direction perpendicular to the tube.

C. Thermal Conductivity in Single-Walled Carbon Nanotubes

The thermal conductivity of SWCNTs from most studies in literature have been seen to depend on several CNT parameters ranging from nanotube length, simulation method for free boundary and periodic boundary conditions [68], [69]; temperature [70], [71]; axial strain [72]; radius and chirality of the tube [73] and interaction between the nanotube with the substrate [74]. Several other studies also emphasized the fact that dependence of thermal conductivity below 30K is reliant on phonons rather than electrons [70]. Therefore, understanding the mechanism of heat conduction in SWCNTs involves investigating the difference between the varieties of phonon modes and to determine which kinds of phonon modes play the dominant role.

D. Temperature Dependent Thermal Conductivity of Single-Walled Carbon Nanotubes

The thermal conductivity of SWCNT measured by [70] was focused on the low temperature range (<100K), which had a linear behavior. At this low temperature, a small diameter most probably affects the phonon properties of single-walled carbon nanotubes [70], [71]. A significant decrease in thermal conductivity was observed as the temperature decreased (Fig 1). The results from the studies revealed an intrinsic thermal conductivity of nanotube bundles rather than sample dependent effects like joints between bundles. Cao et al. [71] reported a peak behavior at about 85K accompanied by a rapid decrease in the temperature dependent thermal conductivity which is caused by the Umklapp scattering freezing out. The peak behaviour will shift to higher temperatures as diameter increases while neglecting dependence on tube chirality [75]. This is because as the temperature increases, the strong Umklapp scattering becomes more effective due to the thermal population of higher-energy phonons (Fig. 2) [71].

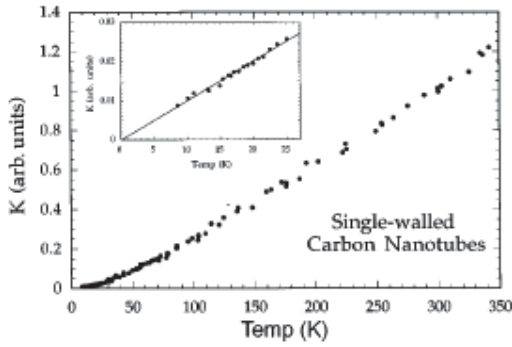


Fig. 1 Thermal conductivity of SWCNT as a function of temperature [70]

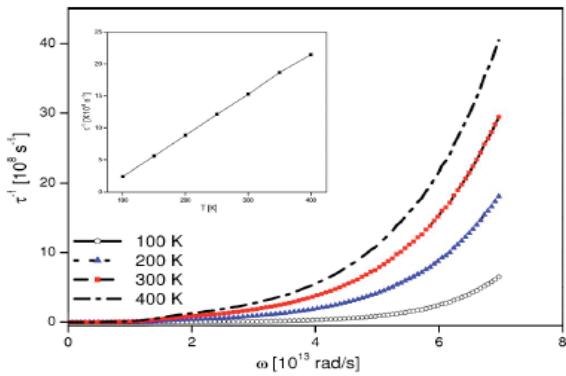


Fig. 2 Relaxation rates of Umklapp process of (6,0) SWCNT [71]

Silotia et al. [76] made an attempt to explain the observed temperature variation of thermal conductivity by [70] using a theoretical anisotropic model. The thermal conductivity based on the model is given as:

$$\kappa = \frac{B_c^2 \theta_{D,eff}^2}{\hbar^2 (6\pi^2 n)^{2/3} B_c} \frac{\pi \hbar}{B_c} \theta_{D,eff}^{d-1} \frac{1}{3} \times l \quad (5)$$

where B_c is the Boltzmann constant, \hbar is the Planck's constant and $\theta_{D,eff}$ is the efficient temperature. The anisotropic model is used because other models like Debye and the extended Debye model do not take into account the presence of the anisotropic nature of SWCNT especially at low temperatures below 30K. In addition, the anisotropic model explains well the temperature variation of specific heat in the entire temperature range 2-300K [76]. The thermal conductivity involves phonon-phonon scattering and phonon-phonon interaction which produces phonon mean free path l or phonon relaxation time τ . Fig. 3 shows the thermal conductivity measurements by [76]. From the figure, it can be seen that the highest thermal conductivity was observed at the highest temperature (350°K) and the lowest conductivity at the lowest temperature (8°K).

At 100K, a clear peak was observed in the study carried out by [77], which gradually decreases with an increasing temperature till it gets to 200K and from 200K-300K, the temperature becomes constant. This behavior is said to be due to the temperature dependent property of phonon. At low

temperature, the phonon relaxation time is inversely proportional to the temperature which translates into a decrease in thermal conductivity with increasing temperature. However at high temperatures, phonon-phonon scattering contributes to the phonon-decay and shows no temperature dependence (the thermal conductivity is constant) [77]. This peaking behavior is also seen in [75]. It was observed by the authors that the peak shifts to higher temperatures with increasing diameter of nanotube due to the onset of Umklapp scattering, which is said to lower the thermal conductivity at higher temperatures, and also depends of nanotube radius. The peak in this study occurred at 400K and then a drop followed at 500K. Recently a technique known as opto-thermal technique was used to determine the intrinsic thermal conductivity and interfacial thermal conductance on thin nanotube films deposited on silicon substrates as a function of temperature in the range 300-450K [78]. The tube diameter was in the range of 1.2-1.7nm with a mean length of 1 μ m. The value of K was found to decrease non-linearly by nearly 60%. This was due to the increase of multi phonon scattering at higher temperatures. The thermal conductivity decreased from 26.4 to 9.2W/mK in the temperature range of 300-450K.

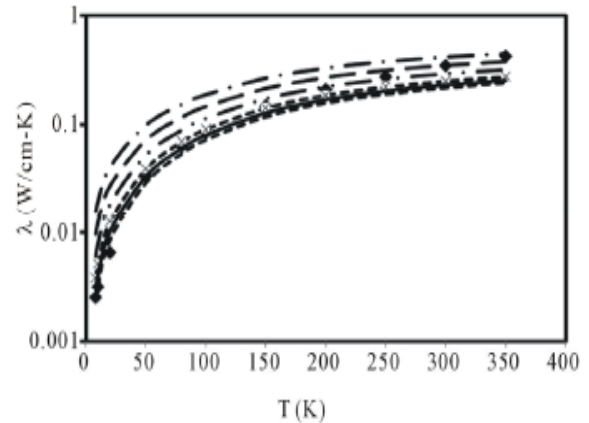


Fig. 3 Thermal conductivity of SWCNT in the temperature range 8-350 at different diameters (0.7, 0.75, 0.8, 0.9, 1, and 1.1.) [76]

The thermal conductivity in higher temperature range of 300-800K has been determined by [79] using reverse fitting based on an existing electro-thermal transport model. The results indicated a restrained decrease in the thermal conductivity of SWCNT near the upper end of the temperature range which is proportional to $1/T^2$. The presence of Umklapp phonon-phonon scattering which gives a temperature dependence of $1/T$ is seen from the graph. In addition, at the upper end of the graph can be seen a drop in thermal conductivity at a rate steeper than $1/T$. The reason given to this is the effect of second order scattering process with scattering rates proportional to T^2 . At the low end of the temperature range, a levelling of thermal conductivity was observed suggesting a transition towards thermal transport limited by phonon boundary scattering due to the finite sample size as seen in Fig. 4.

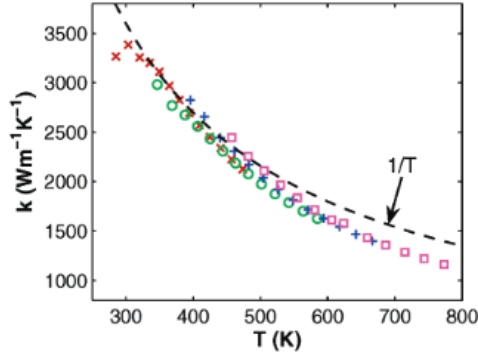


Fig. 4 Thermal conductivity of SWCNT in the temperature range 300-800K [79]

IV. THE EFFECT OF SUBSTRATES ON THE THERMAL CONDUCTIVITY OF SWCNT

The question arose on whether the thermal conductivity of SWCNTs was related to the effects of substrates [74]. This question was answered by carrying out a direct modelling of the heat transfer by means of MD simulations and also by studying the equilibrium multi-particle dynamics based on the Green-Kubo formalism. The study discovered that there was a finite conductivity for nanotubes that were placed on substrates unlike isolated CNT that displayed an anomalous thermal conductivity. The mean free path the heat carries is of the same order or larger than the nanotube length, and for the Knudsen number, $Kn > 1$. This shows that the interaction of CNT with a substrate can change dramatically the character of thermal conductivity, due to the appearance of a narrow gap at the bottom of the frequency spectrum of acoustic phonons.

V. THE ROLE OF PHONON-PHONON SCATTERING IN CARBON NANOTUBES

Heat conduction by phonons is an inclusive process that incorporates a wide range of physics and plays an essential role in applications ranging from space power generation to LED lighting [80]. Acoustic phonons play a dominant role in phonon state [70], [71], [79]. Additional phonon mode, scattering process and rolling-up of graphene sheets have significant effects on the temperature dependence of the thermal conductivity both at low temperature and high temperature [70], [76]. In a perfect isolated SWCNT, the physical mechanics of the thermal transport can be analysed using phonon relaxation rate mainly controlled by boundary scattering and three-phonon Umklapp scattering process [71], [81]. The Umklapp process is made up of the combining process and the splitting process which both contribute to thermal resistance. The total relaxation time can be calculated from Matthiessen's rule and expressed as [71]:

$$\frac{1}{\tau} = \frac{1}{\tau_B} + \frac{1}{\tau_U} \quad (6)$$

with

$$\frac{1}{\tau_U} = \frac{1}{c_p} + \frac{1}{s_p},$$

Therefore, the total relaxation rate can be rewritten as:

$$\frac{1}{\tau} = \frac{1}{\tau_B} + \frac{1}{c_p} + \frac{1}{s_p} \quad (7)$$

with τ_B as the relaxation time for boundary scattering and τ_U as the three-phonon Umklapp scattering process. It was observed that there are more very low lying folded phonon branches as the tubes diameter increases which invariably contributes to thermal conductivity. By using the complete dispersion relations for SWCNT, [81] concentrated on the three-phonon interactions to derive thermal conductivity. [82] has shown that the relaxation rate of Umklapp process is derived by the dispersion data and given lattice characteristics. Because the contribution of low frequency phonon is stronger than that of high frequency, the combining process has been assumed to be more important than the splitting process in the evaluation of thermal resistance.

The combining process and the splitting process respectively satisfy the selection rule:

$$q + q' = q'' + G \quad (8)$$

$$q = q' + q'' + G \quad (9)$$

where q, q', q'' are phonon wave vectors and G is the reciprocal-lattice vector [81]. From (9), the relaxation rate of the three-phonon Umklapp process can be given as [81]:

$$\frac{1}{\tau} = \frac{4\hbar\gamma^2}{3\rho_l v^2} \sum_{j'=1-N/2}^{N/2} \sum_{p'=1}^6 \frac{\omega\omega'\omega''}{v_g} \delta(\delta_\omega) N(\omega', \omega'') \quad (10)$$

and the thermal conductivity calculated for the tube was found to be 474 W/m K at 300 K. The effects of orderly functionalization on the thermal conductivity of SWCNT at 300K was carried out by [83] using a non-equilibrium molecular dynamics (NEMD) simulations. The simulation was carried out to find the character of the thermal conductivity by means of decorated hydrogen atoms. This was done by calculating the phonon power spectra of the SWCNTs from Fourier transform of the velocity autocorrelation function. From Fourier's equation, the thermal conductivity is defined thus:

$$J = -\lambda \nabla T \quad (11)$$

where: ∇T is the gradient of the temperature; T and J is the resulting heat flux density. The result shows that the functionalized CNTs show considerably lesser thermal conductivity than pristine CNT (CNT with attached hydrogen). It was also ascertained that there are more suppressed axial phonon modes of the randomly functionalized SWCNTs than the regular functionalized case. The hydrogen atoms attached to the CNTs act as defects which consequently reduces the thermal conductivity. The study of the phonon spectra indicates that the density of phonon modes is significantly changed for functionalized tubes, which leads to a reduction in the phonon scattering length and the suppression of some vibrational modes. This

results in the degeneration of thermal conductivity. Below room temperature where the phonon-phonon Umklapp scattering is minimal, phonons have only a few scattering events between the thermal reservoirs and the phonon transport is nearly ballistic. This feature is not present in bulk measurements of MWCNT which is possibly due to additional extrinsic phonon scattering mechanisms such as tube-tube interactions [6].

VI. DISCUSSION AND CONCLUSION

Carbon nanotubes undoubtedly are an intriguing next generation materials, which are being continuously improved upon for application in diverse areas including chemical, mechanical and electrical systems. Their synthesis, growth and application is an area of active research.

From literature, significant milestones have been achieved in the field of CNT synthesis with a focus on CVD. Synthesis parameters have been shown to have a direct output on the shape and morphology of as-grown CNTs. The parameters include precursor, synthesis time, temperature, diameter, among others. The inconsistent heat transfer properties such as thermal conductivity of CNTs are attributed to the various conditions such as temperature, diameter, length, and the morphology of growth of the CNT. The present review validates the similarities in the thermal behavior of MWCNTs and graphite. The thermal conductivity of MWCNTs can be modelled assuming the properties and parameters of graphite, although it is possible that the interlayer coupling in MWCNTs might be slightly different than it is in graphite. It was also shown that phonon confinement effects in MWCNTs are important only at very low temperatures. At low temperatures, the thermal conductivity in SWCNT is dominated by phonon boundary scattering. A linear temperature profile exists at low temperatures less than 80K but shows peak behavior at 85K and falls off at higher temperatures.

ACKNOWLEDGEMENT

The authors wish to anticipate the supports from NRF of South Africa and the College of Agriculture, Engineering and Science of the University of KwaZulu-Natal, South Africa.

REFERENCES

- [1] S. K. Das, S. U. Choi, W. Yu, and T. Pradeep, *Nanofluids: science and technology*: John Wiley & Sons, 2007.
- [2] X. Qi, C. Qin, W. Zhong, C. Au, X. Ye, and Y. Du, "Large-scale synthesis of carbon nanomaterials by catalytic chemical vapor deposition: a review of the effects of synthesis parameters and magnetic properties," *Materials*, vol. 3, pp. 4142-4174, 2010.
- [3] S. U. S. Choi and J. A. Eastman, *Enhancing thermal conductivity of fluids with nanoparticles*, 1995.
- [4] S.-S. Choi, "Nanofluid technology: current status and future research," Argonne National Lab., IL (US)1998.
- [5] Y. Arai, Y. Sako and Y. Takebayashi (Eds). *Supercritical fluids: Molecular interactions, physical properties and new applications*. Springer science & business media, 2013. doi: 10.1007/978-3-642-56238-9.
- [6] P. Kim, L. Shi, A. Majumdar, and P. L. McEuen, "Thermal Transport Measurements of Individual Multiwalled Nanotubes," *Physical Review Letters*, vol. 87, 2001.
- [7] S.-G. Jeong, O. Chung, S. Yu, S. Kim, and S. Kim, "Improvement of the thermal properties of Bio-based PCM using exfoliated graphite nanoplatelets," *Solar Energy Materials and Solar Cells*, vol. 117, pp. 87-92, 2013.
- [8] M. R. Snowdon, A. K. Mohanty, and M. Misra, "A Study of Carbonized Lignin as an Alternative to Carbon Black," *ACS Sustainable Chemistry & Engineering*, vol. 2, pp. 1257-1263, 2014.
- [9] J. Prasek, J. Drbohlavova, J. Chomoucka, J. Hubalek, O. Jasek, V. Adam, *et al.*, "Methods for carbon nanotubes synthesis—review," *Journal of Materials Chemistry*, vol. 21, pp. 15872-15884, 2011.
- [10] H. Dai, "Carbon nanotubes: synthesis, integration, and properties," *Accounts of chemical research*, vol. 35, pp. 1035-1044, 2002.
- [11] H. Li, X. He, Y. Liu, H. Yu, Z. Kang, and S.-T. Lee, "Synthesis of fluorescent carbon nanoparticles directly from active carbon via a one-step ultrasonic treatment," *Materials Research Bulletin*, vol. 46, pp. 147-151, 2011.
- [12] B. Zhang, C. y. Liu, and Y. Liu, "A Novel One-Step Approach to Synthesize Fluorescent Carbon Nanoparticles," *European Journal of Inorganic Chemistry*, vol. 2010, pp. 4411-4414, 2010.
- [13] B. De and N. Karak, "A green and facile approach for the synthesis of water soluble fluorescent carbon dots from banana juice," *Rsc Advances*, vol. 3, pp. 8286-8290, 2013.
- [14] S. Manafi, M. Amin, M. Rahimpour, E. Salahi, and A. Kazemzadeh, "High-yield synthesis of multiwalled carbon nanotube by mechanochemical method," *Nanoscale research letters*, vol. 4, pp. 296-302, 2009.
- [15] A. Szabó, C. Perri, A. Csató, G. Giordano, D. Vuono, and J. B. Nagy, "Synthesis methods of carbon nanotubes and related materials," *Materials*, vol. 3, pp. 3092-3140, 2010.
- [16] Ö. Güler and E. Evin, "Carbon nanotubes formation by short-time ball milling and annealing of graphite," *Optoelectronics And Advanced Materials*, vol. 6, pp. 183-187, 2012.
- [17] M. J. Rak, T. Friscic, and A. Moores, "Mechanochemical synthesis of Au, Pd, Ru and Re nanoparticles with lignin as a bio-based reducing agent and stabilizing matrix," *Faraday Discuss*, vol. 170, pp. 155-67, 2014.
- [18] K. Xu, Y. Li, F. Yang, W. Yang, L. Zhang, C. Xu, *et al.*, "Controllable synthesis of single-and double-walled carbon nanotubes from petroleum coke and their application to solar cells," *Carbon*, vol. 68, pp. 511-519, 2014.
- [19] O. V. Kharissova, H. V. Dias, B. I. Kharisov, B. O. Perez, and V. M. Perez, "The greener synthesis of nanoparticles," *Trends Biotechnol*, vol. 31, pp. 240-8, Apr 2013.
- [20] J. Qu, C. Luo, Q. Cong, and X. Yuan, "Carbon nanotubes and Cu-Zn nanoparticles synthesis using hyperaccumulator plants," *Environmental chemistry letters*, vol. 10, pp. 153-158, 2012.
- [21] J. Qu, C. Luo, and X. Yuan, "Synthesis of hybrid carbon nanotubes using Brassica juncea L. application to photodegradation of bisphenol A," *Environmental Science and Pollution Research*, vol. 20, pp. 3688-3695, 2013.
- [22] J. Zhu, J. Jia, F. L. Kwong, D. H. L. Ng, and S. C. Tjong, "Synthesis of multiwalled carbon nanotubes from bamboo charcoal and the roles of minerals on their growth," *biomass and bioenergy*, vol. 36, pp. 12-19, 2012.
- [23] A. K. Mittal, Y. Chisti, and U. C. Banerjee, "Synthesis of metallic nanoparticles using plant extracts," *Biotechnol Adv*, vol. 31, pp. 346-56, Mar-Apr 2013.
- [24] R. Tsao, "Chemistry and biochemistry of dietary polyphenols," *Nutrients*, vol. 2, pp. 1231-46, Dec 2010.
- [25] X. He, H. Li, Y. Liu, H. Huang, Z. Kang, and S.-T. Lee, "Water soluble carbon nanoparticles: hydrothermal synthesis and excellent photoluminescence properties," *Colloids and Surfaces B: Biointerfaces*, vol. 87, pp. 326-332, 2011.
- [26] P. Gonugunta, S. Vivekanandhan, A. K. Mohanty, and M. Misra, "A study on synthesis and characterization of biobased carbon nanoparticles from lignin," *World Journal of Nano Science and Engineering*, vol. 2, p. 148, 2012.
- [27] V. Roshni and D. Ottoor, "Synthesis of carbon nanoparticles using one step green approach and their application as mercuric ion sensor," *Journal of Luminescence*, vol. 161, pp. 117-122, 2015.
- [28] T. A. Hassan, V. K. Rangari, V. Fallon, Y. Farooq, and S. Jeelani, "Mechanochemical and sonochemical synthesis of bio-based nanoparticles," in *Proceedings of the Nanotechnology Conference*, 2010, pp. 278-281.

- [29] T. S. Syamsudin, E. M. Alamsyah, and B. S. Purwasasmita, "Synthesis of Bio-based Nanomaterial from Surian (*Toona sinensis* Roem) Wood Bark Using Conventional Balls Milling Method and its Characterization," *Journal of Biological Sciences*, vol. 14, p. 204, 2014.
- [30] Z. Niu and Y. Fang, "Effects of synthesis time for synthesizing single-walled carbon nanotubes over Mo-Fe-MgO catalyst and suggested growth mechanism," *Journal of crystal growth*, vol. 297, pp. 228-233, 2006.
- [31] S. D. Mhlanga, K. C. Mondal, R. Carter, M. J. Witcomb, and N. J. Coville, "The effect of synthesis parameters on the catalytic synthesis of multiwalled carbon nanotubes using Fe-Co/CaCO₃ catalysts," *South African Journal of Chemistry*, vol. 62, pp. 67-76, 2009.
- [32] W. Zhao, H. S. Kim, H. T. Kim, J. Gong, and I. J. Kim, "Synthesis and growth of multi-walled carbon nanotubes(mwnts) by CCVD using Fe-supported zeolite templates," *Journal of Ceramic Processing Research*, vol. 12, pp. 392-397, 2011.
- [33] E. Dündar-Tekkaya and N. Karatepe, "Effect of reaction time, weight ratio, and type of catalyst on the yield of single-wall carbon nanotubes synthesized by chemical vapor deposition of acetylene," *Fullerenes, Nanotubes and Carbon Nanostructures*, vol. 23, pp. 535-541, 2015.
- [34] S. M. Toussi, A. Fakhru'l-Razi, and A. Suraya, "Optimization of Synthesis Condition for Carbon Nanotubes by Catalytic Chemical Vapor Deposition (CCVD)," in *IOP Conference Series: Materials Science and Engineering*, 2011, p. 012003.
- [35] D. Lopez, I. Abe, and I. Pereyra, "Temperature effect on the synthesis of carbon nanotubes and core-shell Ni nanoparticle by thermal CVD," *Diamond and Related Materials*, vol. 52, pp. 59-65, 2015.
- [36] M. Shamsudin, N. Asli, S. Abdullah, S. Yahya, and M. Rusop, "Effect of synthesis temperature on the growth iron-filled carbon nanotubes as evidenced by structural, micro-Raman, and thermogravimetric analyses," *Advances in Condensed Matter Physics*, vol. 2012, 2012.
- [37] Y. Jiang and C. Lan, "Low temperature synthesis of multiwall carbon nanotubes from carbonaceous solid prepared by sol-gel autocombustion," *Materials Letters*, 2015.
- [38] M. Kumar, "Carbon Nanotube Synthesis and Growth Mechanism " in *Carbon Nanotubes - Synthesis, Characterization, Applications*, D. S. Y. (Ed.), Ed., ed: InTech, 2011, p. 514.
- [39] Š. Kavecký, J. Valúchová, M. Čaplovičová, S. Heissler, P. Šajgalík, and M. Janek, "Nontronites as catalyst for synthesis of carbon nanotubes by catalytic chemical vapor deposition," *Applied Clay Science*, vol. 114, pp. 170-178, 2015.
- [40] Y. Li, J. Liu, Y. Wang, and Z. L. Wang, "Preparation of monodispersed Fe-Mo nanoparticles as the catalyst for CVD synthesis of carbon nanotubes," *Chemistry of Materials*, vol. 13, pp. 1008-1014, 2001.
- [41] I. Abdullahi, N. Sakulchaicharoen, and J. E. Herrera, "Selective synthesis of single-walled carbon nanotubes on Fe-MgO catalyst by chemical vapor deposition of methane," *Diamond and Related Materials*, vol. 41, pp. 84-93, 2014.
- [42] G. Allaedini, S. M. Tasirin, and P. Aminayi, "Synthesis of CNTs via chemical vapor deposition of carbon dioxide as a carbon source in the presence of NiMgO," *Journal of Alloys and Compounds*, vol. 647, pp. 809-814, 2015.
- [43] W.-W. Liu, A. Aziz, S.-P. Chai, A. R. Mohamed, and U. Hashim, "Synthesis of single-walled carbon nanotubes: Effects of active metals, catalyst supports, and metal loading percentage," *Journal of Nanomaterials*, vol. 2013, p. 63, 2013.
- [44] Y. Sun, T. Nakayama, and H. Yoshikawa, "Synthesis of uniform single-wall carbon nanotubes using Mn 12 clusters as the catalyst precursor," *Diamond and Related Materials*, vol. 56, pp. 42-46, 2015.
- [45] H. Cheng, F. Li, G. Su, H. Pan, L. He, X. Sun, et al., "Large-scale and low-cost synthesis of single-walled carbon nanotubes by the catalytic pyrolysis of hydrocarbons," *Applied Physics Letters*, vol. 72, pp. 3282-3284, 1998.
- [46] M. Kumar and Y. Ando, "Chemical vapor deposition of carbon nanotubes: a review on growth mechanism and mass production," *Journal of nanoscience and nanotechnology*, vol. 10, pp. 3739-3758, 2010.
- [47] A. L. M. Reddy, M. Shaijumon, and S. Ramaprabhu, "Alloy hydride catalyst route for the synthesis of single-walled carbon nanotubes, multi-walled carbon nanotubes and magnetic metal-filled multi-walled carbon nanotubes," *Nanotechnology*, vol. 17, p. 5299, 2006.
- [48] P. M. Parthangal, R. E. Cavicchi, and M. R. Zachariah, "A generic process of growing aligned carbon nanotube arrays on metals and metal alloys," *Nanotechnology*, vol. 18, p. 185605, 2007.
- [49] M. Shaijumon, A. L. M. Reddy, and S. Ramaprabhu, "Single step process for the synthesis of carbon nanotubes and metal/alloy-filled multiwalled carbon nanotubes," *Nanoscale Research Letters*, vol. 2, pp. 75-80, 2007.
- [50] F. Xu, H. Zhao, and D. T. Stephen, "Carbon nanotube synthesis on catalytic metal alloys in methane/air counterflow diffusion flames," *Proceedings of the Combustion Institute*, vol. 31, pp. 1839-1847, 2007.
- [51] C. L. Cheung, A. Kurtz, H. Park, and C. M. Lieber, "Diameter-controlled synthesis of carbon nanotubes," *The Journal of Physical Chemistry B*, vol. 106, pp. 2429-2433, 2002.
- [52] X.-Q. Wang and A. S. Mujumdar, "Heat transfer characteristics of nanofluids: a review," *International Journal of Thermal Sciences*, vol. 46, pp. 1-19, 2007.
- [53] V. Khullar and H. Tyagi, "A study on environmental impact of nanofluid-based concentrating solar water heating system," *International Journal of Environmental Studies*, vol. 69, pp. 220-232, 2012.
- [54] M.-S. Liu, M. Ching-Cheng Lin, I. T. Huang, and C.-C. Wang, "Enhancement of thermal conductivity with carbon nanotube for nanofluids," *International Communications in Heat and Mass Transfer*, vol. 32, pp. 1202-1210, 2005.
- [55] Y. Ding, H. Alias, D. Wen, and R. A. Williams, "Heat transfer of aqueous suspensions of carbon nanotubes (CNT nanofluids)," *International Journal of Heat and Mass Transfer*, vol. 49, pp. 240-250, 2006.
- [56] M. Xing, J. Yu, and R. Wang, "Experimental study on the thermal conductivity enhancement of water based nanofluids using different types of carbon nanotubes," *International Journal of Heat and Mass Transfer*, vol. 88, pp. 609-616, 2015.
- [57] T. Maré, S. Halelfadl, S. Van Vaerenbergh, and P. Estellé, "Unexpected sharp peak in thermal conductivity of carbon nanotubes water-based nanofluids," *International Communications in Heat and Mass Transfer*, vol. 66, pp. 80-83, 2015.
- [58] T. Y. Choi, D. Poulikakos, J. Tharian, and U. Sennhauser, "Measurement of thermal conductivity of individual multiwalled carbon nanotubes by the 3- ω method," *Applied Physics Letters*, vol. 87, p. 013108, 2005.
- [59] A. E. Aliev, M. H. Lima, E. M. Silverman, and R. H. Baughman, "Thermal conductivity of multi-walled carbon nanotube sheets: radiation losses and quenching of phonon modes," *Nanotechnology*, vol. 21, p. 035709, 2010.
- [60] L. Lu, W. Yi, and D. L. Zhang, "3 ω method for specific heat and thermal conductivity measurements," *Review of Scientific Instruments*, vol. 72, p. 2996, 2001.
- [61] S. K. Das, S. U. Choi, and H. E. Patel, "Heat transfer in nanofluids—a review," *Heat transfer engineering*, vol. 27, pp. 3-19, 2006.
- [62] S. Vollebregt, S. Banerjee, K. Beenakker, and R. Ishihara, "Thermal conductivity of low temperature grown vertical carbon nanotube bundles measured using the three- ω method," *Applied Physics Letters*, vol. 102, p. 191909, 2013.
- [63] D. J. Yang, Q. Zhang, G. Chen, S. F. Yoon, J. Ahn, S. G. Wang, et al., "Thermal conductivity of multiwalled carbon nanotubes," *Physical Review B*, vol. 66, 2002.
- [64] M. K. Samani, N. Khosravian, G. C. K. Chen, M. Shakerzadeh, D. Baillargeat, and B. K. Tay, "Thermal conductivity of individual multiwalled carbon nanotubes," *International Journal of Thermal Sciences*, vol. 62, pp. 40-43, 2012.
- [65] J. Che, T. Cagin, and W. A. Goddard III, "Thermal conductivity of carbon nanotubes," *Nanotechnology*, vol. 11, p. 65, 2000.
- [66] H. Xie, A. Cai, and X. Wang, "Thermal diffusivity and conductivity of multiwalled carbon nanotube arrays," *Physics Letters A*, vol. 369, pp. 120-123, 2007.
- [67] S. Berber, Y.-K. Kwon, and D. Tománek, "Unusually high thermal conductivity of carbon nanotubes," *Physical review letters*, vol. 84, p. 4613, 2000.
- [68] J. R. Lukes and H. Zhong, "Thermal Conductivity of Individual Single-Wall Carbon Nanotubes," *Journal of Heat Transfer*, vol. 129, p. 705, 2007.
- [69] Z. Wang, D. Tang, X. Zheng, W. Zhang, and Y. Zhu, "Length-dependent thermal conductivity of single-wall carbon nanotubes: prediction and measurements," *Nanotechnology*, vol. 18, p. 475714, 2007.
- [70] J. Hone, M. Whitney, C. Piskoti, and A. Zettl, "Thermal conductivity of single-walled carbon nanotubes," *Physical Review B*, vol. 59, p. R2514, 1999.

- [71] J. X. Cao, X. H. Yan, Y. Xiao, and J. W. Ding, "Thermal conductivity of zigzag single-walled carbon nanotubes: Role of the umklapp process," *Physical Review B*, vol. 69, 2004.
- [72] C. Ren, W. Zhang, Z. Xu, Z. Zhu, and P. Huai, "Thermal conductivity of single-walled carbon nanotubes under axial stress," *The Journal of Physical Chemistry C*, vol. 114, pp. 5786-5791, 2010.
- [73] A. Nasir Imtani, "Thermal conductivity for single-walled carbon nanotubes from Einstein relation in molecular dynamics," *Journal of Physics and Chemistry of Solids*, vol. 74, pp. 1599-1603, 2013.
- [74] A. V. Savin, Y. S. Kivshar, and B. Hu, "Effect of substrate on thermal conductivity of single-walled carbon nanotubes," *EPL (Europhysics Letters)*, vol. 88, p. 26004, 2009.
- [75] M. A. Osman and D. Srivastava, "Temperature dependence of the thermal conductivity of single-wall carbon nanotubes," *Nanotechnology*, vol. 12, p. 21, 2001.
- [76] P. Silotia, S. Dabas, A. Saxena, and S.-P. Tewari, "On the Thermal Conductivity of Single-Walled Carbon Nanotube Ropes," *Soft Nanoscience Letters*, vol. 03, pp. 7-10, 2013.
- [77] H. Li-Jun, L. Ji, L. Zheng, Q. Cai-Yu, Z. Hai-Qing, and S. Lian-Feng, "Thermal properties of single-walled carbon nanotube crystal," *Chinese Physics B*, vol. 20, p. 096101, 2011.
- [78] A. Duzynska, A. Taube, K. Korona, J. Judek, and M. Zdrojek, "Temperature-dependent thermal properties of single-walled carbon nanotube thin films," *Applied Physics Letters*, vol. 106, p. 183108, 2015.
- [79] E. Pop, D. Mann, Q. Wang, K. Goodson, and H. Dai, "Thermal conductance of an individual single-wall carbon nanotube above room temperature," *Nano Lett*, vol. 6, pp. 96-100, Jan 2006.
- [80] A. Minnich, "Advances in the measurement and computation of thermal phonon transport properties," *Journal of Physics: Condensed Matter*, vol. 27, p. 053202, 2015.
- [81] Y. Gu and Y. Chen, "Thermal conductivities of single-walled carbon nanotubes calculated from the complete phonon dispersion relations," *Physical Review B*, vol. 76, 2007.
- [82] Y.-J. Han, "Intrinsic thermal-resistive process of crystals: Umklapp processes at low and high temperatures," *Physical Review B*, vol. 54, p. 8977, 1996.
- [83] R. Pan, Z. Xu, Z. Zhu, and Z. Wang, "Thermal conductivity of functionalized single-wall carbon nanotubes," *Nanotechnology*, vol. 18, p. 285704, 2007.